Deliverable 1.5

Preferential pathways of dispersal and role of the AMOC in connectivity

Project acronym	iAtlantic
Grant Agreement	818123
Deliverable number	1.5
Deliverable title	Preferential pathways of dispersal and role of the AMOC in connectivity
Work package	WP1
Date of completion	March 2024
Author(s)	Didier Jollivet, Elodie Portanier, Adrien Tran Lu Y, Marjolaine Matabos, Florence Pradillon, Sophie Arnaud-Haond

This project has received funding from the European Union's Horizon 2020 research and innovation programme under grant agreement No 818123 (iAtlantic). This output reflects only the author's view and the European Union cannot be held responsible for any use that may be made of the information contained therein.

Contents

List of Tables 3
List of Figures 4
1. Introduction 8
2. Materials & Methods 11
3. Results 14
4. Discussion and conclusion 45
5. References 51
6. Document Information 59

List of Acronyms

AMOC	Atlantic Meridional Overturning Circulation
COI	Mitochondrial Cytochrome Oxidase Subunit 1
CTAB	Cetyltrimethylammonium Bromide
CWC	Cold Water Corals
ddRAD	Double digest restriction-site associated DNA
ENA	European Nucleotide Archive
LEA	Landscape And Ecological Association Studies
MAR	Mid Atlantic Ridge
MED	Mediterranean Lineage
MID	Lusitanian Lineage
NGS	Next-Generation Sequencing
PCA	Principal Component Analysis
PLD	Pelagic Larval Duration
PVP	Polyvinylpyrrolidone
SNPs	Single Nucleotide Polymorphisms
VCF	Variant Call Format
WGS	Whole Genome Sequencing
gDNA	Genomic DNA

List of Tables

Table 1. Number of individual genomic (ddRAD) libraries which are eligible for population genomics studies with more than one million usable reads for SNP detection in *B. boomerang/heckerae*. Barcoded individuals used in the IMa3 analysis corresponded to the same individuals. Listed names represent seep localities. All information concerning geographic coordinates and depth of samples are provided in Portanier *et al.* (2023) and in PANGAEA (Jollivet et al. 2023a,b). 15

Table 2. Number of individual genomic (ddRAD) libraries which are eligible for population genomics studies with more than one million usable reads for SNP detection in G. childressi/mauritanicus. Barcoded individuals used in the IMa3 analysis corresponded to the same individuals. Listed names represent seep localities. All information concerning geographic coordinates and depth of samples are provided in Portanier et al. (2023) and in PANGAEA (Jollivet et al. 2023a,b). 15

Table 3. Sub-sample of barcoded individuals of *P. smaragdina* and *L. atlanticus* for the mtDNA analyses. Listed names represent vent sites along the Mid-Atlantic Ridge. All information concerning geographic coordinates and depth of samples are provided in PANGAEA (Jollivet et al. 2023a). 16

Table 4. Number of individual genomic (ddRAD) libraries which are eligible for population genomics studies with more than 1 million usable reads for SNP detection in hydrothermal vent invertebrates. Listed names represent vent sites along the Mid-Atlantic Ridge and Cayman Ridge. All information concerning geographic coordinates and depth of samples are provided in PANGAEA (Jollivet et al. 2023a). 17

Table 5. Number of individual WGS libraries obtained for the deep corals *D. pertusum* and *M. oculata*. *: three distinct localities. Geographic positions of samples are illustrated in Figure 1 and available in Appendices 1 and 2. 19

Table 6. Parameters estimated using dadi software for *L. atlanticus* and *P. smaragdina* population pairs (population 1 – population 2). Ni : population size of each population i; Ta : time before Ts at which the change in Na occurred, Ts : time of strict divergence; Tsc : time of divergence with migration, bi : the population i's growth factor; hrf : Hill-Robertson factor; Q : proportion of loci that are under the effect of linked selection (i.e., Hill-Robertson effect); P : proportion of loci that have unconstrained migration; Mij : represents the unrestricted migration rate from the population j towards population i; mij : number of migrants per generations from the population j towards population i (calculated as mij = bi*Nui*Mij /2); meij : the restricted migration rate (e.g., barrier loci) from population j towards population i. Times are expressed in years. 28

List of Figures

Figure 1. (A) Sampling maps of *Desmophyllum pertusum* (*Lophelia pertusa*) and *Madrepora oculata* at the Ocean Atlantic scale. (A) sampling of both species with colours representing the main geographic regions and point shapes (square vs triangle) the species. Maps (B) and (C) display the fine scale sampling of *D. pertusum* and *M. oculata*, respectively. Colour points represent localities and small yellow spots record the known occurrence for each species in (B) and (C). 18

Figure 2. Connectivity map obtained by larval dispersal simulations for the seep mussels as extracted from Portanier et al. (2023). Red and purple colours represent the seep localities from which larvae have been emitted (NE: New England seeps, NO: Norfolk Canyon, BC: Baltimore Canyon, BI: Bodie Island, NR1: Brine Pool; AC: Alaminos Canyon, LS: Louisiana Slope, KeJ: Kick'em Jenny volcano, TRI: Trinidad El Pilar seeps, AM: Amazon fan, SP and SPD: Sao Paulo seeps, LOST: Lost City seeps, LOG: Logachev seeps, CA: Darwin volcano in Gulf of Cadiz, SWIM,

ARG: Arguin Bank, CS: Cadamostro Seamount, NIG: Nigerian slope, WAM: West African margin seeps, GUIN: Regab seeps). Polygons in blue represent the main recipient zones for the larval settlement (NE Atlantic: North East Atlantic, NWAM: North western African Margin, US margin: Northeast US coast, GoM: Gulf of Mexico, NMAR: North MAR, MMAR: Mid MAR, SMAR: South MAR). Black arrows correspond to larval fluxes as a proportion of the total number of larvae emitted from a given locality. 20

Figure 3. Pathways of migration for the cold seep complex of mussel species *B. boomerang*/*B. heckerae.* (A) PCA plot of mussel individuals based on their allelic frequencies at the genome scale (KeJ= Barbados accretionary Prism, FE= Florida Escarpment, BR=Blake Ridge and REG= Regab (Gulf of Guinea), (B) Admixture graph of mussel individuals showing three distinct genetic units (FE: *B. heckerae* from Florida Escarpment, KeJ: *B. boomerang* from the Barbados accretionary Prism and Regab: *B. boomerang* from the Gulf of Guinea) with all the individuals of Blake Ridge (BR) and the individual from the Norfolk Canyon (NO) having a boomerang genetic background introgressed by heckerae alleles. (C) Connectivity map showing strong oriented present-days gene flow from both FE and KeJ to BR as obtained from dadi under a population model of secondary contact (SC). 22

Figure 4. Pathways of migration for the cold seep complex of mussel species *G. childressi*/*G. mauritanicus*. (A) PCA plot of mussel individuals based on their allelic frequencies at the genome scale: arrows indicate intermediate individuals between G. childressi (Northeast US Canyons or Gulf of Mexico) and G. mauritanicus from the Barbados accretionary Prism (KeJ), (B) Admixture graph of mussel individuals showing four distinct genetic units (GoM: *G. childressi* from the Gulf of Mexico (ALA: Alaminos C., GRC: Green C., MIS: Mississippi C. and BRP: Brine Pool), US Canyons: *G. childressi* from the Northeast US Canyons (BAL: Baltimore C., CHI: Chincoteague C., NWE: New England seeps, NOR: Norfolk C., SHA: Shallop C., VEA: Veatch C.), KeJ/Barbados: *G. mauritanicus* from the Barbados accretionary Prism and Cadiz: *G. mauritanicus* from the Gulf of Cadiz) with some individuals of the Northeast US Canyons (CHI: Chincoteague and NWE: New England) being hybrids of first or second generation (arrows). (C) Connectivity map showing strong oriented present-days gene flow from both GoM and KeJ to the Northeast US canyons as obtained from dadi under a population model of secondary contact (SC). 24

Figure 5. Past-to-recent oriented gene flows estimated between the seep mussel populations with the Fst-derived method of DivMigrate for (A) *B. boomerang/B. heckerae* and (B) for *G. childressi/G. mauritanicus.* 25

Figure 6. Haplotype networks for the A) *Lepetodrilus atlanticus* and B) *Peltospira smaragdina* species. 26

Figure 7. PCA performed on the SNPs datasets for A) *Lepetodrilus atlanticus* with three distinct geographic isolates and B) *Peltospira smaragdina* with the detection of a continuum of intermediate individuals between two of the three main genetic units (red/yellow vs turquoise points) at Rainbow. 26

Figure 8. ADMIXTURE analyses performed on the SNPs datasets for A) *Lepetodrilus atlanticus* and B) *Peltospira smaragdina*. In both species, populations are separated into three genetic groups (in blue, yellow and green for *L. atlanticus*, and in dark blue, turquoise and yellow for *P. smaragdina*. The admixture graph of *P. smaragdina* clearly shows the presence of F1, F2 and admixed individuals together with the two parental types at Rainbow. 27

Figure 9. Number of migrants per generation (i.e. one year) as estimated by dadi for A) *Lepetodrilus atlanticus* and B) *Peltospira smaragdina* species. NB: these parameters are converted values (number of migrants here = $m_{ij}*b_i*nu_i/2$) and thus depends on other estimated values (nu_i, b_i). The information they give may differ from the information translated by unconverted values shown in Table 6. 29

Figure 11. PCA graph on the shared SNP dataset (2,381 bi-allelic loci) between *Rimicaris chacei* sampled along the Mid-Atlantic Ridge and *Rimicaris hybisae* (Rhyb: in green) sampled on the Cayman

Ridge at the Beebe site. Genetic divergence between the two shrimp species is within the expected genetic variation found within a given species (less than 1% of genetic differentiation) but *R. chacei* populations are not differentiated along the North MAR. 30
Figure 12. Past-to-recent dispersal pathways obtained from the vent shrimp complex of species *R. chacei/R. hybisae* using both the DivMigrate (A) and dadi (B) software. The population model selected by dadi (best fit to the genomic data) is the secondary contact (SC) model with a recent T_{SC}. 31
Figure 13. IMa3 estimates for (A) population splitting times, (B) population sizes and (C) migration rates for the four mitochondrial lineages of vent mussels with pop0=Golden Valley (5°S), pop1= azoricus (35°N), pop2= Lilliput (9°S) and pop3= puteoserpentis (14°N) and the mt genome reference Newick tree: (((0,3),2),1) 34
Figure 14. Past-to-recent dispersal pathways obtained from the vent mussel complex of species *B. azoricus/B. puteoserpentis* using the IMa3 software. 34
Figure 15. Genetic structure of the vent mussels along the Mid-Atlantic Ridge. (A) PCA and (B) Admixture analysis (Structure 2.3.4. With K=2) performed on the SNPs dataset of *Bathymodiolus azoricus* and *B. puteoserpentis* focusing on the hybrid zone located at Broken Spur (29°N)..... 35
Figure 16. (a) Principal component analysis with the first two components for *D. pertusum*. Colour represents localities and each point represents an individual. (b) Identity-by-states (IBS) dendrogram or similarity between samples. Each leaf represents one individual. (c) Plots of admixture for K = 3, where individuals are clustered by localities. Each colour bar represents the proportion of the genetic ancestry for each of the inferred clusters. 38
Figure 17. Heatmap and clustering of the estimated net nucleotide divergence (Da) between European lineages for *D. pertusum*. 38
Figure 18. Connectivity map obtained with the software Moments under the best population model of secondary contact. Gene flows are estimated in terms of number of migrants exchanged between three main geographic areas (Celtic Sea, Bay of Biscay and Mediterranean Sea) indicating the presence of two migration routes: one exporting larvae outside the Mediterranean Sea up to the Celtic Sea and the other one moving down from the Celtic Sea to the Bay of Biscay along the European continental margin. 39
Figure 19. (a) Principal component analysis with the first two components for *M. oculata*. Colour represents localities and each point represents an individual. (b) Identity-by-states dendrogram or similarity between samples. Each leaf represents one individual. (c) Plots of admixture for K = 4 to 7, where individuals are clustered by localities. Each colour bar represents the proportion of the genetic ancestry for each of the inferred clusters. 40
Figure 20. Heatmap and clustering of the net nucleotide divergence (Da) between European margins geographic localities for *M. oculata*..... 41
Figure 21. Principal component analysis (PCA) with first six components for *D. pertusum* with West (US margins) and South (Brazilian and South Africa) Atlantic samples. (A) Bar plot of the first 32 principal components and their proportion of variance explained. (B) PCA for the first two components. (C) PCA for the third and fourth components. (D) PCA for the fifth and sixth components. Colour represents localities and each point represents an individual..... 42
Figure 22. Principal component analysis (PCA) with first six components for *M. oculata* with West (US margins), South (Brazilian) Atlantic and Pacific samples. (A) Bar plot of the first 32 principal components and their proportion of variance explained. (B) PCA for the first two components. (C) PCA for the third and fourth components. (D) PCA for the fifth and sixth components. Colour represents localities and each point represents an individual. 43
Figure 23. Dendrogram plots of genomic similarity between individual estimated with Identity By State for *M. oculata* samples. (A) Colour represents localities. (B) Colour represents species..... 44

Executive summary

Over the course of the iAtlantic project, more than 5 Tb of genomic data were obtained to study the sequence polymorphism of 10 species or species complexes (cold-water corals, vent and seep molluscs, vent shrimp) on a genome-wide scale. These data have been used in population genetics to assess the degree of past and present gene flows between a series of populations at the scale of the Atlantic Ocean, coupling it for certain species (cold seep mussels) with large-scale larval dispersal modelling. Genetic analyses have enabled connectivity maps to be drawn up for all species, establishing past and present preferential migration routes between Atlantic regions. This information is of vital importance in conservation biology and may help in the development of sustainable management tools for deep-sea benthic communities living in fragmented and locally unstable environments. The studied deep-sea species tend to be distributed in geographic isolates, possibly linked by rare and sporadic migration events on a global scale. These species also have complex demographic histories, giving rise to cryptic species complexes that can hybridise locally following secondary contacts. Isolation by distance and the establishment of hydrographic and genetic barriers up to the closing of the Panama seaway has resulted in the regionalisation of most deep-sea species, a fact that must be considered in the current and future exploitation of biological and mineral resources from the deep ocean. The main findings of this work are:

- (1) The hydrothermal vent species along the Mid-Atlantic Ridge (with the exception of Bresiliid shrimp) are distributed in different genetic units that do not exchange much along the ridge axis due to both physical and genetic barriers. These genetic units need to be managed locally, taking into account the genetic information obtained at a regional scale.
- (2) The Atlantic seep mussels are geographically structured at the scale of the Atlantic Ocean with some rare events of long-distance migration. This structure is explained by the demographic history of species. Secondary contacts are probably linked with the closing of the Panama Seaway. However, long-distance migration events are not able to ensure the genetic homogenisation of populations, possibly due to the emergence of genetic barriers.
- (3) Cold-water corals are more genetically structured than previously thought with the co-occurrence of several cryptic species in *Madrepora oculata* at the scale of the Northeastern Atlantic, and the presence of several distinct populations within *Desmophyllum pertusum* at the scale of the whole Atlantic.

1. Introduction

Taxonomic analyses of deep-sea fauna occurring at abyssal depths (>2,000 m depth) has revealed the genetic variability between deep-sea populations, which cluster by broad geographic regions. (Wilson & Hessler 1987, White 1988, Grassle 1989, Rex et al. 1993). Formerly, this clustering was often explained by the depth and geographic extent of the abyssal plains, their partitioning into oceanic basins, and the often-reduced dispersal capacities of the species found there, such as isopod, amphipod and peracarid crustaceans (France et al. 1991, Brandt et al. 2012, Blazewicz-Paszkowycz et al. 2012, Chan et al. 2020), as well as molluscs and annelids (Puillandre et al. 2010, Brazier et al. 2016). The abyssal environment was also previously understood to be a stable and homogeneous environment, relying on trophic fallout from the upper layers of the ocean (Dayton & Hessler 1972) across great distances from which communities slowly diverged according to geography.

However, subsequent studies have shown that the deep seafloor is not as homogeneous as previously understood with a variety of substrata and some local temporal instability (Levin et al. 2001). The discovery of more specialised abyssal communities grouped in underwater oases mostly dependent on specific environmental conditions (hydrothermal vents, seeps, whale carcasses, cold-water coral reefs) has definitively undermined this paradigm of habitat homogeneity and stability by showing just how fragmented and temporally unstable deep-sea environments can be (Ramirez-Llodra et al. 2010).

In the context of habitat variability, the search for a favourable habitat to settle and reproduce can represent a big challenge for species with benthopelagic life cycles, for which the dispersal phase occurs as a larva. Regarding a fragmented and potentially unstable environment, the theory of metapopulations predicts that long-distance dispersal should be favoured to avoid inbreeding and to compensate for the local extinction of certain populations (Hamilton & May 1977, Levin et al. 1984, McPeek & Holt 1992). However, the resilience of a species depends also on its ability to both (re)colonise empty habitats and replenish source populations. Therefore, resilience also depends on the probability of individuals to be able to establish themselves and have offspring out of the total number of propagules released in the water-column (Chevaldonné et al. 1997). This can lead to alternative or mixed dispersal strategies that mainly depend on the dynamics and the carrying capacity of the environment itself for a given species (McPeek & Holt 1992, Doebeli & Ruxton 1997). These strategies have strong consequences on the genetic structure of species and/or the formation of new species. Over the past two decades, increasing evidence has been uncovered from genomic and barcode datasets to highlight that deep-sea species are much more genetically diversified than previously thought. Numerous cryptic species have formed in allopatry due to tectonism (Plouviez et al. 2009, Johnson et al. 2016, Matabos & Jollivet 2019, Breusing et al. 2020, Poitrimol et al. 2023, Tran Lu Y et al. 2023, in prep), depth, or the insularity of some habitats (Castelin et al. 2012, Jennings et al. 2013, Rogacheva et al. 2013). These species may secondarily meet again to produce species ranges superimposition or hybrid zones (Faure et al. 2009, Johnson et al. 2013, Taboada et al. 2022, Paulus et al. 2022, Castel et al. 2023).

Assessing genetic variability of species from genomic analyses over their range now makes it possible to trace back their demographic history and identify the dispersal patterns that led to their current distribution (Gagnaire et al. 2016). Fitting single nucleotide polymorphism (SNP) frequency spectra onto specific demogenetic models gives promising results in terms of estimating past and present-days gene flows and the time elapsed since the genetic exchanges were ceased or reactivated (Gagnaire et al. 2016, Cayuela et al. 2018, Gagnaire 2020). The information on genetic variation carried by the genome

is sufficiently robust to identify the origin of first- and second-generation migrants or hybrids (Nussberger et al. 2013), which have established themselves in a given population. From this, it is possible to infer present-days exchanges between the sampled populations, providing that they differ to some extent (Wilson & Rannala 2003, Huisman 2017). These newly developed methods have been shown to be useful to determine patterns of dispersal and colonisation pathways. These methods are particularly well-suited for the marine fauna (Gagnaire et al. 2016, 2018, Rougeux et al. 2019, Gagnaire 2020, Tran Lu Y et al. 2023, in prep) for which tracking larvae still remains difficult (but see: Mouchi et al. 2023). This approach can be used to detect putative long-distance migrants in a given population, and their impact in the replenishment of populations. For deep-sea fauna, many questions remain unanswered regarding (i) the degree of exchanges between populations in a species range, (ii) the identification of source populations for other populations replenishment and (iii) the larval dispersal strategies (lecithotrophy vs. planktotrophy, long-range vs. short-range dispersal) that have been adopted by species to optimise their resilience in a given marine landscape.

Previous studies on Atlantic seep fauna and cold-water reef corals suggest that these species could disperse long-distances and may eventually be able to exchange larvae between active margin faunas on both sides of the North Atlantic Ocean. For cold seep fauna, this hypothesis was proposed because of the absence of genetic differentiation observed between them with the use of classical genetic markers such as *Cox1* or microsatellites (Andersen et al. 2004, Olu-LeRoy et al. 2007, Hilario et al. 2011, Teixeira et al. 2013, LaBella et al. 2017). A similar idea was proposed by Boavida et al. (2019) and Gary et al. (2020) for cold-water framework-forming corals *Desmophylum pertusum* (also referred to as *Lophelia pertusa)* situated along the European continental slope on the Atlantic and the Mediterranean Sea (although a differentiation between basins was demonstrated in the case of *D. pertusum*), but not for another reef coral *Madrepora oculata*, which appears much more geographically structured. Similar studies have been performed for hydrothermal vent species along the Mid-Atlantic Ridge. For some species, panmixia over several thousands of kilometres was suggested (i.e. shrimps, Teixeira et al. 2012, *Shinkailepas*, Yahagi et al. 2019), questioning the hypothesis of the lack of physical barriers to dispersal for this fauna. The presence of divergent geographic lineages, possibly cryptic species was however detected for the hydrothermal vent mussels between vent sites of both the northern and southern parts of the ridge (i.e. *Bathymodiolus* sp., van der Heijden et al. 2012, Breusing et al. 2016).

Focusing on the MAR, a comparative approach of several iconic species must be implemented to get a picture of larval dispersal along the ridge. Gastropods are pioneer species in ecological successions, being one of the first to colonise newly-formed hydrothermal vents or to recolonise them after disturbance (Mullineaux et al. 2010, Bayer et al. 2011, Marticorena et al. 2021, Sarrazin et al. 2022), and thus should be compared with shrimps and mussels using the same kind of genomic markers. Gastropods are thought to play an important role in the functioning and resilience of hydrothermal ecosystems (Sarrazin et al. 2022). While *L. atlanticus* has recently been listed as 'Least Concern' on the Vent Red List for molluscs, *Peltospira smaragdina* is listed as 'Near Threatened' (Thomas et al. 2021). Therefore, it is important to determine if several genetic groups exist and the extent to what they are connected. In addition, the comparative approach between species could help disentangle the role played by demographic history, life history traits and environmental factors (water chemistry or depth characteristics of sampled vent fields) in shaping genetic connectivity.

To date, these analyses have not been sensitive enough to assess with accuracy the relative parts of the demographic history and present-days exchanges across and along the continental slopes of the Atlantic Ocean. As such a coupling between high resolution studies of present-days population

connectivity through genome-wide genetic approaches and 'large-scale' modelling of larval dispersal at different depths based on our knowledge of the biology and ecology of the same species, offers particularly promising prospects (Breusing et al. 2016; 2023). Larval dispersal modelling by simulating Lagrangian trajectories of particles can be used to test the hypothesis of a long-distance migration that can ensure efficient exchanges between seep mussel beds or cold-water coral reefs of the American, European and African margins, or along oceanic ridges. While such approaches have been widely used in coastal waters (Pineda et al. 2007, Nicolle et al. 2017, Ayata et al. 2018, Handal et al. 2020) they remain quite rare at the scale of an ocean. Larval dispersal simulations have been performed at the scale of the North Atlantic oceanographic model VIKING20X to explore the putative routes of migration for deep fauna, including cold-water coral species (Gary et al. 2020). Such an approach was used to estimate population connectivity of hydrothermal vent sites along the Mid-Atlantic Ridge with and without genetic validation (Breusing et al. 2016, Yearsley et al. 2020). However, most of these predictions were validated by genetic data at the genome scale over a multiple species approach.

The Atlantic Ocean monitoring program through the H2020 iAtlantic project has developed such a modelling-genetic coupling through the use of the VIKING10/20 and INALT10/20 ocean circulation models developed by the GEOMAR partner (Kiel, Germany) and the production of individual genomic libraries targeting cold seep mussels from the American, African and European active margins by the SU partner (Roscoff, France). This novel work was for the first time made possible by collecting and barcoding nearly all currently available seep mussel collections that have been obtained by European and American deep-sea researchers (i.e. C. L. Van Dover (Duke University), C. M. Young (Oregon Institute of Marine Biology), E. Cordes (TEMPLE University), C. L. Morrison (US Geological Survey), M. R. Cunha (Aveiro University), K. Olu-LeRoy (IFREMER) over the last two decades. This first step enabled the visualisation and assessment of the pertinence of contemporary exchange pathways between the main cold seepage areas discovered so far. The existence of these larval-dispersal corridors was then validated or invalidated by genetic data from populations living in the same areas by population genomics analyses. This part of the work is presented herein and has been already published in Frontiers in Marine Science (Portanier et al. 2023) together with some connectivity maps that are now archived in PANGAEA (Jollivet et al. 2023a).

Genomic analyses were also performed on hydrothermal vent fauna along the Mid-Atlantic Ridge by barcoding and genotyping several hundreds of gastropods (*Peltospira smaragdina* and *Lepetodrilus atlanticus*), mussels (*B. azoricus* and *B. puteoserpentis*) and shrimps (*Rimicaris exoculata* and *R. chacei*). We therefore combined high-throughput double-digest Restriction-site Associated DNA sequencing (ddRADseq) with population genetics and demographic inferences approaches. We relied on a comprehensive sampling scheme encompassing a large spatial scale, from the south of the MAR (5°S) to the northernmost site of Moytirra (45°N), representative of the known distribution range for the 'classical' vent fauna (Sarrazin et al. 2022). Such an approach was also performed on cold-water reef corals found in canyons along both the American and European Atlantic margins by using Whole Genome Sequencing (WGS) using collections previously sampled during the European Union ATLAS project (2016-2020), and completed with additional ones coming from Brazilian waters and the Gulf of Mexico from a joint effort of IFREMER (MARBEC) with several US and Brazilian Institutes (i.e. M.V. Kitahara (University of Sao Paulo), C.L. Morrison (US Geological Survey) and Santiago Herrera (Lehigh University). This provided new ways to investigate whether previous larval dispersal modelling predictions were correct and reliable (Breusing et al. 2016, Yearsley et al. 2020, Gary et al. 2020) and

could be used as a tool for the preservation of marine life in the face of deep-sea mining and climate change.

This Deliverable Report presents results of the larval dispersal modelling and genomic works that have been done so far by the partners SU, IFREMER and CNRS to contribute to our knowledge of the past-to-recent dispersal pathways that shape the present-days distribution of emblematic species of deep-sea fauna.

2. Materials & Methods

Source of specimens

A comprehensive genomic survey of several deep-sea benthic species was performed using either ddRAD or WGS sequencing of hundreds of individuals for each species. Collections of seep mussels were obtained by SU on both sides of the North Atlantic (Barbados, GoM, Northeast US coast, Gulf of Cadiz and Gulf of Congo) from a Consortium of deep-sea researchers (i.e. C. L. Van Dover (Duke University), C. M. Young (Oregon Institute of Marine Biology), E. Cordes (TEMPLE University), C. L. Morrison (US Geological Survey), M. R. Cunha (Aveiro University), K. Olu-LeRoy (IFREMER)). Collections of vent gastropods, shrimps and mussels were obtained on the North Mid-Atlantic Ridge between 5°S to 45°N depending on the species from several oceanographic cruises (Momareto, 2007, chief scientist P.M. Sarradin; Biobaz, 2013, chief scientist F. Lallier; Momarsat, 2016 and 2019, chief scientist P.M. Sarradin; Bicose1 2014 and Bicose2 2018, chief scientist M.A. Cambon-Bonavita; Transect 2018, chief scientist N. LeBris; the VENTuRE Survey 2011 (A. Wheeler) and RV Meteor M78/2 2009, chief scientist R. Seifert). Cold-water coral samples of *D. pertusum* and *M. oculata* came primarily from the IFREMER collections from the Northeastern Atlantic and Mediterranean: most samples came from collections initiated during the CoralFISH EU project BobGeo (2009), CE0908 (2009) and BobEco (2011) cruises (Mission chiefs Jean-François Bourillet, Anthony Grehan and Sophie Arnaud-Haond), MAGIC (2010; mission chief Alexandra Savini) and IceCTD (2012; mission chiefs Norbert Franck and Sophie Arnaud-Haond), and ATLAS EU project's Medwaves expedition (Mission chief Covadonga Oreja) and IFREMER Mediterranean surveys (cruises Videocor 20017, Caladu 2018 and Caladu2 2021; mission chief Marie-Claire Fabri). Precious samples from Southern Açores were also collected during the Athena cruise M151 (mission chief Norbert Franck Heidelberg). Samples of *D. pertusum* from North Sea oil platforms collected by industry were supplied by L.-A. Henry (UEDIN). Additional partners cruises contributed with few samples from interesting locations of the North Atlantic: samples from a Sonne cruise So276 (Saskia Bricks) and from Sweden (Ann Larsson). An important contribution of iAtlantic to this large dataset was the ability to collaborate more broadly to better understand the phylogeography of these species. S. Arnaud-Haond and ATLAS/iAtlantic coordinator J. M. Roberts initiated a collaboration with members of the cold-water coral (CWC) research community during. Ricardo Tomas Pereyra Ortega (Univ. of Goteborg) shared genome sequences obtained in Sweden, and Marcelo Kitahara (University of Sao Paulo) from Brazil. An additional collaborative effort was finally funded and planned during the 8th International Symposium of Deep-Sea Corals (8 ISDSC) in Early June 2023, with US and Brazil was added, thanks to additional iAtlantic funds derived from the non-use of the ROV Luso budget to extend the dataset to a pan Atlantic scale. Data were thus obtained from the Brazilian, South African and Gulf of Mexico waters with several US Institutes , C.L. Morrison (US Geological Survey) and Santiago Herrera (Lehigh University)

Vent and seep invertebrates

Most of the molecular methods presented in this report for seep mussels are similar between all the vent and seep species studied by the SU partner which also include the vent gastropods (*P. smaragdina*

and *L. atlanticus*) and the shrimp *Rimicaris* spp. Deep corals were studied following the WGS technology that uses a different bioinformatic suite of analyses which is presented here as a second paragraph in the Materials & Methods.

Genomic DNA (gDNA) was extracted from frozen or ethanol-preserved whole animals (gastropods) or tissues of pleopods, foot, mantle or gills depending on their preservation state and availability. Extractions were performed using a 2% cetyltrimethylammonium bromide (CTAB)/1% polyvinylpyrrolidone (PVP) protocol following Jolly et al. (2003) for vent and seep mussels or using Macherey-Nagel NucleoSpin Tissue DNA extraction kits for the other vent species (shrimp and limpets), following the supplier recommendations (Macherey-Nagel, Düren, Germany). The mitochondrial cytochrome oxidase subunit 1 (CO1) gene was then amplified using degenerated version of universal-applicable primers (Folmer et al. 1994) for *Bathymodiolus* species and newly derived primers for gastropod species. ddRAD libraries were produced on the same gDNA samples following the protocol detailed in Daguin-Thiébaut et al. (2021). The libraries were sequenced in 150-bp paired-end reads using the Illumina technology on a Novaseq 6000. Number of sequenced individuals are shown in Tables 1, 2, 3 and 4.

Raw reads were demultiplexed using the process_radtags module of Stacks software version 2.52 (Catchen et al. 2013) to remove adapters and reads with low quality scores. The single nucleotide polymorphisms (SNPs) were then identified by Stacks and filtered in R version 4.1.1 (R Core Team, 2021) to keep the SNPs present in at least 90% of the individuals and only keep the individuals which were genotyped for at least 80% of the total number of SNPs. Mitochondrial haplotypes were determined using DnaSP v.6 (Rozas et al. 2017) and used to produce minimum spanning haplotype networks using PopArt v.1.7 (Leigh & Bryant 2015) to visually represent the relationships among haplotypes from different geographic locations within each species complex. For multiloci datasets, genetic interactions of individuals within a given species were visualised using the software Admixture or LEA (Alexander et al. 2009, Zhou et al. 2011) and multivariate analyses such as PCA.

To identify effective migration routes for both the vent mussels belonging to *Bathymodiolus* and the seep mussels of the genera *Gigantidas* and *Bathymodiolus*, we used the IMa3 software (Hey et al. 2018) which implements hierarchical Bayesian, Markov-chain Monte Carlo simulations of gene genealogies under an Isolation with Migration model to estimate splitting times, effective population and migration rates between multiple populations from mitochondrial data. Additionally, we used the software dadi (Gutenkunst et al. 2009) when using SNPs derived from the ddRAD data. This later software implements 28 population models encompassing different demographic scenarios which is highly time-consuming. The full set of simulations to infer strength and orientation of gene flow were thus obtained only for hydrothermal gastropods along the Mid-Atlantic Ridge. For the other species, diffusion approximations for demographic inference (dadi; Gutenkunst et al. 2009 analyses were performed only for the four basic population models (SI, IM, AM & SC with and without population growth). Lastly, the software DivMigrate (Sundqvist et al. 2016) was used to estimate past Fst-derived bidirectional gene flow from the SNP data using the individual genotypes of the bi-allelic loci archived in a Genepop format in PANGAEA (Jollivet et al. 2023b).

Finally, larval dispersal modelling was only performed on the seep mussels using VIKING20X, an updated and expanded version of the VIKING20 ocean general circulation model aiming at hindcast simulations of Atlantic Ocean circulation variability on monthly to multi-decadal timescales. The spatial resolution was sufficient to capture mesoscale processes into subarctic latitudes (see a detailed description in Biastoch et al. 2021). Larval trajectories were modelled with the offline 3D Lagrangian code Parcels v2.0 (Probably A Really Computationally Efficient Lagrangian Simulator) based on the 3D velocities provided by the VIKING20X model. Mussel larvae were released monthly during a unique spawning event that

occurred the first day of each month from November to March during the natural spawning period of *Gigantidas childressi*, from 2014 to 2019 to consider year-to-year variations in current patterns. Biological characteristics of larvae in terms of Planktonic Larval Duration (PLD), behaviour and mortality were defined according to field observations and laboratory experiments performed on *G. childressi* (Arellano *et al.* 2011, 2014*)*.

Deep cold-water corals

Population genomic analyses were performed on *D. pertusum* and *M. oculata* samples from the Mediterranean Sea and North-East Atlantic. These samples were remapped on two high-quality, annotated reference genomes (one for *D. pertusum*/*L. pertusa* and one for *M. oculata*) assembled by Genoscope of Evry (project eDNAbyss, France Génomique 2017-2021) at the end of 2021 (sequencing) and early 2022 (annotation), resulting in 626 and 1,325 contigs for *D. pertusum* and *M. oculata* respectively. More recently, data from colleagues in Eastern Atlantic (Brazil and US coasts) were added for both species, in order to obtain a better pan-Atlantic picture.

Samples preparation

European scale

For the European Atlantic coast and the Mediterranean Sea, 91 samples of *D. pertusum* and 83 samples of *Madrepora oculata* were used for WGS analysis (Figure 1, Table 5).

Whole Genome resequencing (shotgun) libraries were produced in late 2022 for the European samples with a targeted coverage of 30X per sample. The whole *D. pertusum* libraries for EU samples were produced by the company Genotoul (Toulouse[1]) and *M. oculata* at Integragen (Evry[2]), in both case funded by national projects ("*Pourquoi Pas les Abysses*", IFREMER 2017-2021 and Clonix 2D, ANR-18-CE32-0001, respectively). Libraries were sequenced on a Novaseq sequencer (150 pb paired-end reads). The raw data for these WG sequencing libraries were obtained in early to mid-January 2023. For European samples, technical replicates (the same DNA sample sequenced twice) and few biological replicates (different polyps from the same colony and different colony displaying the same genotype) were included in the sequencing effort to ensure and assess possible technical, sequencing errors and to assess clonality effect on next-generation sequencing (NGS) data.

Pan-Atlantic scale

The collaborations mentioned above have allowed gathering a pan-Atlantic consortium to expand our European scale to a Pan-Atlantic scale to provide a first comprehensive view of the genetic divergence of these species. This added 59 samples from Brazil, 3 from South Africa, 16 from the Northwestern Atlantic and 8 from Gulf of Mexico for *D. pertusum*. In addition, 6 samples from Brazil, 5 from Pacific Ocean and 7 from Gulf of Mexico were also processed for *Madrepora*. (See Figure 1, Table 5). WGS libraries for Brazilian and African samples were produced by our Brazilian collaborator (Dr M.V. Kithara) using extra-funding from iAtlantic while libraries for US coast samples were produced by Genohub (US) thanks to a collaborative effort (US, IFREMER/CNRS). As European samples, these libraires were sequenced using a Novaseq sequencer (150 pb paired end reads) and raw data were obtained in mid-July 2023 for Brazilian and African samples and mid-August 2023 for US samples.

Mapping & calling

Raw read quality was assessed with FastQC (v0.11.9) prior to the mapping and assembly. Raw reads were pre-processed with fastp (v.0.23.4) and trimmomatic (V.0.36) to filter Adapter content and trim

[1] https://www.genotoul.fr
[2] https://integragen.com/fr

the first 10 base pairs. Pre-processed reads were mapped to the reference genome using BWA-MEM2 (v2.2.1) with default settings. The resulting individual samples SAM files were sorted and transformed with SortSam (Picard v2.21.1), duplicate reads were marked with MarkDuplicates (Picard v2.21.1), and individual sample information was then added using AddOrReplaceReadGroups (Picard v2.21.1). The mapping quality was assessed using samtools (v1.9). Variant calling was performed using the caller BCFTOOL mpileup (v1.13) with default settings.

Data filtering

A first Variant Call Format (VCF) file (dataset) was generated with only European samples independently for both species with different stages of filtering to minimise erroneous SNPs and the effect of missing data. For *D. pertusum*, the filtering steps were realised with VCFTOOLS (v.0.1.16) to minimise the effect of low-quality variants and missing data, with the following arguments (--minDP 5, --min quality 40, --mean DP 10, max missingness per variant and individual at 25% and then max missingness per variant at 10%). We excluded indels and kept only bi-allelic variants in the dataset. We then kept only one variant per 1,000 base pairs (--thin 1,000) to minimise the effect of linkage disequilibrium. To minimise the effect of clonal replicates on downstream population genetics analysis, we also excluded clonal samples and technical replicates. Similarly, the *Madrepora* dataset was filtered with the same approach and slightly different parameters (--minDP 5, --min quality 40, --meanDP10_40, max variant and individual missingness at 25%, only bi-allelic variants, removed clones and technical replicates and --thin 1,000).

Population analyses

The contemporary genetic population structure for both species was examined using several approaches and methods. Principal Component Analysis (PCA) with SNPrelate (v1.32.2: Zheng et al. 2012) was performed to explore the signal of structuration without prior. Ancestry proportion and admixture analyses were performed using Admixture (v.1.3.0). Individual genetic relatedness was estimated by using the Identity-by-State (IBS) between pairs of individuals with SNPrelate (v1.32.2). Additional analyses such as *f3* statistic and Treemix were also used to investigate introgression and admixture between populations (Pickrell & Pritchard 2012). Pairwise F_{st} and F_{is} per locality was assessed with snpR (v1.2.8.0). Windowed differentiation statistics along the genome, including Fst, (Raw nucleotide divergence) dxy, and nucleotide diversity (π), per lineages or population, was calculated with the python scripts from 'Genomics_general'[3]. Preliminary demo-genetic inferences were performed with the software moments (v.1.1.15: Jouganous et al. 2017) with four basic models (SI, IM, AM and SC) only for *Desmophyllum pertusum*.

3. Results

Seep mussels

Both larval dispersal modelling and genetic data were used to examine efficient larval exchange pathways across the Atlantic in the two main species complexes of deep-sea mussels exploiting these hydrocarbon/methane seeps, namely: *Bathymodiolus heckerae*, *B. boomerang* and *Gigantidas childressi*, G. *mauritanicus*. Simulations of larval dispersal were carried out on 20 localities distributed on both sides of the Atlantic based on a pelagic larval duration (PLD) of one year with the progressive ascent of larvae in the surface layer until they reach the thermocline (around a depth of 200 m). These dispersal simulations showed possible present-days exchanges at the latitude of the Atlantic equatorial belt (Figure 2). These dispersal results agree with mitochondrial data, which were used to barcode individuals (*mtCox1*). In particular, genetic data supports the probable arrival of migrants on the

[3] https://github.com/simonhmartin/genomics_general

Nigerian coast from seeps of the Barbados accretion prism in the species *B. boomerang*, and the recent connection of *G. childressi* and *G. mauritanicus* across the Caribbean Sea (three *mauritanicus* migrants sampled there) and a possible old corridor of larval exchanges with Europe at the level of the north-eastern overturning loop of the AMOC. Conversely, the mitochondrial data unexpectedly refute the existence of exchanges between the Barbados accretionary prism and the Gulf of Mexico, despite the incoming flow of larvae predicted by the physical models of water-mass circulation. A similar discrepancy between the two methods was also found along the African coasts where a lack of larval transport associated with the dispersal model is invalidated by the genetic data. As part of these results, a paper has been published in Frontiers in Marine Science in a special iAtlantic issue (Portanier et al. 2023). All genetic data and larval dispersal simulations over 20 localities and 25 dates have been archived in Geonode and PANGAEA (Jollivet et al. 2023a) and sequences have been archived in a European Nucleotide Archive (ENA) repository.

Table 1. Number of individual genomic (ddRAD) libraries which are eligible for population genomics studies with more than one million usable reads for SNP detection in *B. boomerang/heckerae*. Barcoded individuals used in the IMa3 analysis corresponded to the same individuals. Listed names represent seep localities. All information concerning geographic coordinates and depth of samples are provided in Portanier *et al.* (2023) and in PANGAEA (Jollivet et al. 2023a,b[4]).

	B. boomerang	*B. heckerae*	Total
Blake Ridge		26	26
Florida Escarpment		19	19
Kick'em Jenny (KeJ) volcano -Barbados	12		12
Nigeria Slope	12	18	30
Norfolk Canyon		1	1
Regab seeps (Gulf of Congo)	88		88
Total	**112**	**64**	**176**

Table 2. Number of individual genomic (ddRAD) libraries which are eligible for population genomics studies with more than one million usable reads for SNP detection in *G. childressi/mauritanicus*. Barcoded individuals used in the IMa3 analysis corresponded to the same individuals. Listed names represent seep localities. All information concerning geographic coordinates and depth of samples are provided in Portanier et al. (2023) and in PANGAEA (Jollivet et al. 2023a,b[5]).

	G. childressi	*G. mauritanicus*	Total
Alaminos Canyon	16		16
Baltimore Canyon	36		36
Barbados Prism		13	13

[4] https://doi.org/10.1594/PANGAEA.961199, https://doi.org/10.1594/PANGAEA.955455
[5] https://doi.org/10.1594/PANGAEA.961199, https://doi.org/10.1594/PANGAEA.955455

	G. childressi	*G. mauritanicus*	Total
Gulf of Cadiz		40	40
Chincoteague Canyon	52		52
Green Canyon	25		25
Kick'em Jenny volcano		23	23
Mississippi Canyon	22		22
New England Seeps	20	2	22
Nigeria Slope		8	8
Norfolk Canyon	29		29
NR-1 Brine Pool	27		27
Shallop Canyon	17		17
Veatch Canyon	26		26
Total	**270**	**86**	**356**

Table 3. Sub-sample of barcoded individuals of *P. smaragdina* and *L. atlanticus* for the mtDNA analyses. Listed names represent vent sites along the Mid-Atlantic Ridge. All information concerning geographic coordinates and depth of samples are provided in PANGAEA (Jollivet et al. 2023a[6]).

	P. smaragdina	*L. atlanticus*	Total
Moytirra (45°N)	8		8
Menez Gwen (37°N)		5	5
Lucky Strike (37°N)	14	8	22
Rainbow (35°N)	25	8	33
Broken Spur (29°N)	8	7	15
TAG (26°N)	8		8
Snake Pit (23°N)	12		12
Golden Valley (5°S)		6	6
Total	75	34	109

[6] https://doi.org/10.1594/PANGAEA.961199

Table 4. Number of individual genomic (ddRAD) libraries which are eligible for population genomics studies with more than 1 million usable reads for SNP detection in hydrothermal vent invertebrates. Listed names represent vent sites along the Mid-Atlantic Ridge and Cayman Ridge. All information concerning geographic coordinates and depth of samples are provided in PANGAEA (Jollivet et al. 2023a[7]).

	P. smaragdina	*L. atlanticus*	*R. exoculata*	*R. chacei/hybisae*	Total
Moytirra (45°N)	26				26
Menez Gwen (37°N)		28			28
Lucky Strike (37°N)	28	22		19	69
Rainbow (35°N)	25	16	26	2	69
Broken Spur (29°N)	43	25	18	27	113
TAG (26°N)	42		23	32	97
Snake Pit (23°N)	43		22	30	95
Logachev (14°N)			26		26
Golden Valley (5°S)		24			24
Beebe (Cayman)				23	23
Total	207	115	115	133	570

[7] https://doi.org/10.1594/PANGAEA.961199

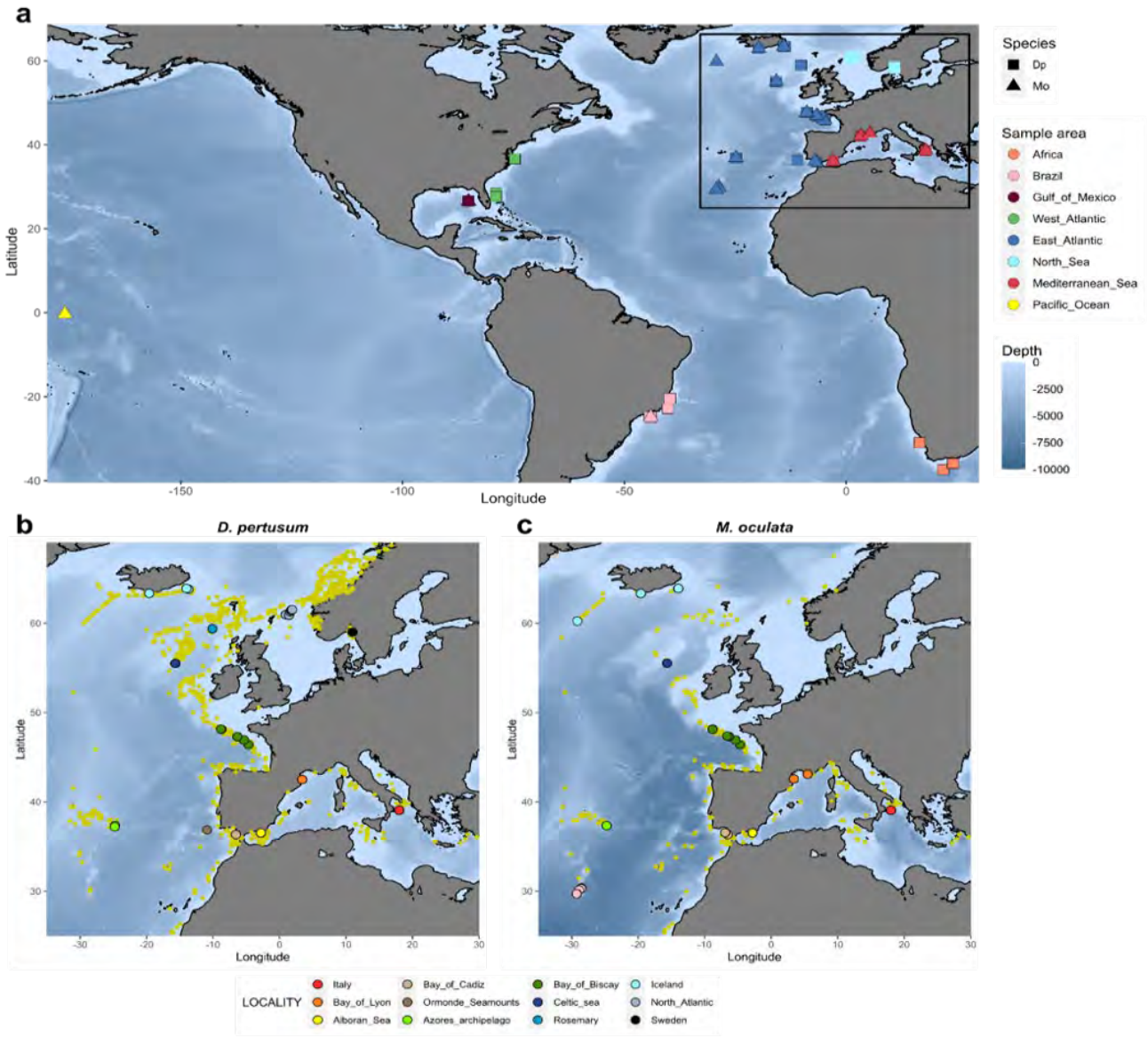

Figure 1. (A) Sampling maps of *Desmophyllum pertusum (Lophelia pertusa)* and *Madrepora oculata* at the Ocean Atlantic scale. (A) sampling of both species with colours representing the main geographic regions and point shapes (square vs triangle) the species. Maps (B) and (C) display the fine scale sampling of *D. pertusum* and *M. oculata*, respectively. Colour points represent localities and small yellow spots record the known occurrence for each species in (B) and (C).

Table 5. Number of individual WGS libraries obtained for the deep corals *D. pertusum* and *M. oculata*. *: three distinct localities. Geographic positions of samples are illustrated in Figure 1 and available in Appendices 1 and 2.

Basin	Locality	Coordinates	*D. pertusum (N)*	*M. oculata (N)*
West Atlantic	Norfolk Canyon	37.09/74.55	7	
West Atlantic	Canaveral	28.11/78.78	9	
Azorean archipelago	Meteor	29.74 to 30.36		7
		-28.53 to -29.26		3
	Formigas	37.34/-27.74	3	
Bay of Biscay	Croisic Canyon	46.38/-4.68	2	4
	Guivinec Canyon	46.93/-5.36	1	3
	Morgat Canyon	47.32/-6.35	3	5
	Petite Sole	48.12/-8.80	8	6
Bay of Cadiz	Mud volcano	36.56/-6.93	1	7
Celtic Sea	Logachev	55.52/-15.65	8	5
Iceland	Londsjup	63.87/-14.00	3	3
	Hafadjup	63.34/-19.60	2	3
	Ormonde Seamounts	63.34/-19.60	1	1
Atlantic	Rockall	-59.40/-10.10	6	
Mediterranean Sea	Bay of Lyon	42.55/3.41	4	6
		43.11/5.46		6
Mediterranean Sea	Santa Maria di Leuca (Italy)	39.06/18.01	4	8
Mediterranean Sea	Alboran Sea Seco_de_los_Olivos	36.54/-2.82	3	9
North Sea	Norway -Tisler	59.00/10.97	10	
Gulf of Mexico	Mississippi Canyon	27.00/-85.00	8	8
South Atlantic	Brazil	-24.40/-43.93	26*	6
South Atlantic	South Africa	-30.52/16.65	2	
		-36.88/22.00	1	
Total			**112**	**90**

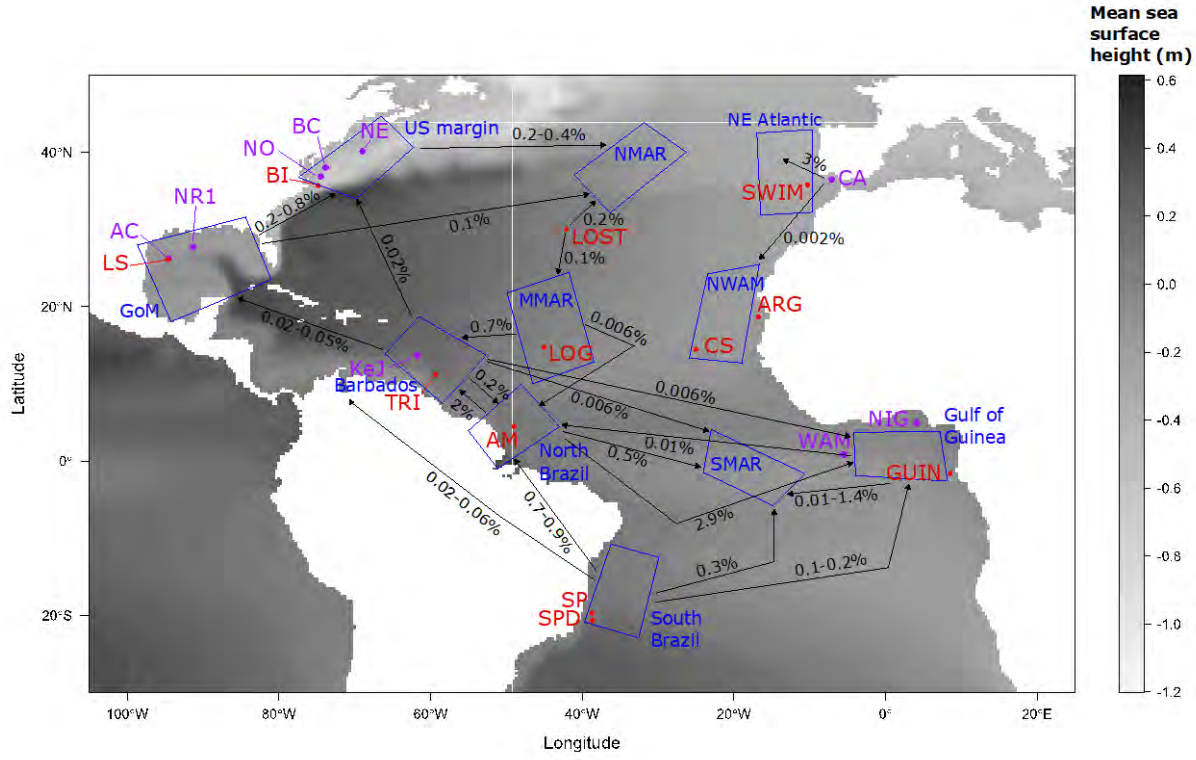

Figure 2. Connectivity map obtained by larval dispersal simulations for the seep mussels as extracted from Portanier et al. (2023). Red and purple colours represent the seep localities from which larvae have been emitted (NE: New England seeps, NO: Norfolk Canyon, BC: Baltimore Canyon, BI: Bodie Island, NR1: Brine Pool; AC: Alaminos Canyon, LS: Louisiana Slope, KeJ: Kick'em Jenny volcano, TRI: Trinidad El Pilar seeps, AM: Amazon fan, SP and SPD: Sao Paulo seeps, LOST: Lost City seeps, LOG: Logachev seeps, CA: Darwin volcano in Gulf of Cadiz, SWIM, ARG: Arguin Bank, CS: Cadamostro Seamount, NIG: Nigerian slope, WAM: West African margin seeps, GUIN: Regab seeps). Polygons in blue represent the main recipient zones for the larval settlement (NE Atlantic: North East Atlantic, NWAM: North western African Margin, US margin: Northeast US coast, GoM: Gulf of Mexico, NMAR: North MAR, MMAR: Mid MAR, SMAR: South MAR). Black arrows correspond to larval fluxes as a proportion of the total number of larvae emitted from a given locality.

Genomic data were then used to validate the occurrence of specific dispersal corridors for the two seep mussel complexes of species using RADseq, leading to a high number of nuclear loci (SNPs, n = 5,878 for *B. boomerang/heckerae*, and n = 6,344 for *G. childressi/mauritanicus*) but without the individuals coming from the Nigerian slope for which DNA was too much degraded to get nuclear markers. These bi-allelic loci indicated a clear spatial segregation of the seep mussel populations and validated the hypothesis, that these two species complexes are formed by 3 (*Bathymodiolus* group) and 4 (*Gigantidas* group) distinct genetic units as previously shown with the mitochondrial analysis. These units represent geographic isolates on both sides of the North Atlantic, with the clear geographic isolation of *G. mauritanicus* in the Gulf of Cadiz, and *B. boomerang* in the Gulf of Guinea (see Figure 3A & 4A). A small proportion of alleles (0.5-1%) in African populations come from the western Atlantic seep localities and could represent rare events of trans-Atlantic migration. In the specific case of *Bathymodiolus*, both the PCA and Landscape and Ecological Association Studies (LEA) analyses placed the Blake Ridge population (reference type *heckerae*) as a collection of intermediate (admixed) individuals between the Florida Escarpment population (type *heckerae*) and the Barbados Prism population (reference type *boomerang*) (Figure 6A), suggesting an 'old' pathway of colonisation across the Caribbean Sea, at least for *B. boomerang*. In the specific case of *Gigantidas*, both the PCA and Admixture analyses clearly

showed the presence of F1/F2 hybrids between *childressi* and *mauritanicus* at a minimum of three locations (KeJ, Mississippi Canyon, New England seeps & Chincoteague canyon: see **Figure 5B**). Hybrids and backcrosses were however more numerous in the Northeast US canyons with a greater level of allele introgression in the Norfolk canyon for both alleles coming from GoM and Barbados.

A

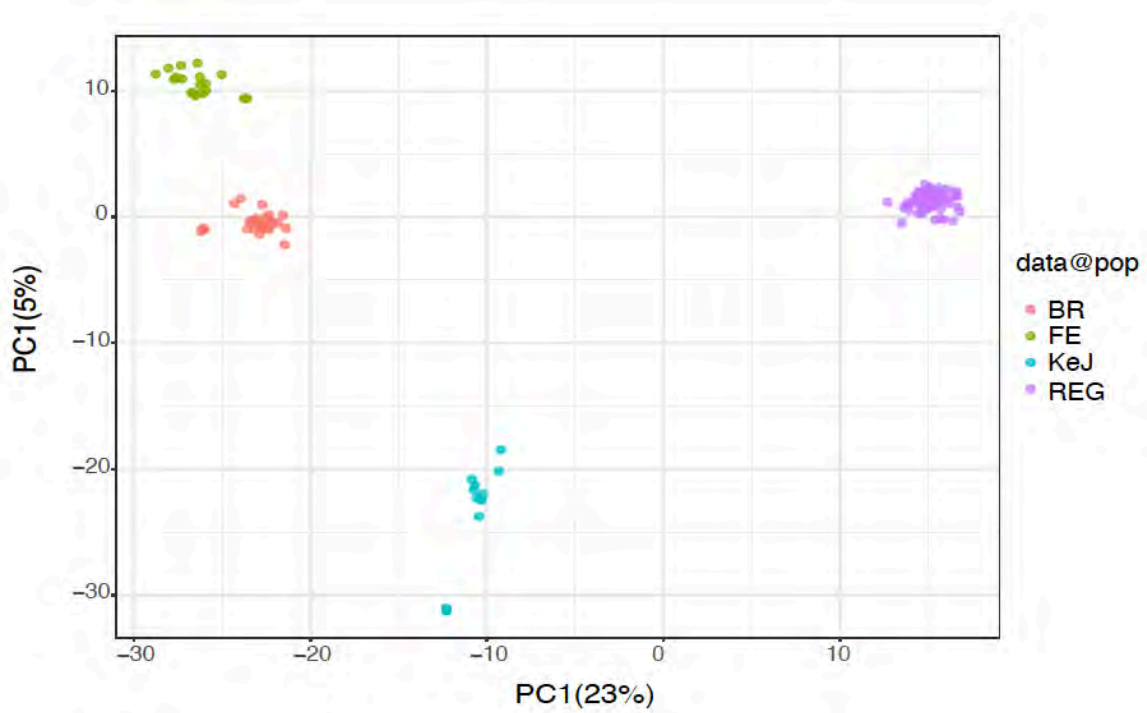

B

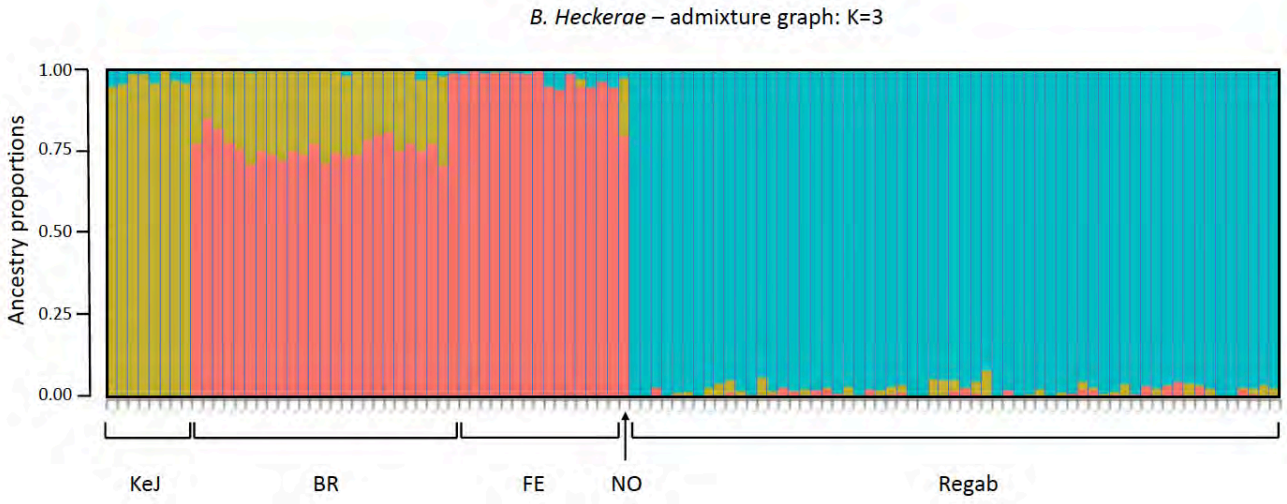

C

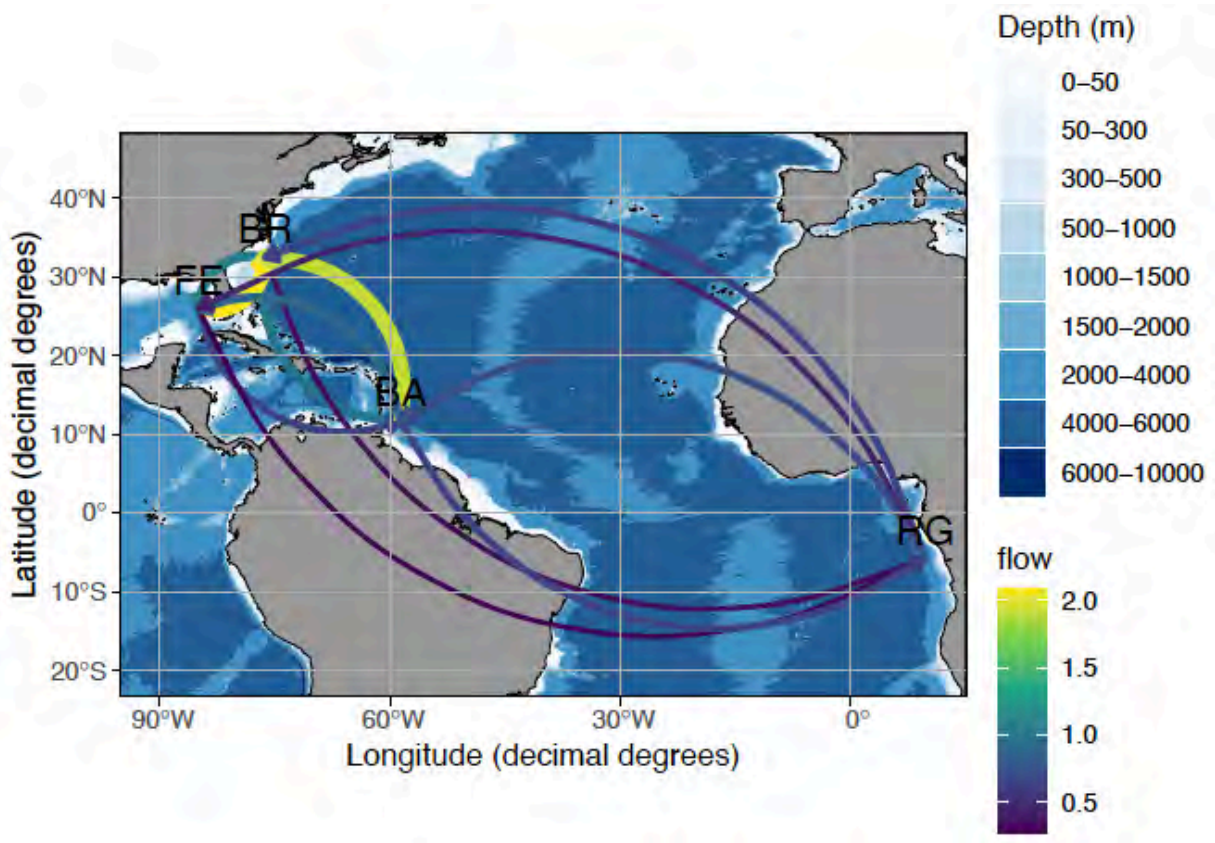

Figure 3. Pathways of migration for the cold seep complex of mussel species *B. boomerang/B. heckerae*. (A) PCA plot of mussel individuals based on their allelic frequencies at the genome scale (KeJ= Barbados accretionary Prism, FE= Florida Escarpment, BR=Blake Ridge and REG= Regab (Gulf of Guinea), (B) Admixture graph of mussel individuals showing three distinct genetic units (FE: *B. heckerae* from Florida Escarpment, KeJ: *B. boomerang* from the Barbados accretionary Prism and Regab: *B. boomerang* from the Gulf of Guinea) with all the individuals of Blake Ridge (BR) and the individual from the Norfolk Canyon (NO) having a boomerang genetic background introgressed by *heckerae* alleles. (C) Connectivity map showing strong oriented present-days gene flow from both FE and KeJ to BR as obtained from dadi under a population model of secondary contact (SC).

A

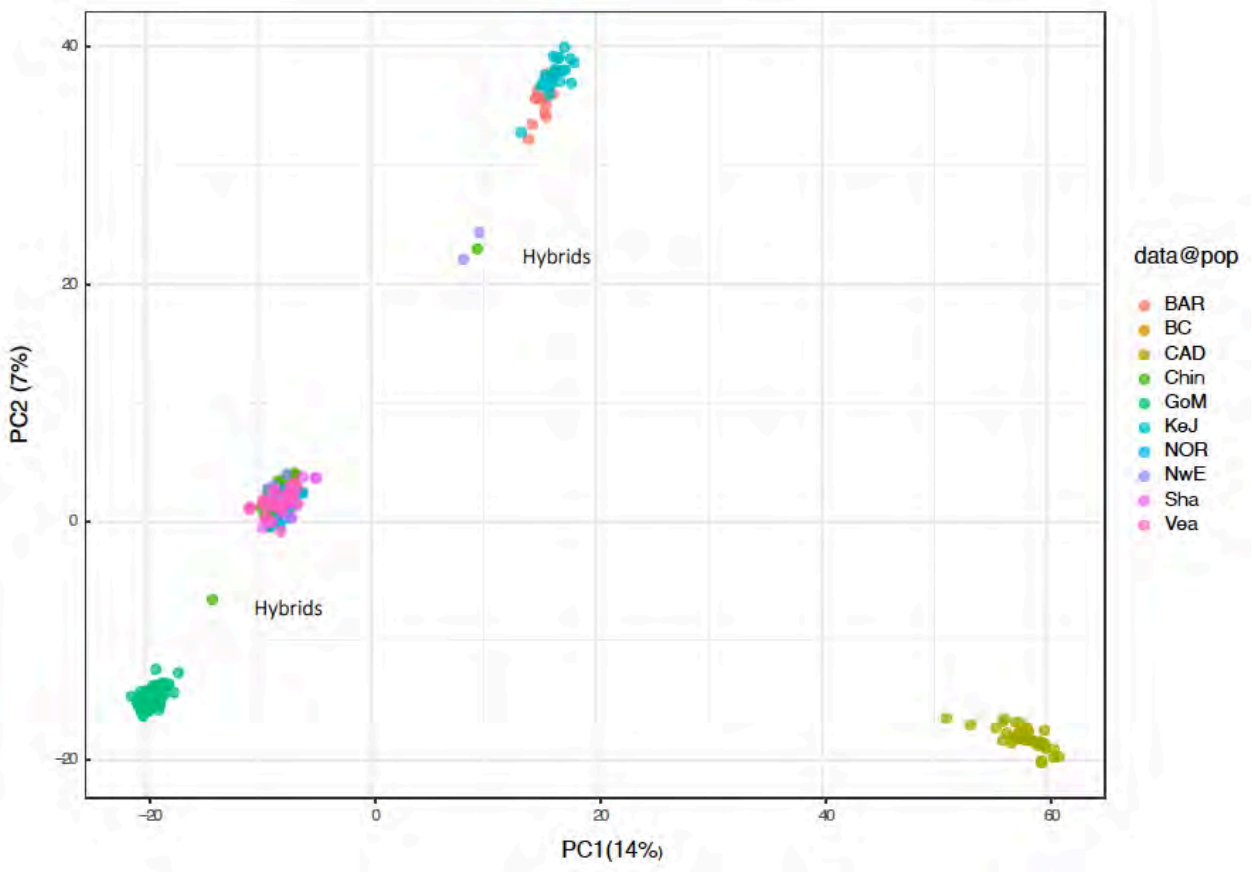
Hybrids
Hybrids
PC2 (7%)
PC1(14%)
40
20
0
−20
−20
0
20
40
60
data@pop
BAR
BC
CAD
Chin
GoM
KeJ
NOR
NwE
Sha
Vea

B

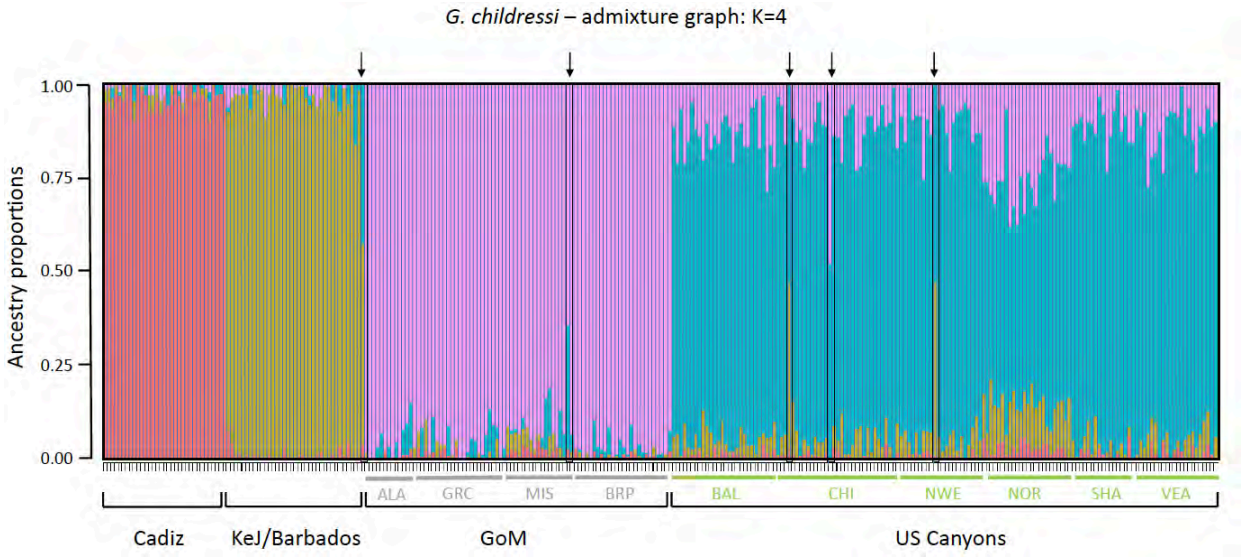
G. childressi – admixture graph: K=4
Ancestry proportions
1.00
0.75
0.50
0.25
0.00
ALA
GRC
MIS
BRP
BAL
CHI
NWE
NOR
SHA
VEA
Cadiz
KeJ/Barbados
GoM
US Canyons

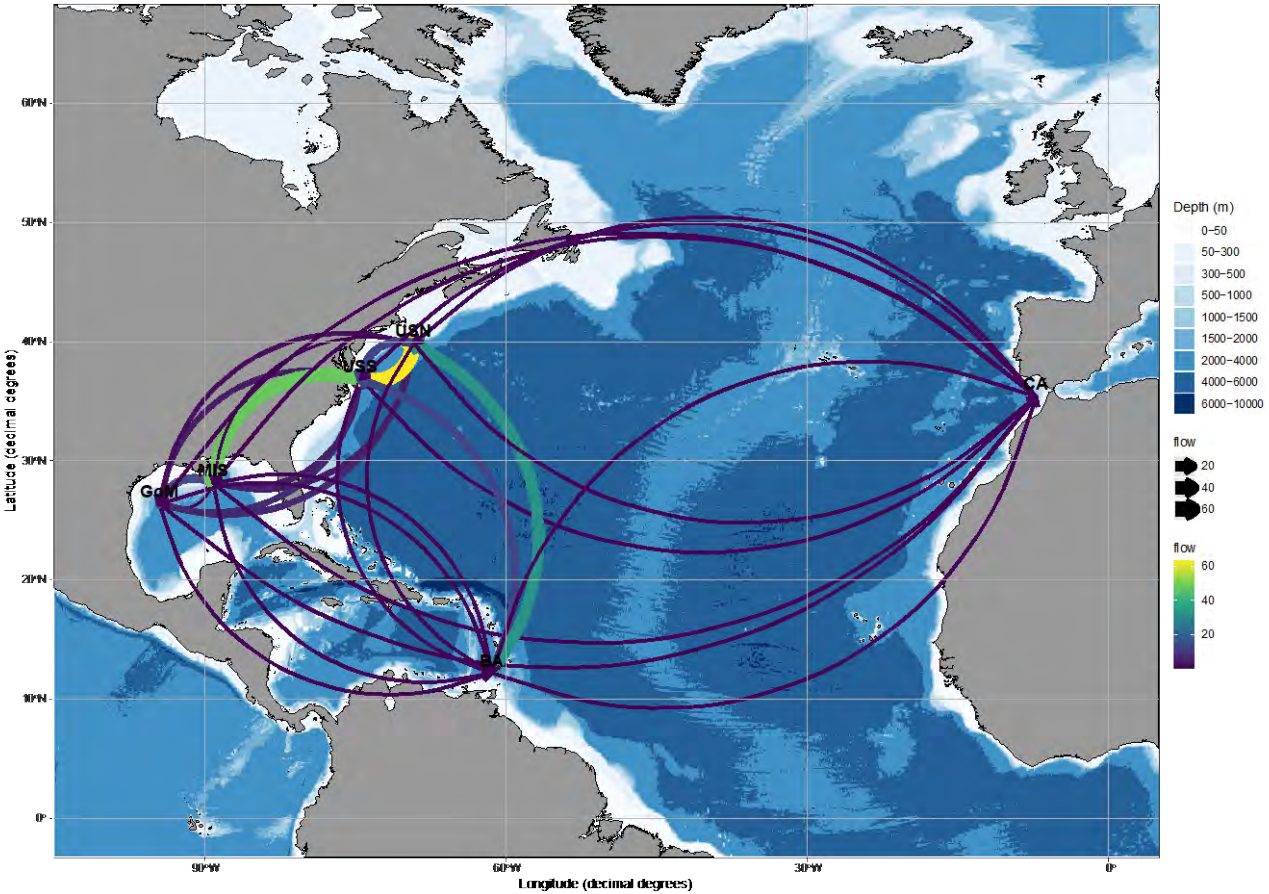

Figure 4. Pathways of migration for the cold seep complex of mussel species *G. childressi/G. mauritanicus*. (A) PCA plot of mussel individuals based on their allelic frequencies at the genome scale: arrows indicate intermediate individuals between *G. childressi* (Northeast US Canyons or Gulf of Mexico) and *G. mauritanicus* from the Barbados accretionary Prism (KeJ), (B) Admixture graph of mussel individuals showing four distinct genetic units (GoM: *G. childressi* from the Gulf of Mexico (ALA: Alaminos C., GRC: Green C., MIS: Mississippi C. and BRP: Brine Pool), US Canyons: *G. childressi* from the Northeast US Canyons (BAL: Baltimore C., CHI: Chincoteague C., NWE: New England seeps, NOR: Norfolk C., SHA: Shallop C., VEA: Veatch C.), KeJ/Barbados: *G. mauritanicus* from the Barbados accretionary Prism and Cadiz: *G. mauritanicus* from the Gulf of Cadiz) with some individuals of the Northeast US Canyons (CHI: Chincoteague and NWE: New England) being hybrids of first or second generation (arrows). (C) Connectivity map showing strong oriented present-days gene flow from both GoM and KeJ to the Northeast US canyons as obtained from dadi under a population model of secondary contact (SC).

The software dadi and DivMigrate provided congruent information about past-to-recent gene flows with strong to moderate gene flows from Gulf of Mexico and the Barbados accretionary prism to the canyons of the Northeastern US coast of the Atlantic (see Figures 3C & 4C), and the best fit of the genomic data to a population model obtained by dadi was the secondary model for the two seep mussel complexes of species with short to moderate Tsc (time since the secondary contact) when compared to the total isolation time since the initial population split. The statistical analysis of preferential Gst-based gene flow directions between the different populations done with DivMigrate (100 bootstraps) clearly indicated that the main gene flow orientations are from the South American coast (Barbados) to the North American coast, and to lesser extent from East to West across the Atlantic, with some recipient populations along the US coast (Chincoteague, Norfolk, Baltimore and New England).

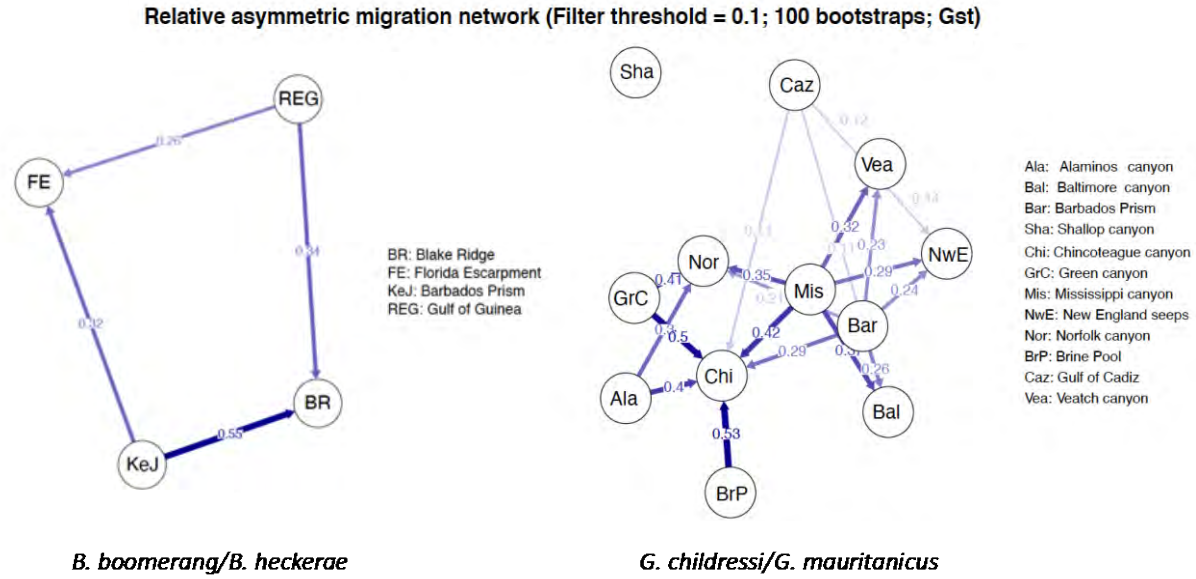

Figure 5. Past-to-recent oriented gene flows estimated between the seep mussel populations with the Fst-derived method of DivMigrate for (A) *B. boomerang/B. heckerae* and (B) for *G. childressi/G. mauritanicus*.

Vent gastropods

A first study was initiated on barcoded individuals (mt*Cox1* gene) to evaluate whether the two morphological species of vent gastropods *P. smaragdina* and *L. atlanticus* represented 'true' genetic species. Then, a second genetic analysis was done on each species at the genome scale to estimate the direction and strength of gene flow between a series of geographic populations along the Mid-Atlantic Ridge. Both mitochondrial (*Cox1* sequences) and nuclear (SNPs, n = 16,603 for *P. smaragdina*, 15,529 for *L. atlanticus*) markers indicated a clear spatial segregation of the vent gastropod populations for the two species investigated.

The haplotype network showed a clear separation between the three divergent genetic lineages for *L. atlanticus* (Figure 7A) and this relatively high level of divergence clearly indicated that these three lineages fall into the grey zone of speciation (dxy = 1.0 to 1.5%). Mitochondrial divergence and spatial arrangement of haplotypes were less pronounced between *P. smaragdina* populations (dxy = 0.5% between Moytirra and the other populations, Figure 7B) but still indicated that this latter species is also geographically highly structured.

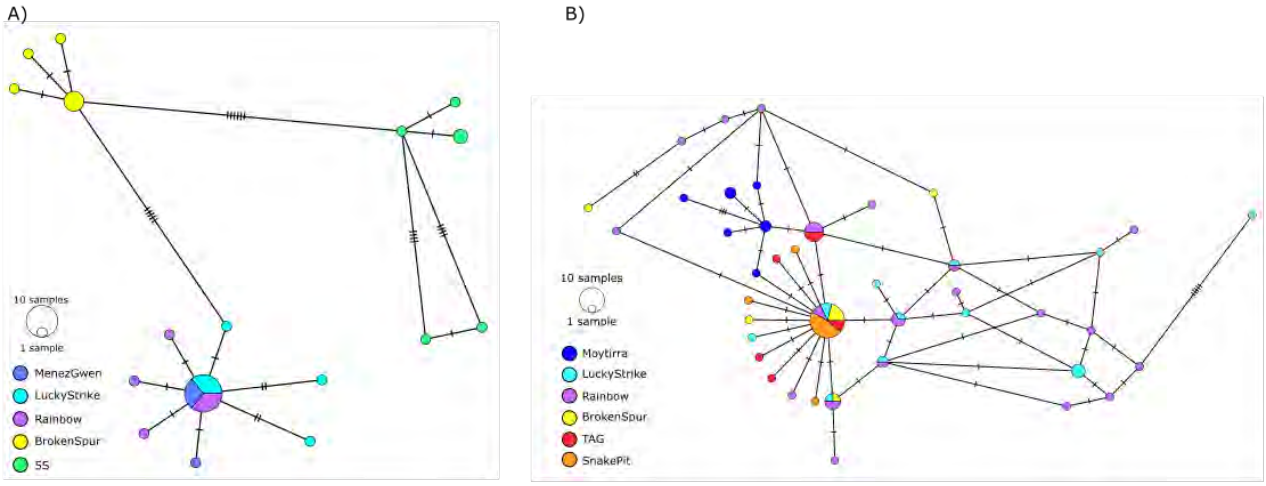

Figure 6. Haplotype networks for the A) *Lepetodrilus atlanticus* and B) *Peltospira smaragdina* species.

Genetic patterns estimated from SNPs were quite similar with at least three nearly independent genetic units spatially separated indicating low to no gene flow between them for both species. These metapopulations correspond to South MAR, mid (14-29°N) MAR and the Azorean triple junction for *L. atlanticus* (Figure 8A and 9A), and mid MAR, the Azorean triple junction and North MAR (45°N) with the presence of a contact zone near Rainbow (35°N) for *P. smaragdina* (Figure 8B and 9B). The presence of parental individuals of genetic cluster 1 from Lucky Strike (membership probability of 1.0 to cluster 1), but not from the southernmost cluster 3 (Figure 9B) and the strong allele introgression of cluster 1 into cluster 3 at Rainbow indicates that most gene flow occurs in a southward direction. The presence of both F1 and F2 hybrids at Rainbow however indicates that gene flow, although low, is currently occurring in both directions on this portion of ridge. In *L. atlanticus*, no gene flow was detected using the SNPs dataset (no admixed individuals, Figure 9A) and ASAP analyses on the mitochondrial DNA pointed to the presence of three separated OTUs. As also illustrated by the lower percent of variance explained by the PCA axes, the genetic differentiation was overall lower for *P. smaragdina* than for *L. atlanticus*, suggesting more exchanges of more contemporary migrants between populations of the former species.

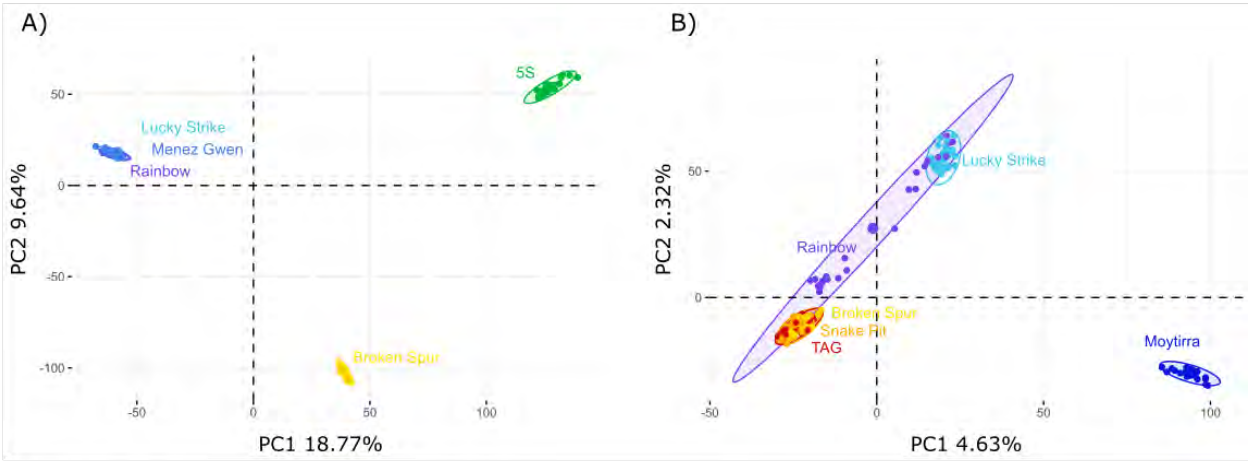

Figure 7. PCA performed on the SNPs datasets for A) *Lepetodrilus atlanticus* with three distinct geographic isolates and B) *Peltospira smaragdina* with the detection of a continuum of intermediate individuals between two of the three main genetic units (red/yellow vs turquoise points) at Rainbow.

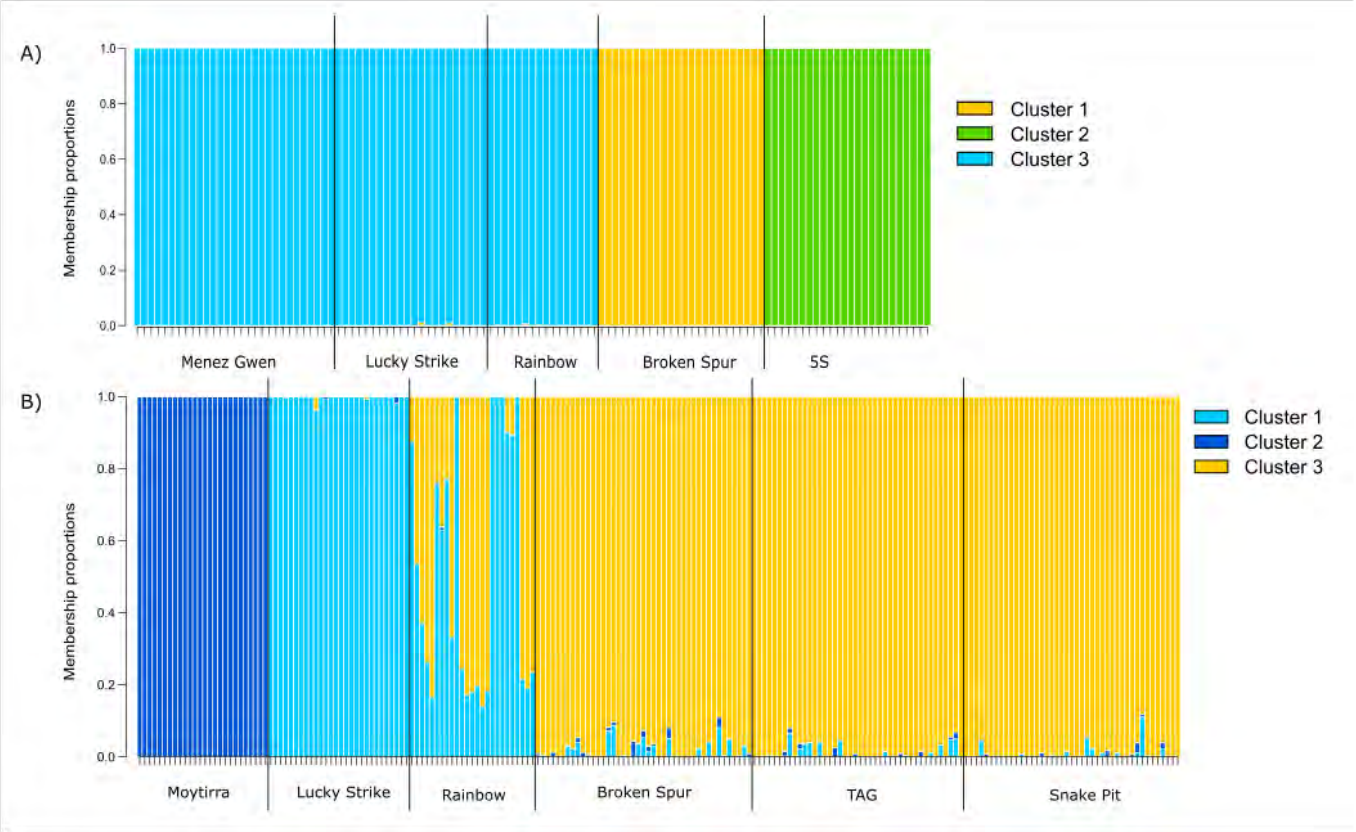

Figure 8. ADMIXTURE analyses performed on the SNPs datasets for A) *Lepetodrilus atlanticus* and B) *Peltospira smaragdina*. In both species, populations are separated into three genetic groups (in blue, yellow and green for *L. atlanticus*, and in dark blue, turquoise and yellow for *P. smaragdina*. The admixture graph of *P. smaragdina* clearly shows the presence of F1, F2 and admixed individuals together with the two parental types at Rainbow.

Although close to a strict isolation (SI) model from both the PCA and ADMIXTURE analyses, demographic inferences suggested that the best demographic scenarios between the three genetic *L. atlanticus* groups were secondary contact scenarios with a strong effect of linked selection and population size changes (all pairs) as well as heterogenous migration rates along the genome (i.e. barrier loci, pairs Menez-Gwen-5°S, Broken Spur-5°S, Table 6). It thus seemed that the three previously evidenced genetic units may have been recently reconnected. The number of migrants per generations were indeed very low and the times spent isolated (Ts) very large as compared to the time spent since the secondary contact (Tsc, Table 6, Figure 10A). Migration seemed to be slightly biased in a northward direction (Table 6, Figure 10A). Regarding *P. smaragdina*, an isolation with migration model with an effect of linked selection and population size changes was the best supported between clusters 1 and 3 (Table 6) but the analysis did not include the Rainbow population, which clearly gave credit to the hypothesis of secondary contact between these two clusters. Between Moytirra cluster and the Snake Pit or Lucky Strike clusters, the best model was a secondary contact model with population size changes (both pairs) and the effect of linked selection with heterogeneous migration along the genome (Moytirra-Snake Pit pair). Overall, the presence of both non-negligible northward and southward present-days migration was detected along the ridge (Table 6, Figure 10B) although the main direction of migration was clearly southward using both dadi and DivMigrate. This southward pathway of the ridge colonisation may be therefore dictated by bottom currents, at least for the vent gastropods.

Table 6. Parameters estimated using dadi software for *L. atlanticus* and *P. smaragdina* population pairs (population 1 – population 2). Ni : population size of each population i; Ta : time before Ts at which the change in Na occurred, Ts : time of strict divergence; Tsc : time of divergence with migration, bi : the population i's growth factor; hrf : Hill-Robertson factor; Q : proportion of loci that are under the effect of linked selection (i.e., Hill-Robertson effect); P : proportion of loci that have unconstrained migration; Mij : represents the unrestricted migration rate from the population j towards population i; mij : number of migrants per generations from the population j towards population i (calculated as mij = bi*Nui*Mij /2); meij : the restricted migration rate (e.g., barrier loci) from population j towards population i. Times are expressed in years.

	L. atlanticus			*P. smaragdina*		
Pop pair	MG-BS	MG-5°S	BS-5°S	MO-LS	MO-SP	LS-SP
Best model	SC2NG	SC2N2mG	SC2N2mG	SC2mG	SC2N2mG	IM2NG
N1	4,926	1,329	549	3,027	1,772	729
N2	3,223	5,902	1,301	9,826	8,908	2,940
Na	25,155	573	5,982	457	1,038	21,748
Ta	8,539	1,103	11,900	4,143	714	7,957
Ts	4,255	12,709	10,873	10,776	4,083	794
Tsc	1,614	837	390	1,182	586	
b1	1.644	1.272	0.393	0.356	0.351	7.443
b2	0.358	0.033	0.256	0.308	0.208	21.464
hrf	0.179	0.087	0.042		0.124	
P		0.008	0.031	0.087	0.001	
Q	0.493	0.169	0.274		0.255	0.233
M12	0.986	1.305	5.517	0.068	0.726	8.031
M21	2.314	1.954	1.018	0.466	1.244	1.113
m12	1.159	0.874	0.995	0.032	0.673	8.999
m21	0.388	0.149	0.283	0.609	1.155	14.495
me12		0.138	0.323	0.606	0.782	
me21		3.125	3.113	1.935	4.084	
Theta	2,088.593	765.054	363.001	643.725	553.133	1,345.138

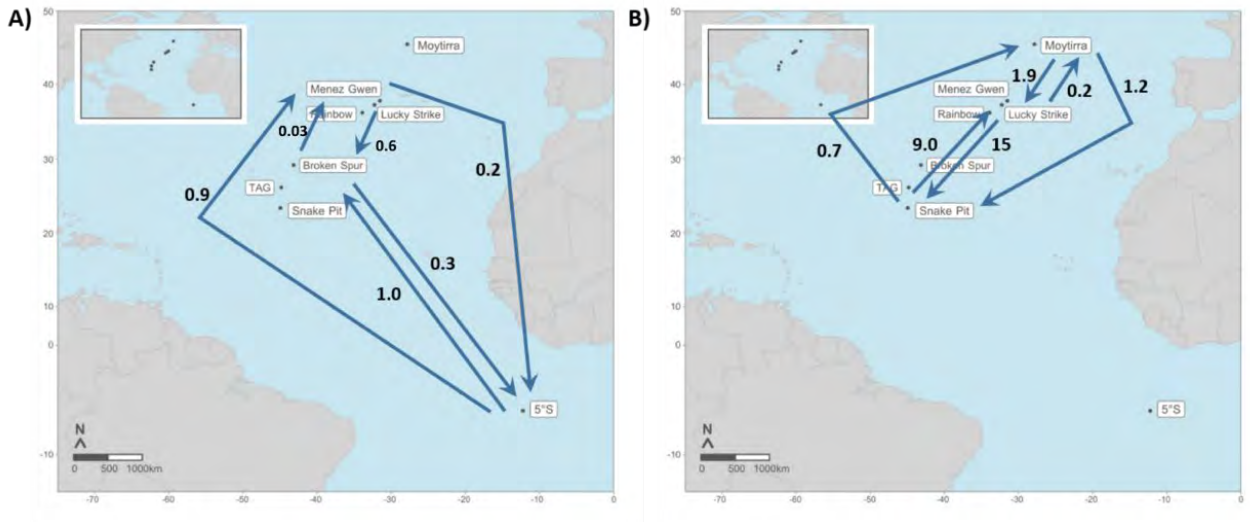

Figure 9. Number of migrants per generation (i.e. one year) as estimated by dadi for A) *Lepetodrilus atlanticus* and B) *Peltospira smaragdina* species. NB: these parameters are converted values (number of migrants here = m_{ij}*b_i*nu_i/2) and thus depends on other estimated values (nu_i, b_i). The information they give may differ from the information translated by unconverted values shown in Table 6.

Vent shrimps

Previous work on both mitochondrial and nuclear (microsatellites) markers clearly gave support to a lack of spatial structure at the scale of the Mid-Atlantic Ridge, with no genetic differentiation between the investigated populations of *Rimicaris exoculata* (including samples from the south of the MAR, Teixeira et al. 2012). Our results, using ddRAD sequencing and SNPs datasets (n= 1,808 for *R. exoculata*, n= 2,844 for *R. chacei*) confirmed the lack of geographical barriers to gene flow for *R. exoculata* and evidenced a similar pattern for *R. chacei* (Figure 11A & B). All individuals of each species grouped together in the multivariate analyses with a low percentage of variance explained by the two first axes (Figure 11). F-statistics were not significantly different from zero and clearly indicated that shrimps are able to freely migrate as larvae, adults or both between vent sites at the ridge scale (i.e. over > 3,000 km). In contrast, a slight and significant geographic structure was observed between *R. chacei* (Mid-Atlantic Ridge) and *R. hybisae* (Caiman Ridge in the Caribbean Sea) (Figure 12). Although genetically differentiated at this greater spatial scale, the genetic data obtained at the genome scale confirmed that they probably belong to the same species despite their morphological differences (highly pronounced cephalothorax enlargement due to epibiosis in the specific case of *R. hybisae*), as previously suggested by Methou et al. (2023) using the mitochondrial marker *Cox1*.

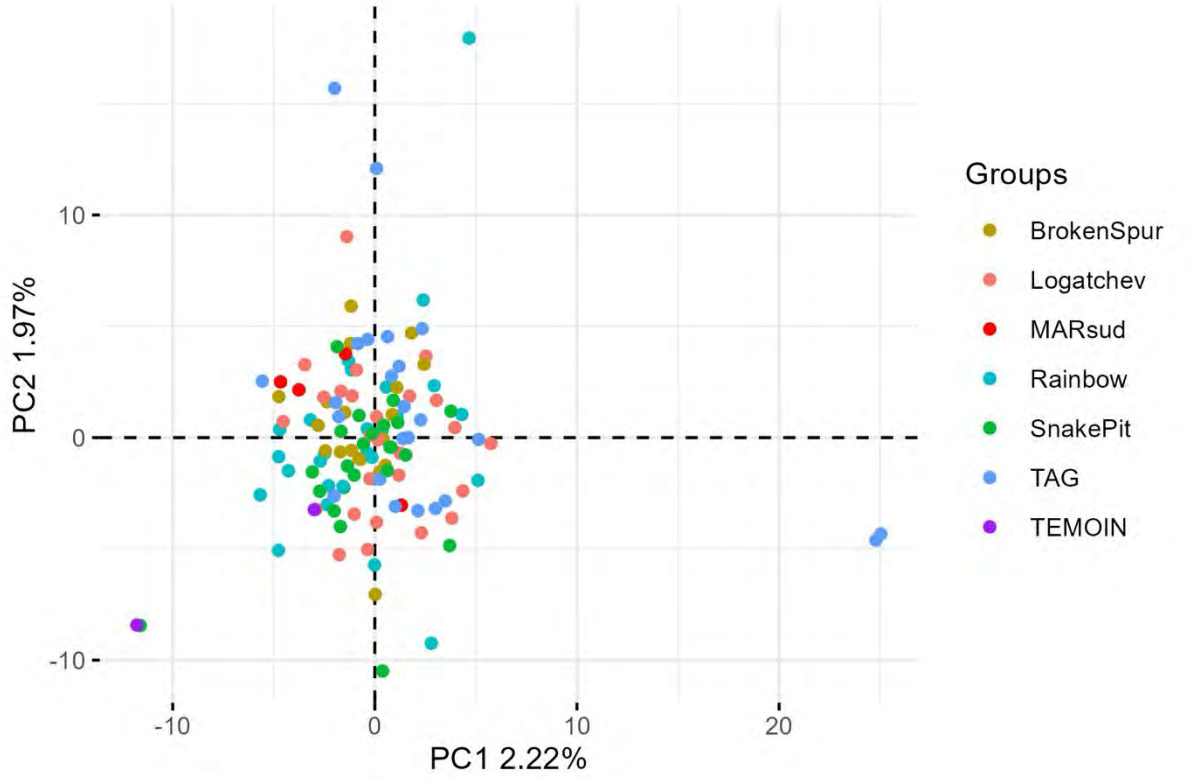

Figure 10. PCA graph with a SNPs dataset (1,040 bi-allelic loci) for *Rimicaris exoculata* with no genetic differentiation of individuals (one single panmictic group) along the whole MAR.

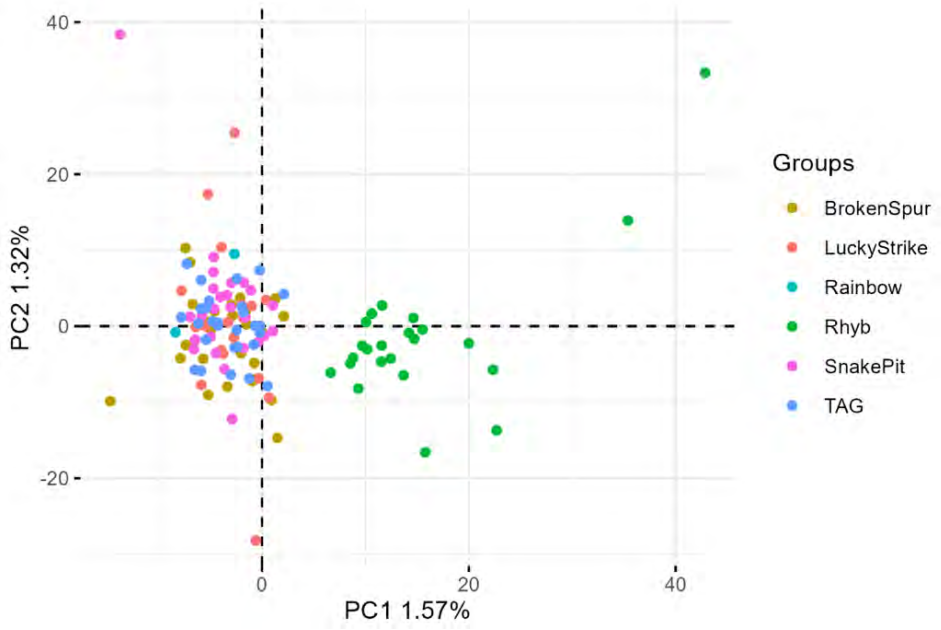

Figure 11. PCA graph on the shared SNP dataset (2,381 bi-allelic loci) between *Rimicaris chacei* sampled along the Mid-Atlantic Ridge and *Rimicaris hybisae* (Rhyb: in green) sampled on the Cayman Ridge at the Beebe site. Genetic divergence between the two shrimp species is within the expected genetic variation found within a given species (less than 1% of genetic differentiation) but *R. chacei* populations are not differentiated along the North MAR.

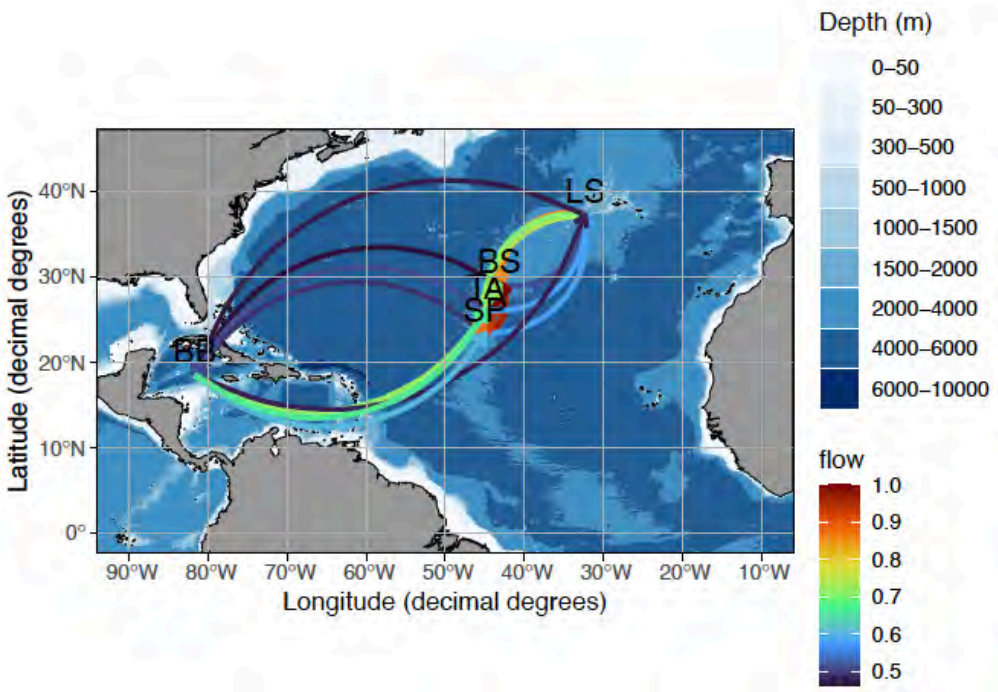

A. *R. chacei/hybisae* - DivMigrate (Gst-based gene flow)

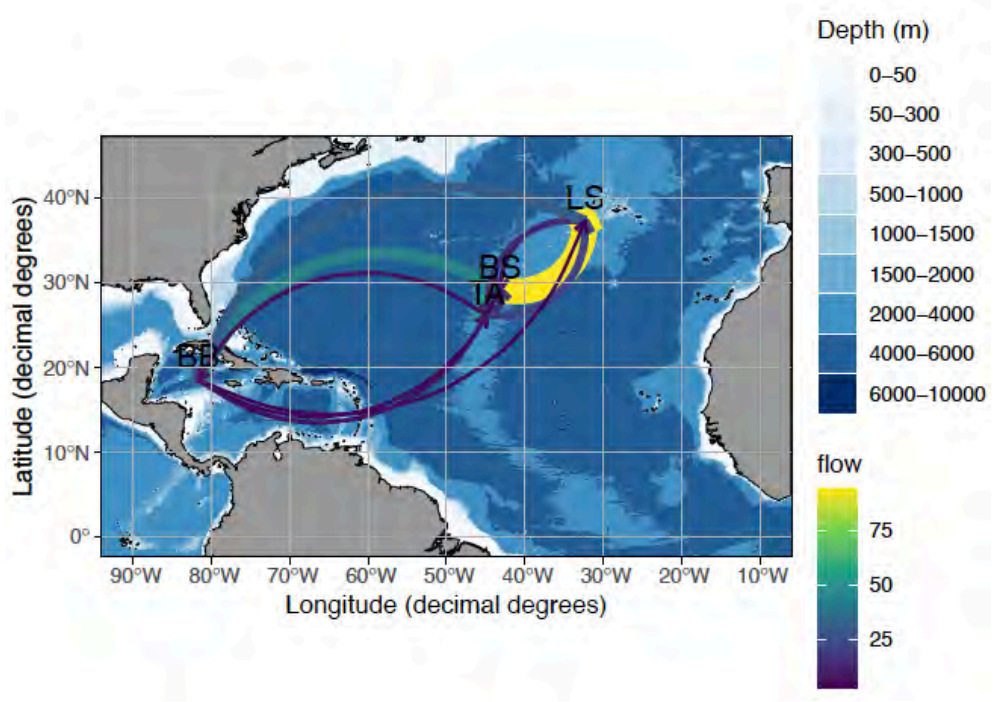

B. *R. chacei/hybisae* - dadi (present-day gene flow following SC model)

Figure 12. Past-to-recent dispersal pathways obtained from the vent shrimp complex of species *R. chacei/R. hybisae* using both the DivMigrate (A) and dadi (B) software. The population model selected by dadi (best fit to the genomic data) is the secondary contact (SC) model with a recent T_{SC}.

Since *R. chacei* and *R. hybisae* fall within the same species with the existence of a slight but significant geographic structure, these two morphological/geographic forms of the same species were grouped together to better understand the demographic history of this polymorphic (highly developed vs restricted cephalothoracic epibioses) species, and the relationship between the MAR and Cayman Ridge populations. The direction and strength of gene flows between the main shrimp populations were obtained using both DivMigrate and dadi with 2,381 bi-allelic loci (SNPs) to have a better idea of past and present-days exchanges between these two disjunct ridges and presented in Figure 13. Interestingly, patterns of gene flow obtained using the two methods were not congruent with a past-to-recent flow clearly oriented from the Caribbean Sea to the southern part of the MAR (DivMigrate, Figure 13A) and a much more recent flow (following a secondary contact: SC model) secondarily oriented from the northern part of MAR to the Caribbean Sea.

Vent mussels

A first analysis was performed on the four geographic mitochondrial lineages of the Atlantic vent mussels that presently belong to the previously described species *Bathymodiolus azoricus* and *B. puteoserpentis*. These mussel populations form geographic isolates along the Mid-Atlantic Ridge at the locations 35-37°N (*B. azoricus*), 14-26°N (*B. puteoserpentis sensu stricto*), 5°S (*B. puteoserpentis*-like) and 9°S (*B. azoricus*-like) (Van der Heijden et al. 2012) with a well-described hybrid zone between the two former species localised near the site Broken Spur at 29°N/MAR. This analysis was performed in collaboration with C. Borowski (MPI Bremen) on polymorphic sequences of 10 nuclear (gene) markers (see Faure et al. 2009) and the mitochondrial gene *Cox1* using the software IMa3 (Figure 14). Results showed that the mussel populations form a continuum of hybridisation along the MAR between the two most geographic extremes, with at least two secondary tension zones occurring between them.

For the vent mussels, gene flow was mainly oriented southward down to the Equator (from the Azorean triple junction to Logachev (14°N) and Logachev to Golden Valley (5°S) with subsequent allele introgression from *B. azoricus* in *B. puteoserpentis* (with the presence of a hybrid zone at Broken Spur, 29°N) and the expansion of *B. puteoserpentis* further south (Figure 15). The direction of gene flow was northward was mirroring this in the southern Atlantic with southward migration and the formation of a second hybrid zone near 5°S, the Golden Valley mussel population at this site receiving foreign alleles both from Logachev (14°N) and Lilliput (9°S). The highest possible population splitting time (T1) between *B. puteoserpentis* and the mussel population from 5°S was estimated to occur about 1.7 Mya (Figure 14) with episodic migration events between them. The population model of secondary contact still needs to be tested using dadi and our newly gained RADseq datasets obtained from the mussel populations of Lilliput (9°S) and Golden Valley (5°S) again in collaboration with C. Borowski (MPI Bremen).

The hybrid zone of Broken Spur (29°N) was then better characterised using a RADseq dataset (1,800 bi-allelic loci, 4,251 SNPs) obtained from *B. azoricus* and *B. puteoserpentis* populations (Lucky Strike, Menez Gwen, Rainbow, Snake Pit and Logachev) taking advantage of new adults and young mussel settlers collected at Broken Spur in 2018. The PCA clearly showed the clear separation of *B. azoricus* and *B. puteoserpentis* on the first axis (with 63.6% of the genetic variance explained by this axis: Figure 16). The analysis also showed that some individuals from Snake Pit and nearly all individuals of Broken Spur are intermediate between the two species, but some differences exist between adults and young settlers. Most of intermediate adults are closer to *B. puteoserpentis* or 'pure' *B. puteoserpentis* whereas intermediate settlers are either closer to *B. puteoserpentis* or 'pure' *B. azoricus.* This finding was confirmed by the Admixture analysis (Structure 2.3.4 with K=2: Figure 16) in which the young settlers sampled at Broken spur were all F2 hybrids with the exception of three 'pure' *azoricus* whereas most

of the adults were either 'pure' *puteoserpentis,* F2 or introgressed individuals with a '*puteoserpentis*' genetic background.

The origin of the three 'pure' *azoricus* postlarvae that settled at the basis of the vent chimney named 'abondance' in the Broken Spur vent field was traced back from 20,402 bi-allelic loci using a DAPC approach on *B. azoricus* populations only. The analysis clearly showed that these three settlers were genetically different from the populations sampled at the triple Azorean junction (i.e. Menez Gwen, Lucky Strike and Rainbow), indicating that they have been produced elsewhere on the Mid-Atlantic Ridge.

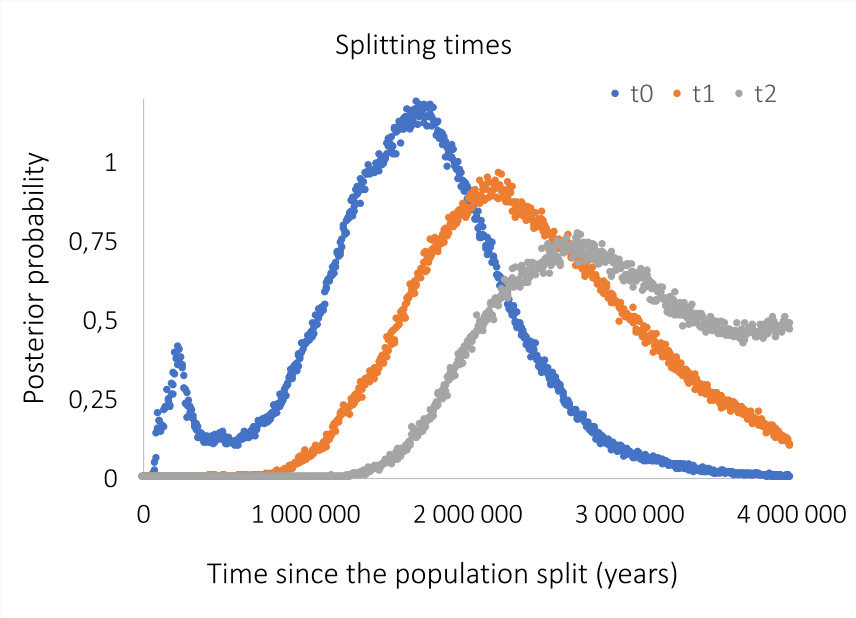

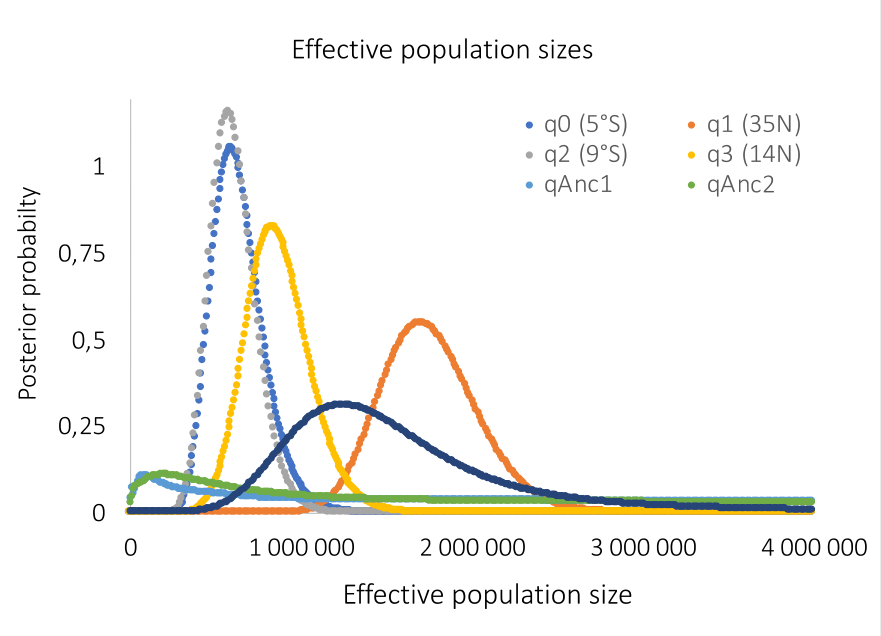

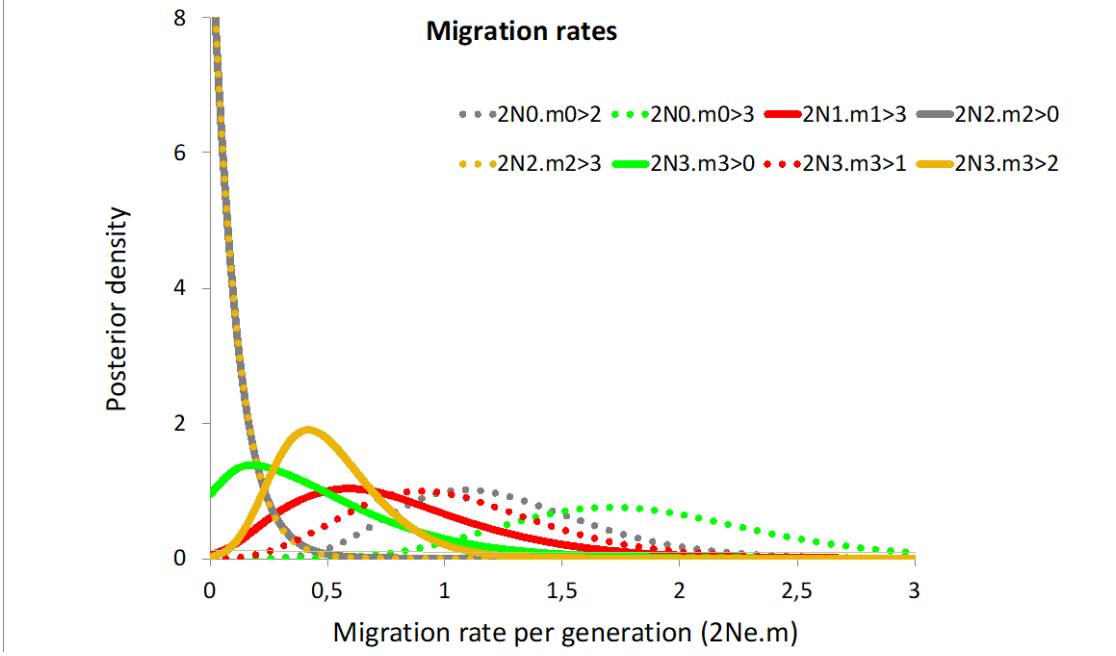

Figure 13. IMa3 estimates for (A) population splitting times, (B) population sizes and (C) migration rates for the four mitochondrial lineages of vent mussels with pop0=Golden Valley (5°S), pop1= *azoricus* (35°N), pop2= Lilliput (9°S) and pop3= *puteoserpentis* (14°N) and the mt genome reference Newick tree: (((0,3),2),1)

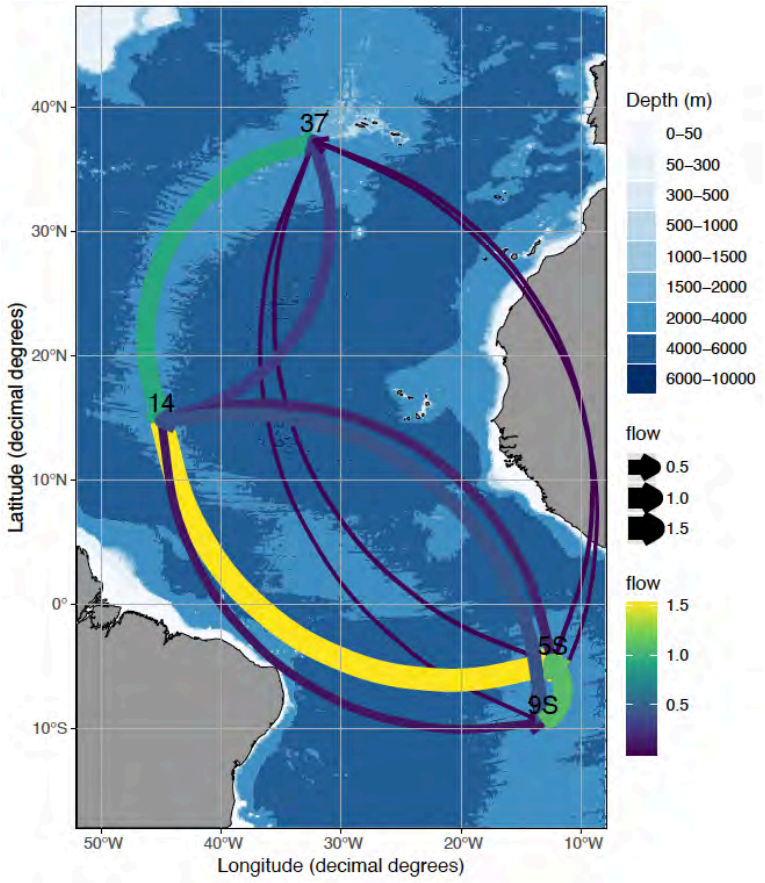

Figure 14. Past-to-recent dispersal pathways obtained from the vent mussel complex of species *B. azoricus/B. puteoserpentis* using the IMa3 software.

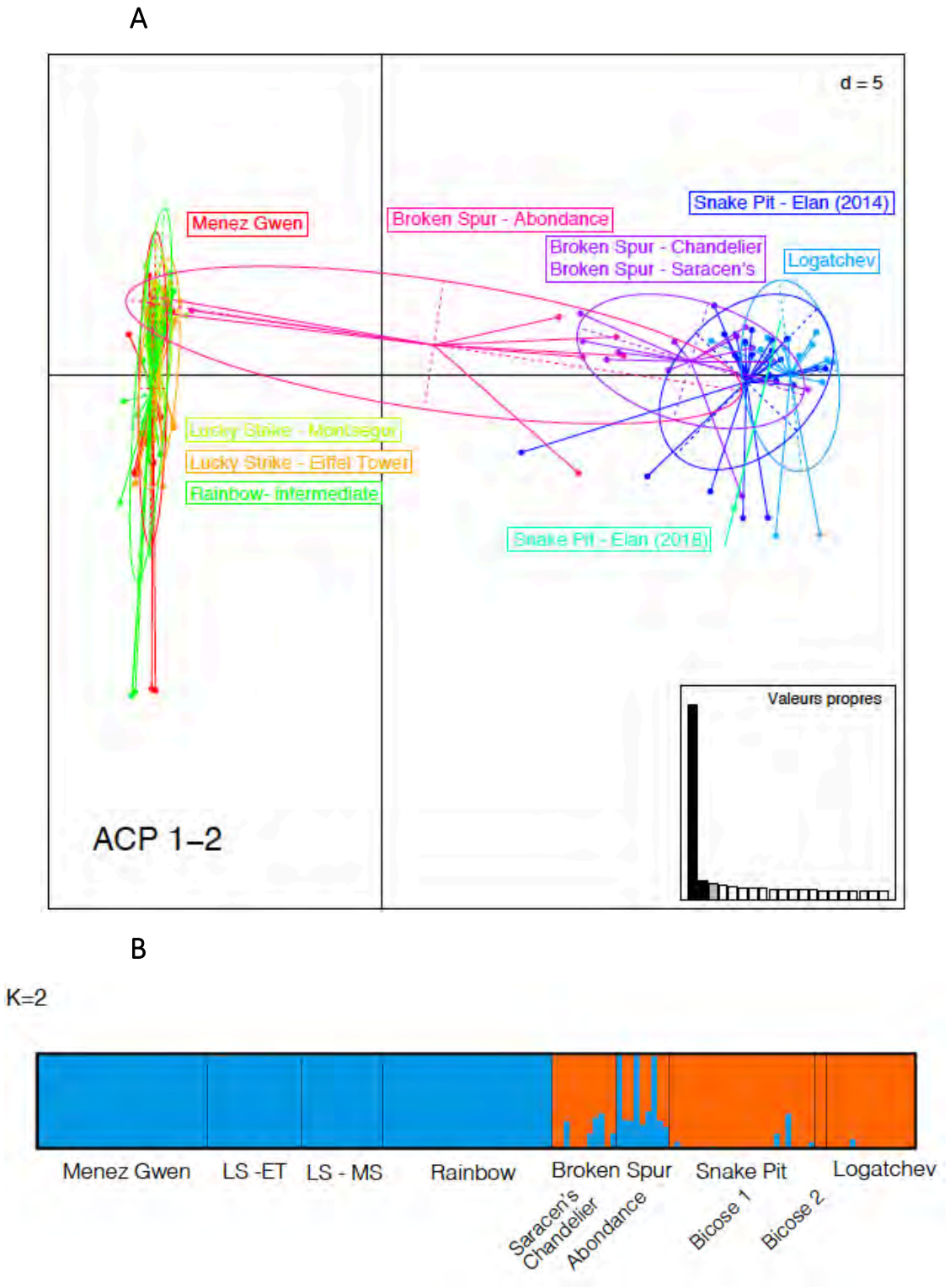

Figure 15. Genetic structure of the vent mussels along the Mid-Atlantic Ridge. (A) PCA and (B) Admixture analysis (Structure 2.3.4. With K=2) performed on the SNPs dataset of *Bathymodiolus azoricus* and *B. puteoserpentis* focusing on the hybrid zone located at Broken Spur (29°N).

Deep-sea corals

The first results presented in this deliverable were obtained between August and November 2023 and focussed on the European margins. Additional data from US and Brazilian coasts were and are still under

analyses as the raw sequencing results arrived only in late August to early September 2023. Whole genome sequencing requires detailed and time-consuming bioinformatic work, followed by biostatistics analyses on a calculation cluster with much script development. Thus, only preliminary results were available for this report, showing that corals from those areas represent different divergent OTUs (see Results and Discussion sections).

Filtered dataset

So far, only *D. pertusum* and *M. oculata* (.vcf) files have been filtered for several quality threshold and missingness (individual and SNPs) to minimise the effect of low-quality variant and missing data, then variants were kept with a minimal distance of 1,000 base pair between them. This resulted on a VCF with 360,391 variants for 53 *D. pertusum* samples and 348,847 variants for 71 *M. oculata* samples for the European dataset. The remaining part of the dataset is still under bioinformatic analysis.

An additional effort is provided in this revision, where most recent data from US and Brazilian margins for both species are now added to the datasets, resulting in 28 and 3 samples for *D. pertusum* and *M. oculata* respectively for the South Atlantic (Brazil), 22 and 6 for the West Atlantic (US margins) and 5 samples of *M. oculata* from the Pacific Ocean.

Identification of cryptic species and geographic patterns of dispersal

Exploratory analyses of the deep cold-water coral population structure revealed highly contrasting patterns between the species *D. pertusum* and *M. oculata*.

D. pertusum

The genomic data analyses of *D. pertusum* revealed population structures that can be divided into three genetic groups along the coasts of Europe. In the European group, the spatial composition consists of (i) a Mediterranean lineage (referred to as MED), (ii) a Lusitanian lineage (MID), which includes samples from the Azores, the Bay of Biscay, and some individuals of the Celtic Sea and Iceland, and (iii) a third and last boreal lineage (NORTH) consisting of individuals from Iceland, the Celtic Sea and the North Sea (Sweden and Norway) (Figure 17a, b). These analyses highlight that the Bay of Biscay, the Celtic Sea and the Iceland represent a tripartite transition zone between the MED, the Azores archipelagos and NORTH lineages with numerous admixed individuals if not all sampled ones in the MID area (Figure 17b, c). Furthermore, most analyses demonstrated a considerable genetic resemblance between the North and MED lineages, while the MID lineage is somewhat more divergent (Figure 18) with net divergence (Da) values up to 0.0045. The Treemix and *f3* statistics analyses do not show any substantial gene flow between these lineages. However, demogenetic inferences using moments with the most suitable models IM and SC clearly indicated that a nearly one directional gene flow oriented from the Mediterranean Sea (MED lineage) and the North Sea/Arctic Sea (NORTH lineage) toward the Bay of Biscay/Celtic Sea to compose the MID group (Figure 19). These inferences are still preliminary and further inferences need to be performed with these models and including the simulation of genomic heterogeneity. F_{is} estimates obtained for each locality and each lineage were nearly all significantly negative, possibly due to the clonal effect, by generating inbreeding signal.

Additional preliminary results on a pan-Atlantic scale show a clear signal of geographical differentiation in three major genetic lineages, the first comprising all samples from the South Atlantic, the second those from the North West Atlantic (US margins) and the last comprising samples from Europe (Figure 21a). In addition, genetic structure is also observed within North Atlantic lineages (Figure 21a, b, c). The first is between the Canaveral and Gulf of Mexico/Norfolk Canyon samples (Figure 21a, b). The second split is that observed within Europe with the three lineages presented in the previous paragraph (Figure 21b, c).

M. oculata

For *M. oculata*, genetic analyses also revealed highly structured and differentiated lineages along European coasts (Figure 20a, b) but the level of divergence between these lineages was much more pronounced (Da ranged between 0.3-0.65: see Figure 21) supporting the existence of a species complex rather than a single species. This structure is made up of at least four major, highly divergent genetic lineages (Figures 20 & 21). The first and most divergent lineage encompasses populations from the Mediterranean Sea and the Bay of Cadiz. The second is found in the Bay of Biscay. The third is made up of individuals from the Azores archipelago, and some individuals from the Bay of Biscay and Brazil. Finally, the last lineage groups most of the northern localities, the Celtic Sea, Iceland and individuals from the southern part of the Azores (Meteor area). Within this lineage structure, a sub-structuring is also observed at the scale of localities (Figure 20 a, b, c). Additionally, Treemix and *f3* analyses revealed that the Celtic Sea should represent a mixing zone between Iceland (lineage 3) and the Bay of Biscay (lineage 2). Such an observation also held for the individuals sampled in the Bay of Cadiz where admixed individuals between the Mediterranean lineage 1 and lineage 2 from the Bay of Biscay were depicted. F_{is} estimates per locality were also mostly significant and negative, possibly due to inbreeding signal potentially from clonality when compared to sexual reproduction.

Preliminary pan-Atlantic results on *M. oculata* plus additional samples from the Pacific Ocean showed different results compared to those observed for *D. pertusum*. Firstly, it is clearly identified that within the Atlantic Ocean, for the localities sampled, two very distinct genetic lineages are observed with no clear geographic congruency (Figure 22b, c, d & Figure 22a). The first observed lineage is that comprising the samples from the North-East Atlantic, presented previously, and a few samples from Brazil. The second observed line is composed of the remaining samples from Brazil grouping with those from the Gulf of Mexico and the Pacific Ocean. These two major lineages correspond to the two recently recognised distinct species, *M. oculata* and *M. piresae* sp. nov (Capel et al. 2023).

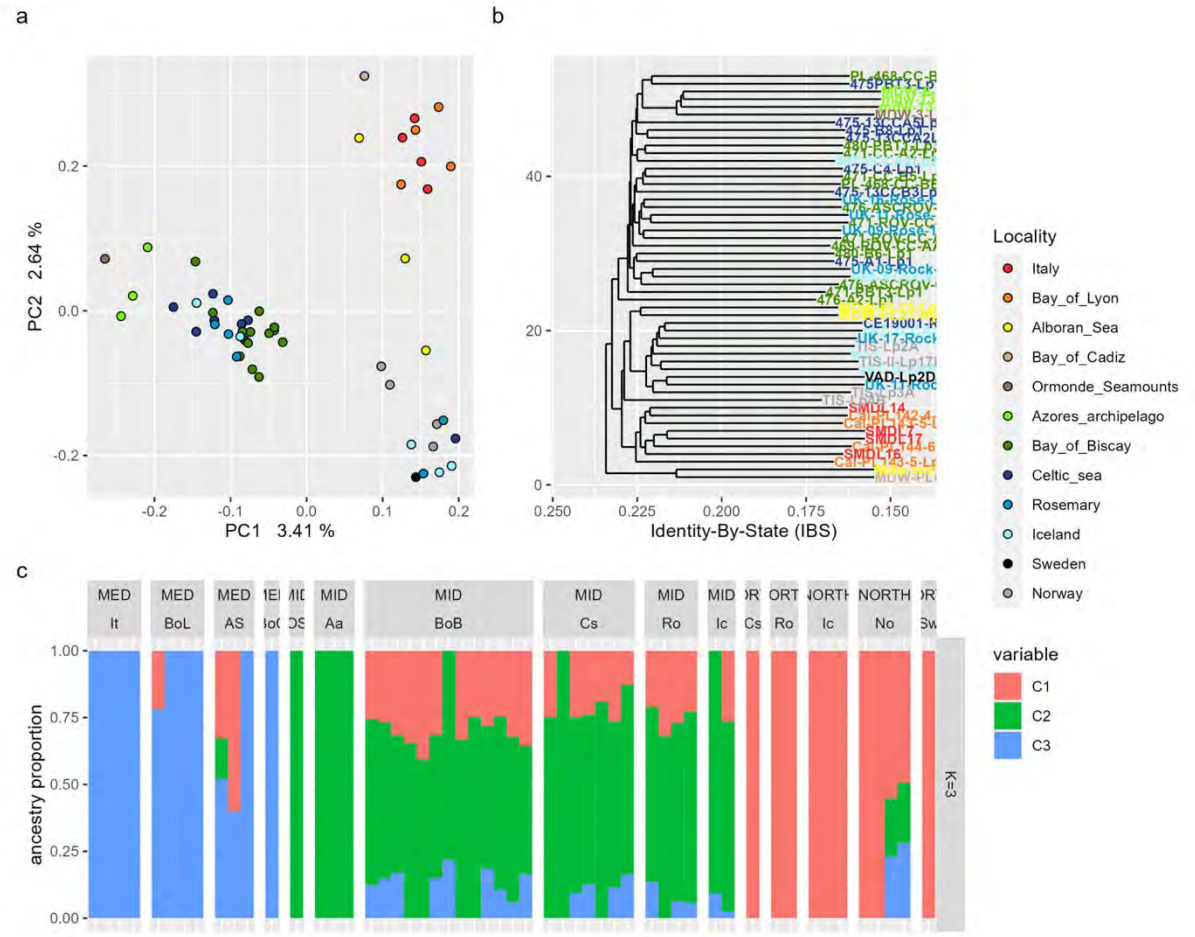

Figure 16. (a) Principal component analysis with the first two components for *D. pertusum*. Colour represents localities and each point represents an individual. (b) Identity-by-states (IBS) dendrogram or similarity between samples. Each leaf represents one individual. (c) Plots of admixture for K = 3, where individuals are clustered by localities. Each colour bar represents the proportion of the genetic ancestry for each of the inferred clusters.

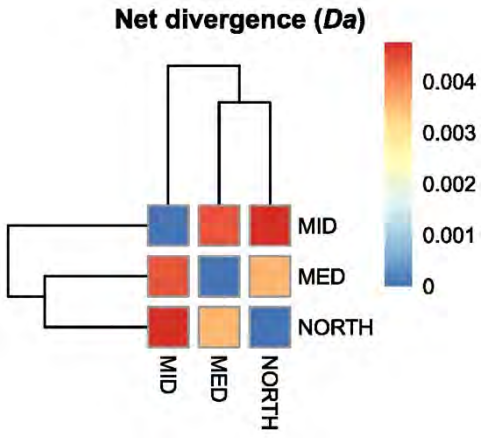

Figure 17. Heatmap and clustering of the estimated net nucleotide divergence (Da) between European lineages for *D. pertusum*.

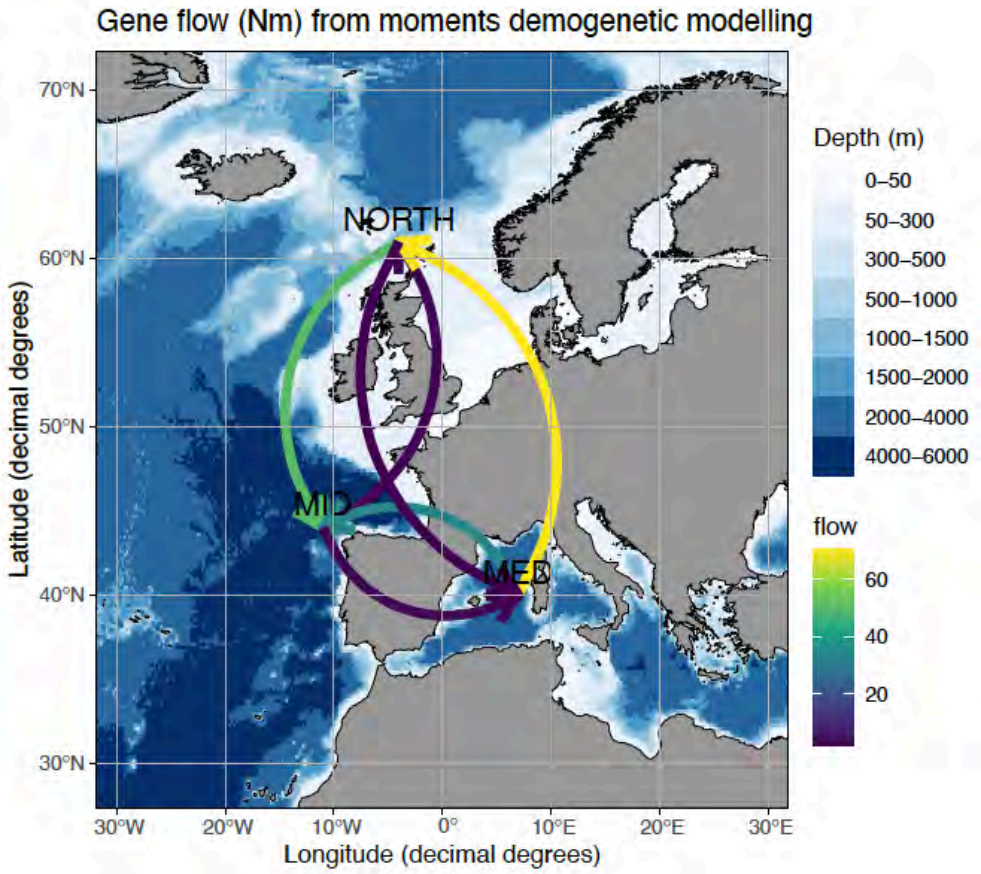

Figure 18. Connectivity map obtained with the software Moments under the best population model of secondary contact. Gene flows are estimated in terms of number of migrants exchanged between three main geographic areas (Celtic Sea, Bay of Biscay and Mediterranean Sea) indicating the presence of two migration routes: one exporting larvae outside the Mediterranean Sea up to the Celtic Sea and the other one moving down from the Celtic Sea to the Bay of Biscay along the European continental margin.

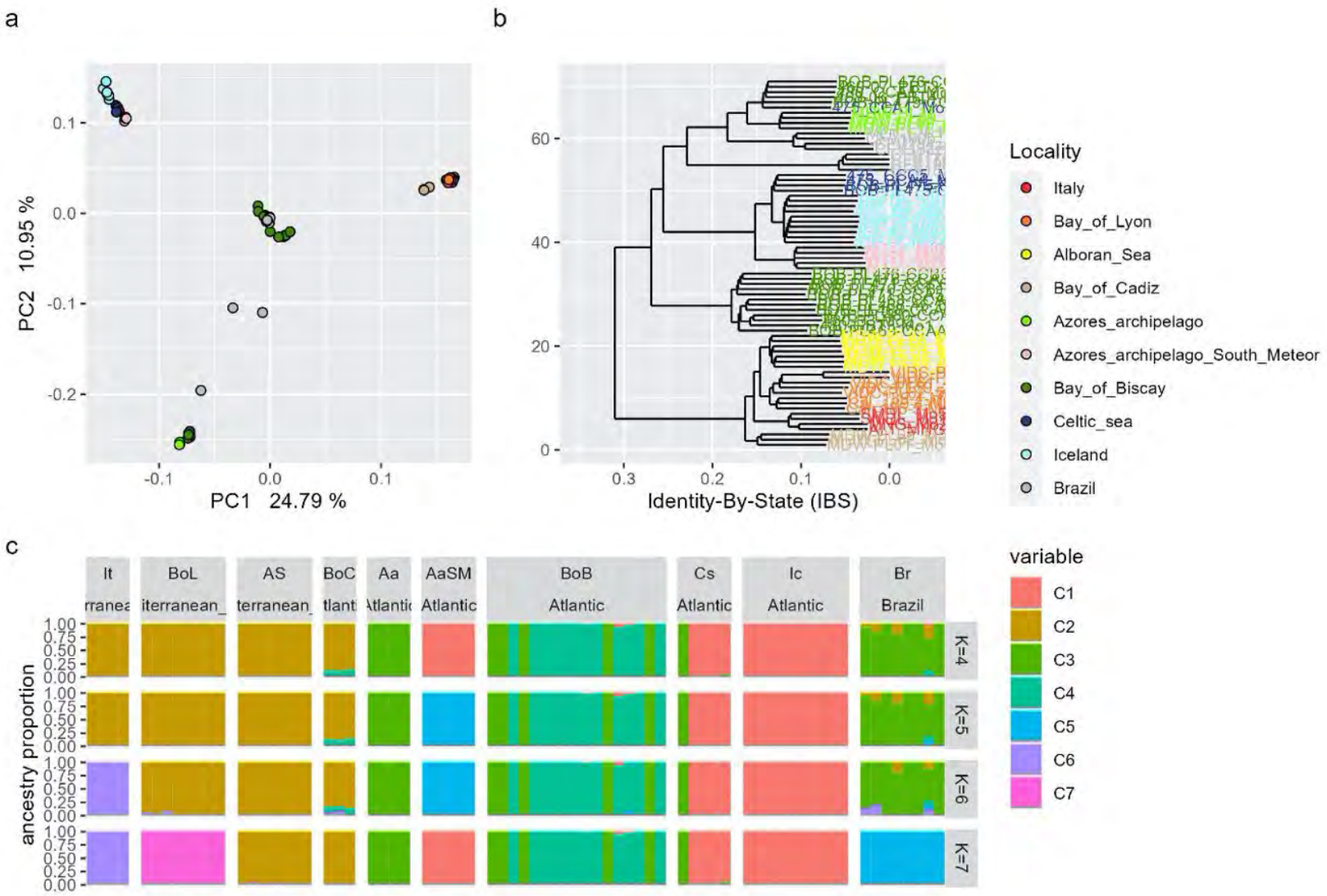

Figure 19. (a) Principal component analysis with the first two components for *M. oculata*. Colour represents localities and each point represents an individual. (b) Identity-by-states dendrogram or similarity between samples. Each leaf represents one individual. (c) Plots of admixture for K = 4 to 7, where individuals are clustered by localities. Each colour bar represents the proportion of the genetic ancestry for each of the inferred clusters.

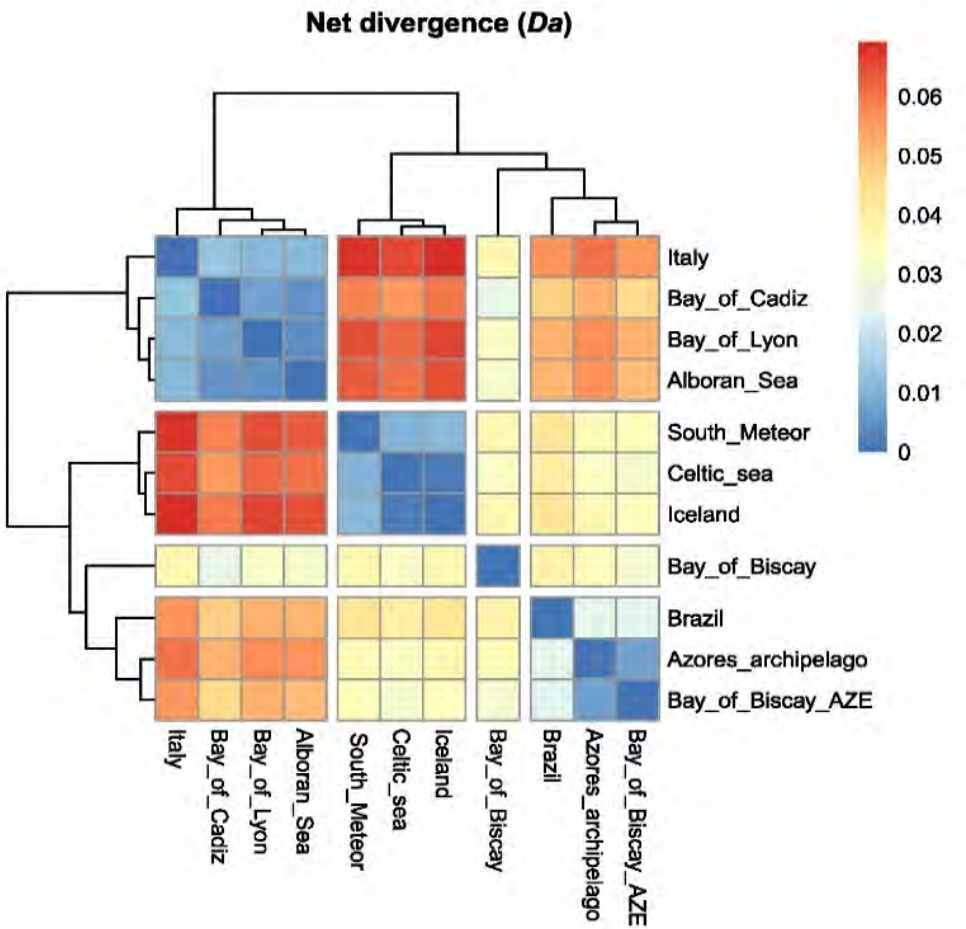

Figure 20. Heatmap and clustering of the net nucleotide divergence (Da) between European margins geographic localities for *M. oculata*.

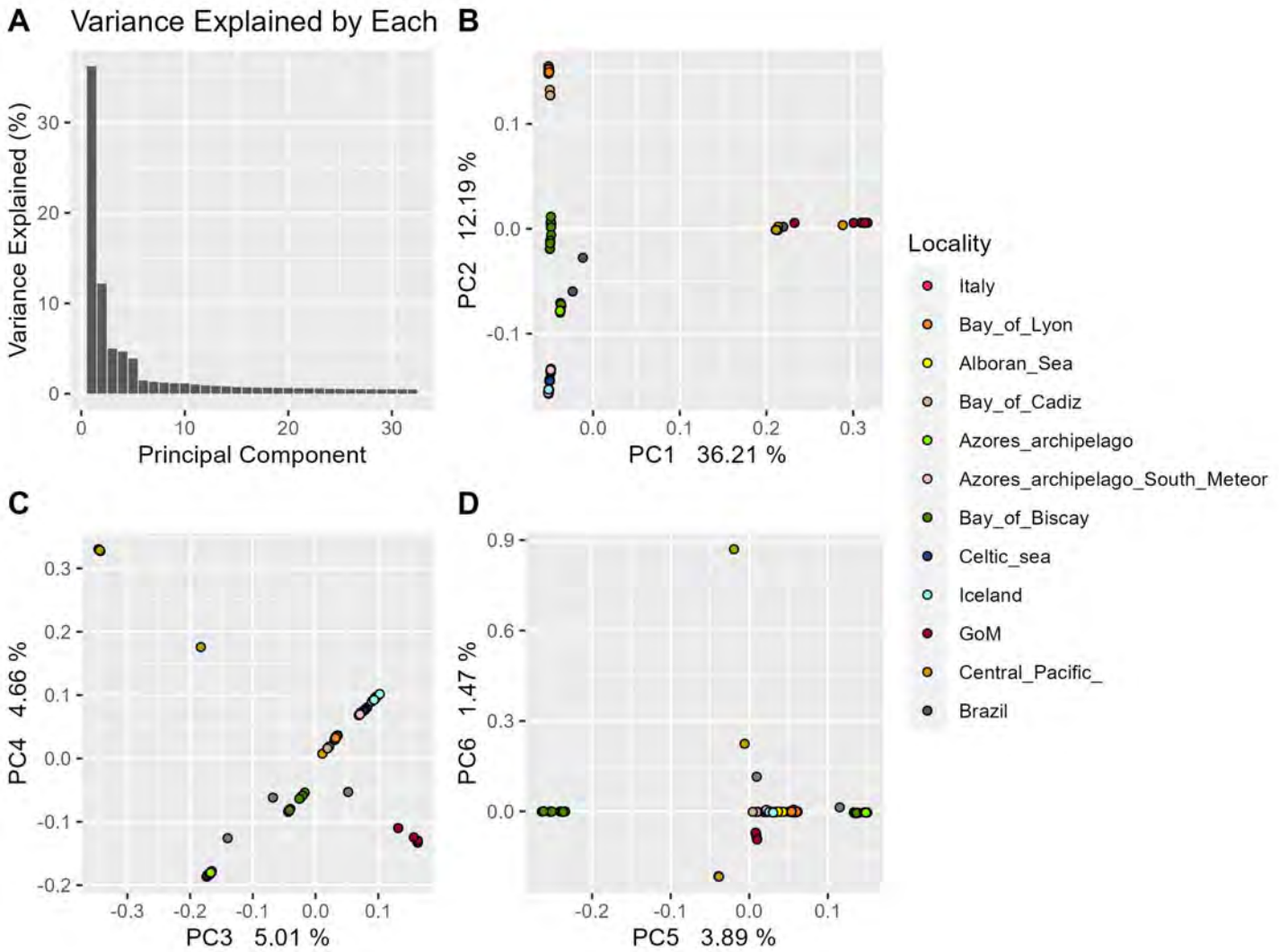

Figure 21. Principal component analysis (PCA) with first six components for *D. pertusum* with West (US margins) and South (Brazilian and South Africa) Atlantic samples. (A) Bar plot of the first 32 principal components and their proportion of variance explained. (B) PCA for the first two components. (C) PCA for the third and fourth components. (D) PCA for the fifth and sixth components. Colour represents localities and each point represents an individual.

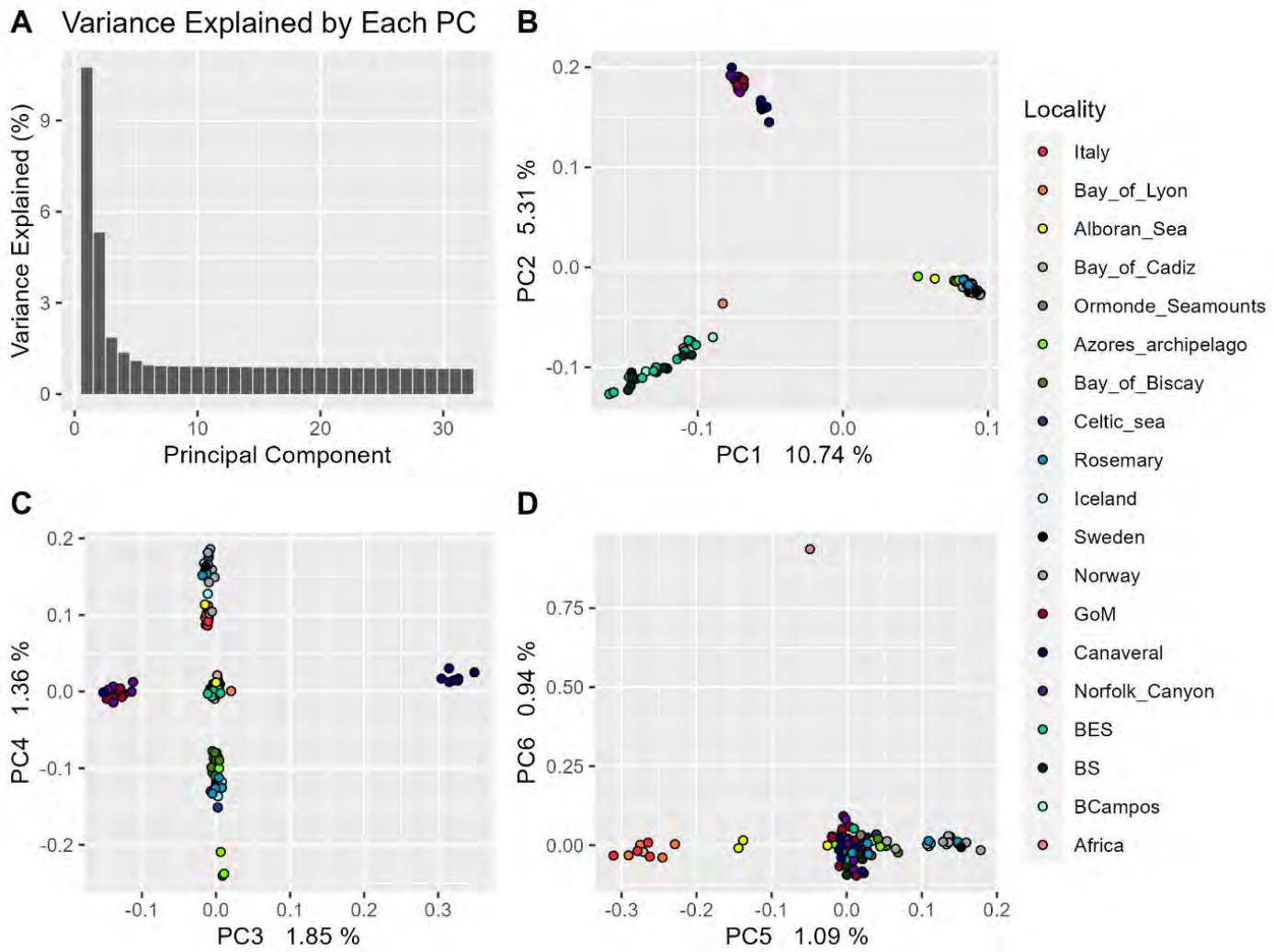

Figure 22. Principal component analysis (PCA) with first six components for *M. oculata* with West (US margins), South (Brazilian) Atlantic and Pacific samples. (A) Bar plot of the first 32 principal components and their proportion of variance explained. (B) PCA for the first two components. (C) PCA for the third and fourth components. (D) PCA for the fifth and sixth components. Colour represents localities and each point represents an individual.

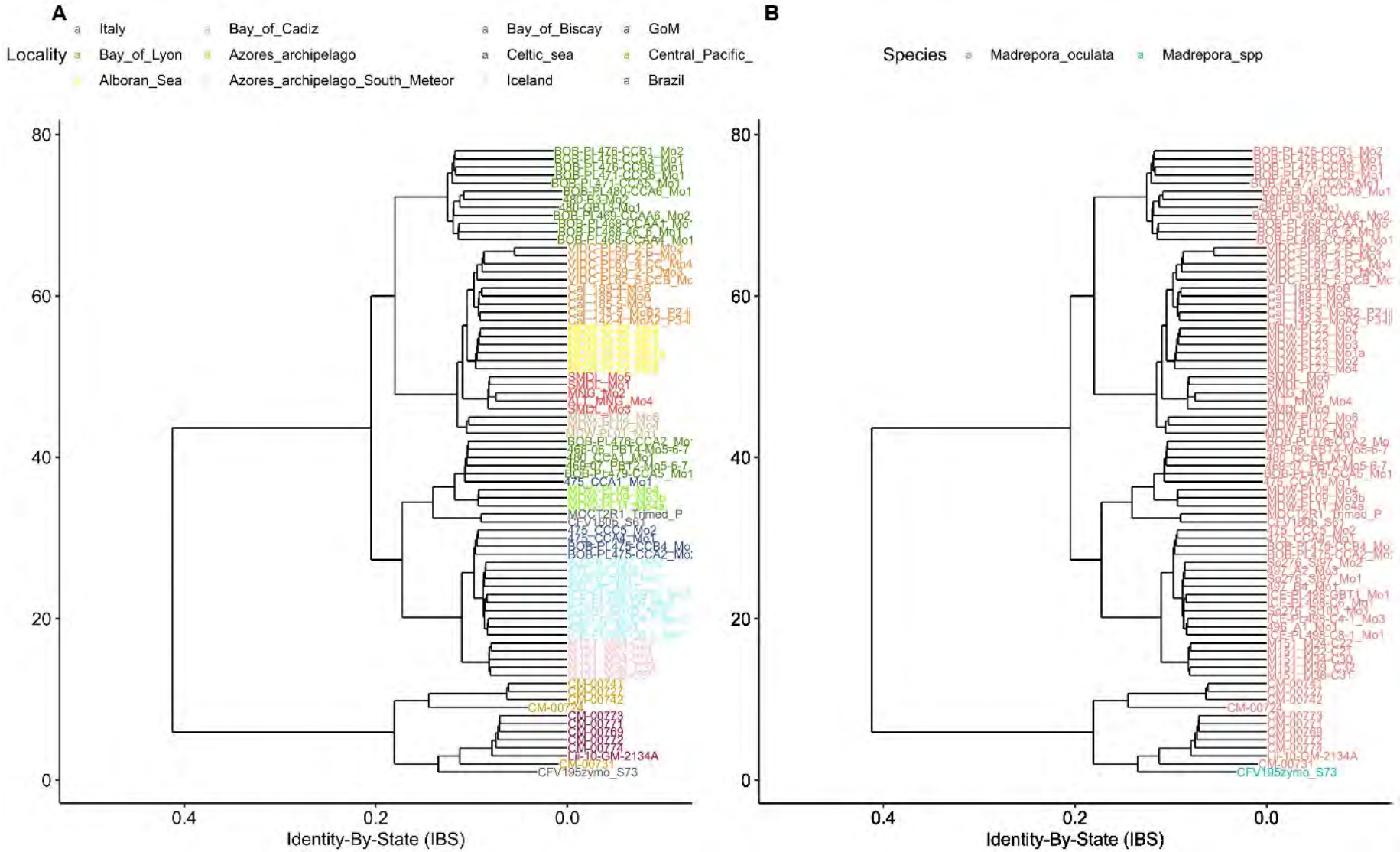

Figure 23. Dendrogram plots of genomic similarity between individual estimated with Identity By State (IBS) for *M. oculata samples*. (A) Colour represents localities. (B) Colour represents species.

4. Discussion and conclusion

For several decades, molecular data obtained on marine fauna have shown that it is often difficult to grasp the concept of biological species on the basis of morphological criteria alone. Species should be considered first and foremost as working hypotheses, especially when they are geographically widespread and have not been the subject of any cross-breeding experiments (Pante et al. 2015). To date, very few studies have assessed the degree of diversification of abyssal species using molecular approaches based on several genes, although some have shown the importance of depth and seabed topology in the diversification of certain taxa (Raupach et al. 2007, Castelin et al. 2012, Pante et al. 2012, 2015, Ritchie et al. 2017, Chan et al. 2020, Mohrbeck et al. 2021). In the deep-sea, very few samples are available, and species biology is poorly understood and it is generally impossible to carry out *in situ* and *in vivo* experiments.

In this deliverable, we therefore propose for the first time an integrated genome-wide study of the genetic differentiation of several emblematic species of three fragmented deep-sea habitats - hydrothermal vents, cold seeps and cold-water coral reefs - to assess both species range and population connectivity within this range at the scale of the Atlantic Ocean. The present genomic data clearly indicate that most of morphological species fall into the grey zone of speciation and form cryptic species complexes that exchange more or less well with each other depending on their degree of genetic and geographic isolation (Roux et al. 2016). In such context, population connectivity is often difficult to trace back as physical barriers to dispersal may be at the same place where genetic barriers could also be positioned leading to complex gene histories possibly leading to a gradient of isolation and gene flow recovery due to secondary contact (Bierne et al. 2011).

Deep sea is made up of collection of isolated genetic entities

Our genetic analyses point toward a clear spatial segregation of nearly all deep-sea species under scrutiny at the scale of the North Atlantic, with the exception of the apparently unique and widely distributed population of *Rimicaris exoculata*. Those differentiated genetic entities span from well-separated cryptic species in cold-water reef corals to geographic isolated populations, possibly evolving toward the formation of new species as observed for the vent and seep molluscs (Vrijenhoek et al. 2009). In all cases, the genetic information that many of the species showed on the basis of morphological data as cosmopolitan are in fact cryptic species complexes or made up of a collection of populations that exchange very little due to physical barriers to dispersal, or even genetic barriers that formed during long-term isolation (Johnson et al. 2008, Plouviez et al. 2009, 2010, 2013, Breusing et al. 2016, Matabos & Jollivet 2019, Tran Lu Y et al. 2023, Poitrimol et al. 2023). Analyses of genomic data and their coupling with larval dispersal simulations for some species show that deep-sea species are in general highly structured at the Atlantic scale if we exclude the atypical case of hydrothermal shrimps (Breusing et al. 2016, Portanier et al. in prep). Long-distance migratory flows, even if they clearly exist, are rare and do not ensure the demographic maintenance of local populations and their genetic re-homogenisation at the species level. This fragmentation of species into more or less distinct genetic entities has major consequences for the management of their populations in the face of the many constraints currently being exerted by man (destruction of reefs by fishing) or planned for the future (deep-sea mining). In particular by combining potential and realised dispersal, one should allow to specify the most probable conditions of larval migration both in terms of positioning and effective duration in the water column (Breusing et al. 2016, 2023, Portanier et al. 2023). Partial genetic isolation of deep-sea species populations however is also a formidable means of tracing past and present migration routes by studying the demographic history of species (preferred routes and directions of flow, isolation with past migration or secondary reconnection with present gene flow).

In the seep mussel populations, genomic data clearly supports the view of two pairs of closely-related species in the genera *Bathymodiolus* and *Gigantidas* with rare long-distance migration events across both the Caribbean Sea and/or the Atlantic Equatorial belt (Portanier et al. 2023). This finding agrees with the previous description of the morphological species *B. heckerae* and *B. boomerang* on one hand, and *G. childressi* and *G. mauritanicus*, on the other hand, that diverged prior to the closing of the Panama Seaway before secondarily meeting around 2 Mya (Portanier et al. 2023). Despite this divergence (quite similar between the two pairs of species) and some possible genetic incompatibilities, the fact that we were able to pick up several F1/F2 hybrids between the Barbados, Gulf of Mexico and the Northeast US Canyons clearly indicate that mussels are able to widely disperse across the Caribbean Sea with the settlement of long-distance dispersers at some locations (North East US Canyons, African coasts) that were able to hybridise with local individuals recently (within one or two generation times).

In hydrothermal vent mussels and gastropods, a strong genetic differentiation of populations was also observed leading to different genetic groups and very low estimates of gene flow between them. Such a situation was previously depicted for the vent mussels with the presence of two distinct morphological species (*B. azoricus* and *B. puteoserpentis*), which were still able to interact through a hybrid zone located at the Broken Spur vent field (29°N) (O'Mullan et al. 2001, Faure et al. 2009). Two additional OTUs were also found in the South Mid-Atlantic Ridge at 5° and 9°S by sequencing their mitochondrial DNA (Van der Heijden et al. 2012), suggesting that, despite a long larval pelagic duration assumed to occur in the surface waters, vent mussels are also in the grey zone of speciation and could represent a complex of closely related species. We found that this complex of mussel species forms geographically isolated populations that separated between 1.7 and 2.5 million years ago, but continue to exchange locally due to the co-occurrence of two hybrid (tension) zones located on either side of the Russian-French mining exploration zones. These new data suggest that these two highly faulted and offset portions of the ridge represent zones of restricted migration. The same situation seems to occur for the vent gastropods *P. smaragdina* and *L. atlanticus*, for which genetic data undeniably indicate that population connectivity is low or null at the scale of the ridge even if secondary contacts are likely to explain some punctual exchanges in the same area of restricted migration (between Rainbow and Broken Spur for *P. smaragdina*). Resilience of these species may be low in the face of mining activities, since low effective migration can be enhanced with mining between 26 and 36°N and may result in the absence of the rescue effect after disturbances. The exploitation of polymetallic sulphides may indeed cause biodiversity and habitat loss for numerous species, changes in seafloor shape and sediment texture, deviation of hydrothermal fluids, creation of sediment plumes, noise and light pollution (Van Dover 2011, Ramirez-Llodra et al. 2011, Gollner et al. 2017). All these factors may in turn have impacts on larvae circulation and resilience of species (Levin et al. 2016, Morato et al. 2020). Connectivity and the degree to which populations are exchanging migrants thus need to be accounted for in the design of protected areas (Balbar & Metaxas 2019) and in the authorisation of mining exploitation. Isolated populations (e.g. Moytirra for *P. smaragdina*, or 5°S and Broken Spur for *L. atlanticus*) may not be able to recover from disturbances caused by mining and should be managed independently. The fact that nearly all retained models were however SC models may suggest that populations previously isolated are being reconnected to some extent. The initial isolation may be the result of physical barriers to gene flow such as fracture zones or large areas of less venting activity. For instance, the Azorean triple junction point or the Kurchatov and Pico fracture zones may represent topographic impediments to gene flow between Moytirra and Lucky Strike populations for *P. smaragdina*. Similarly, the Oceanographers, Atlantis or Hayes fracture zones may represent physical barriers between Rainbow and Broken Spur, for *B. azoricus*, *P. smaragdina* and *L. atlanticus*. The co-occurrence of the Vema or Romanche fracture zones can also explain the genetic break observed for *L. atlanticus* between the northernmost and the southernmost parts of the ridge, which coincide with the break observed

between *B. puteoserpentis* and the south MAR *Bathymodiolus* species and the presence of a hybrid zone at 5°S (Van der Heijden et al. 2012, Breusing et al. 2016, present data).

The population genomics study on two emblematic cold-water coral species on the European margin also provides new information on their phylogeography, and strikingly on their taxonomy as they are in fact a complex of several distinct species hitherto not recognised as distinct base on their morphology. First, our analyses support the evidence of three genetic lineages along the European Atlantic margin and the Mediterranean Sea. *Madrepora* genomic analyses revealed some kind of parallelism of divergence, while being much more pronounced. Firstly, it appears that *M. oculata* reefs along the European coast shelter a complex of distinct cryptic species and preliminary analyses clearly show that this is also the case at a wider scale, where two already recognised species co-exist within localities in Brazil, and North West Atlantic (US margins) samples of *M. oculata* are probably actually *M. piresae* sp. nov (Capel et al., 2023). The addition of more samples from the Pacific Ocean suggests the existence of another divergent lineage of this newly described *Madrepora* species.

The case of *D. pertusum* is a bit different, as a clear structure is observed on the Atlantic scale, but genomic divergence is less strong than the one observed on the European scale for *M. oculata*, suggesting *D. pertusum* may still be considered as encompassing very differentiated or isolated populations across the Mediterranean and Atlantic.

The levels of divergence for *Madrepora* are well above those typifying the grey zone of speciation in animals (Roux et al. 2016). These major results are consistent with previous results obtained by Boavida et al. (2019) where the population structure and differentiation estimated between *Madrepora* lineages was important. The most divergent cryptic lineages appear to be those from the Mediterranean, extending as far as the Bay of Cádiz at the entrance to the Mediterranean on the Atlantic side. The North-East Atlantic lineages are slightly less divergent but remains still too divergent to be simply considered as isolated populations of a single species (Roux et al. 2016). The other localities and lineages show clear divergence and differentiation, with the exception of the Bay of Biscay. This latter locality shelters a mosaic of genetic lineages, with one dominant lineage and a few individuals with a distinct genetic signature otherwise retrieved in the Azores. We therefore showed that the species *M. oculata*, currently considered to be a single morphological species across the European margin, is in fact a highly divergent cryptic species complex. This partition of morphological cold-water coral species has therefore strong implications in terms of species conservation, management and connectivity, revealing the need to re-evaluate dispersal patterns across the scale of each genetic entity. The impressive and remarkable mosaic of cryptic species for *Madrepora* at restricted regional scale, also provides evidence for a complex phylogeographic history of species as the result of past climatic events (i.e. glacial episodes with several refugia), highlighting the need to re-evaluate habitat suitability and dispersal models. Although counter-intuitive, this juxtaposition of divergent *Madrepora* lineages along the European margin could indicate that this later species was able to recolonise the North-East Atlantic Ocean more rapidly than *Desmophyllum*, would these corals have shared the same glacial refugia.

Pathways of migration and connectivity maps

Our genomic analyses were used to produce both past and present-day connectivity maps in order to better highlight the main dispersal corridors for this specific benthic fauna. These data will be valuable in the conservation biology of species from highly fragmented deep-sea environments and their putative evolution in the face of deep-sea mining and global warming with its associated modification of the oceanic circulation. In particular by combining potential and realised dispersal, we can now better specify the most probable conditions of larval migration both in terms of positioning and effective duration in the water column. Nearly all genomic datasets fitted a secondary contact population model

allowing us to estimate recent to contemporary gene flows using the dadi/moments software. Results obtained from these methods were not always in agreement with those estimated using DivMigrate, suggesting that some patterns of connectivity may have changed with time. DivMigrate produced oriented Fst-based gene flows that are the result of migrant exchanges over a more integrated period of time. In this respect, maps bear the imprint of the most recent part of the species' dispersal history, which often dates back to the last glacial maximum.

For seep mussels, they clearly indicate colonisation patterns from the Caribbean Sea and the Gulf of Mexico to the Northeast US canyons with some rare but past genetic (mitochondrial) exchanges across the Atlantic (Portanier et al. 2023). This finding agreed with the clear spatial segregation of mussel populations at the scale of the North Atlantic and the co-existence of two pairs of geographic mussel species that diverged prior to the closing of the Panama Seaway (Atlantic outflow in the Pacific) but met again after this closing two to three Mya following the newly emerged Atlantic circulation (beginning of the AMOC reinforcement, 4.5 Mya: Haug & Tiedemann 1998). Rare long-distance migration events clearly occur nowadays across the Caribbean Sea for both seep mussels *Gigantidas* and *Bathymodiolus* and were validated by the finding of F1/F2 hybrids along the Northeast US coast. Present-days long-distance migration was however not validated by the genomic data along the Atlantic Equatorial belt in contrast to the expectations of the larval dispersal simulations done along the South American coast in which trans-Atlantic larval transportations by surface waters were strong and able to reach the African coast (Portanier et al. 2023). As *G. childressi* larvae have been collected in the first 200 m depth (Arellano et al. 2011), this could be explained by the sea surface temperature which may be too high for the survival of mussel larvae above the thermocline at the Equator as sensitivity to temperature may be great for larvae of abyssal species (Tyler & Dixon 2000, Arellano et al. 2014). However, larvae may stay for a restricted proportion of their PLD in surface waters with a possible long period of descent that needs to be adjusted in larval dispersal models.

For the species complex of vent shrimp *hybisae/chacei*, DivMigrate flows are also clearly oriented from the Caribbean Sea to the Mid-Atlantic Ridge suggesting a recent colonisation of the MAR sites by *R. hybisae*. Unlike *R. chacei*, *R. hybisae*, initially described from the Caiman Ridge, forms swarms around 'black smoker' chimneys and represents the ecological analogous of the MAR shrimp *R. exoculata*, with an enlarged cephalothorax bearing a well-developed Campylobacteria epibiosis (Nye et al. 2012, Versteegh et al. 2023). The unexpected genomic finding that *R. hybisae* and *R. chacei* belong to the same species may explain why *R. chacei*, present on MAR sites, has a reduced cephalothoracic epibiosis and failed to occupy the ecological niche presently associated with the other shrimp species *R. exoculata* (Methou et al. 2020, 2023). If recent, the arrival of *R. hybisae* to become *R. chacei* on the MAR vent sites may have indeed forced this species to adapt to new vent conditions at the base of the vent edifices where venting is less strong and diffuse because of its trophic competition with *R. exoculata*: an ecological situation that remains to be tested. Analysing the genetic structure of the species complex *hybisae/chacei* as a single species indicated that, despite massive exchanges between populations, the main present-days flow is northward, feeding vent sites of the Azorean triple junction, from where a significant proportion of juveniles are likely to return to the Caiman Ridge in the Caribbean Sea. Such a coupling between the Mid-Atlantic Ridge and the Cayman Ridge is however interesting as it may explain why most of the large *chacei* juvenile populations are collapsing at TAG and Snake Pit with the presence of very few reproductive adults in the vicinity of 'black smoker' chimneys (Methou et al. 2023). The presence of massive populations of *R. chacei* juveniles at TAG, Snake Pit or Broken spur that could then migrate elsewhere to swarms at vents where *R. exoculata* is absent could represent a strong argument to protect these zones from deep-sea mining.

Conversely, the main flow direction along the Mid-Atlantic Ridge is southward for both the vent mussels and the vent gastropods (Faure et al. 2009, Breusing et al. 2016, Portanier et al. in prep, present study). Genetic exchanges appear to be very low if not null between populations of vent gastropods, suggesting that dispersal strategies should greatly differ between vent species. The southward direction of gene flow suggest that gastropods may use intermediate waters to disperse. However, even if to a lower extent, gene flow estimates were not null in the northward direction. This was particularly true for *P. smaragdina*, for which a hybrid zone with F1/F2 hybrids and the two parental types were found at the Rainbow site. The formation of a tension zone (as opposed to the mosaic hybrid zone found in *Mytilus edulis/M. galloprovincialis*: Bierne et al. 2003) is often indicative of a stepping-stone model of colonisation, within which hybrids are often positioned in the area of less migration (Bierne et al. 2011). This can suggest that larvae may be constrained to travel with deeper currents close to the bottom and not in shallow waters: a situation more likely expected for the vent mussels. It is noteworthy that genetic structure was lower and gene flow estimates higher for *P. smaragdina* than for *L. atlanticus*. This is surprising since *L. atlanticus* was expected to have a longer PLD thanks to a planktotrophic larval development while *P. smaragdina* larvae are hypothesised to have a lecithotrophic development (Lutz et al. 1986, Matabos & Thiébault 2010, Matabos & Jollivet 2019). Differences in the number of larvae produced (fecundity), the proportion of larvae using upper and faster currents, or other factors may be responsible of such an observation. One hypothesis may be that a higher proportion of *P. smaragdina* larvae are using intermediate currents than what occur for *L. atlanticus*.

In the cold-water coral reefs, analyses of whole genome data revealed unexpected and different patterns of dispersal along European coast. The two deep-water corals *D. pertusum* and *M.oculata* display indeed very different geographic architecture, suggesting different ways of dispersing, and confirm previous studies done with mitochondrial markers and microsatellites (Le Goff-Vitry et al. 2004, Boavida et al. 2019). At a first glance, *M. oculata* clearly represent a mosaic of assemblages formed by several divergent cryptic species that superimpose at some locations such as the Bay of Biscay and the Azorean archipelago. Although estimating migration events between *M. oculata* populations was not possible with our present sample sizes and the diversification of this complex of cryptic species, the co-occurrence of several genetic lineages along the continental slope may be an indication of rapid population expansions from several glacial refugia that led to a fast recolonisation event in this area. Such mosaic of cryptic species may be therefore the reflection of some propensity to disperse over a much more important geographic range. However, this mosaic of lineages has been only observed in the Bay of Biscay, suggesting that despite this possible propensity to disperse, these lineages still remain mainly geographically segregated. By contrast, *D. pertusum* is also sub-divided in less divergent genetic units, but these groups or populations are more geographically segregated. The presence of three genetic lineages (MED, MID and NORTH) could be explained also by a complex phylogeographic history, with the existence of an ancestral lineage of the MED and NORTH lineages along the European coasts: the Mediterranean lineage indeed shares more genetic background with the NORTH lineage than the MID. This ancestral lineage was likely isolated by the last glacial maximum (LGM) along the European coasts. After the LGM, another and more divergent genetic lineage (MID) may have recolonised the Bay of Biscay from the South, possibly with the reinforcement of the AMOC. This third lineage possibly originating from off the Atlantic coast of Africa was able to secondarily come into contact with the NORTH lineage at the level of the Celtic Sea. This scenario could explain both the polymorphism shared by the MED and NORTH lineages and their isolation and divergence with the MID lineage. Nevertheless, additional samples and more detailed analyses are needed to draw conclusions about these possible hypotheses. A demo-genetic analysis, although tricky using moments, was however done by assigning individuals to these three genetic groups and pointed to a strong northward flow from the Mediterranean Sea to the Celtic Sea, in line with the Mediterranean Outflow water, suggesting that

Mediterranean and the NORTH populations may share genomic background still unsorted by the genetic drift (e.g. with no clear dichotomy in a phylogenetic reconstruction) in the face of migration. Gene flows out of the Mediterranean Sea should therefore indicate that *D. pertusum* larvae are probably not transported by surface water-masses. This finding fully agrees with the study done by Henry et al. (2014) who, using elemental fingerprints in fossil records, the sediment archive of the AMOC strength and historic gene flow, postulated that the cold-water reef coral *D. pertusum* had a rapid post glacial range expansion along the European continental slope fuelled by the Mediterranean Outflow Water after the Younger Dryas 11.6 kyr ago.

In terms of population connectivity, these preliminary results suggest limited exchanges between the three geographic groups of *D. pertusum*. First, it appears that the MED lineage is isolated from the two others, while MID and NORTH are found to live in sympatry at few localities off the Ireland coast. Additionally distinct clonal colonies found in the dataset and F_{is} estimation revealed that clonal reproduction is possibly non-negligible as suggested by the modelling of Stoeckel et al. (2021). While our results and study provide some strong evidence of restricted dispersal, data are still currently analysed to better contain dispersal corridors. On the one hand, the genomic results obtained for *D. pertusum* suggest that a non-negligible fraction of shared polymorphism is retained between lineages even after being isolated prior to the last glacial episodes, potentially due to the effect of clonality. On the other hand, they also show that these lineages possibly found in sympatry, are not able to exchange much of their genetic background as could be expected in the absence of reproductive incompatibility (at least partial).

Although pan-Atlantic analyses are only preliminary, it seems that the *D. pertusum* phylogeographic pattern of differentiation of the three major lineages (South, West, East Atlantic) could be related to the AMOC, where West Atlantic localities are closer genetically to each other than to the East (the European margin). On the other hand, for *M. oculata*, it is much more difficult to interpret data due to the existence of highly divergent genetic lineages and cryptic species at different geographic scales (oceanic and regional), leaving an incomplete sampling to assess connectivity among conspecific populations.

In conclusion, the patterns of connectivity of Atlantic abyssal species, whether migration occurred in the recent past of populations or is more contemporary, seem to correspond to the general trend of water masses circulation in the Atlantic (Gary et al. 2020, Biastoch et al. 2021), whatever the deep-sea habitat studied (hydrothermal vents, seeps, reefs on continental slopes). As far as species from deep hydrothermal vents are concerned, migratory flows are mainly directed southwards in the North Atlantic and probably in the opposite direction in the South Atlantic, at least for the vent bathymodiolins following the general circulation pattern of the North Atlantic drift (Biastoch et al. 2021). Following this trend, it is therefore quite possible that most of the larvae are not necessarily transported in surface waters but rather entrained in the sinking vein of AMOC waters located along the Mid-Atlantic Ridge as already shown by Breusing et al. (2016) and Yearsley et al. (2020) with dispersal restricted to tens to hundreds of kilometres: a situation clearly highlighted by the low levels of gene flow estimated here for nearly all species. The only exception to this rule is the hydrothermal vent shrimp, which tend to migrate in a northerly direction, with the *chacei/hybisae* species potentially returning to the Caribbean Sea, and therefore migrating against the Gulf Stream. This is contradictory to the cold seep mussels whose larvae seem to be transported from the Gulf of Mexico towards the North-eastern coast of United States. This oddity is probably explained by the active migratory behaviour of post-larvae or juvenile shrimp near the bottom, although the lack of genetic differentiation of their populations over the Mid-Atlantic Ridge prevents us from validating with certainty a particular direction of migration at this spatial scale. In cold-seep mussels of the genera *Bathymodiolus* and *Gigantidas*, migration patterns clearly follow the North

Atlantic drift across the Caribbean Sea, confirming the hypothesis of larvae being driven towards the surface as proposed by Arellano et al. (2011, 2014) and Young et al. (2012). However, long-distance migrations seem to be rare and do not appear to be sufficiently effective in re-homogenising populations located on either side of the Caribbean Sea or the Atlantic Equatorial Belt. Such a hypothesis of restricted dispersal with rare long-range dispersal has been proposed by Benestan et al. (2021) to explain some discrepancies between population genetic analyses and larval dispersal modelling of several species in the Mediterranean Sea. In our specific case, demo-genetic models and the presence of F1/F2 hybrids on the North-East coast of the USA clearly support a recent history of secondary contacts. Having this in mind, it is also possible that crosses with long-distance recruits are strongly counter-selected by the establishment of genetic barriers during the period of isolation of these populations in allopatry during the last glaciations or, even dating back to the Isthmus of Panama closure about 2.8 Mya (O'Dea et al. 2016). This barrier to migration, whether physical (by the distance to be covered and/or the hydrodynamic regime encountered by larvae at the travelling depth) or genetic (emergence of genetic incompatibilities), appears to be even greater in deep-water corals, with the presence of highly divergent cryptic species. Even if larval dispersal modelling was likely to predict some possibility for trans-Atlantic migration for *D. pertusum* with realistic pelagic larval duration at the surface of the ocean (Gary et al. 2020), there may be genomic incompatibilities limiting the realised dispersal among those distinct lineages. In fact, in the particular case of cold-water corals, the notion of cosmopolitan species, as initially suggested by the morphological data, seems to be meaningless and raises questions about the scale of conservation measures in the absence of rescue effect, and the regional management of reefs in the face of global warming and deep trawling.

5. References

Alexander, D. H., Novembre, J., & Lange, K. (2009). Fast model-based estimation of ancestry in unrelated individuals. *Genome research*, *19*(9), 1655-1664. http://www.genome.org/cgi/doi/10.1101/gr.094052.109

Andersen, A. C., Hourdez, S., Marie, B., Jollivet, D., Lallier, F. H., & Sibuet, M. (2004). *Escarpia southwardae*, a new species of vestimentiferan tubeworm (Annelida, Siboglinidae) from West-African cold seeps. *Journal of Canadian Zoology*, 82, 980-999. https://doi.org/10.1139/z04-049

Arellano, S. M., Van Gaest, A. L., Johnson, S. B., Vrijenhoek, R. C., & Young, C. M. (2014). Larvae from deep-sea methane seeps disperse in surface waters. *Proceedings of the Royal Society B: Biological Sciences*, *281*(1786), 20133276. https://doi.org/10.1098/rspb.2013.3276

Arellano, S. M., & Young, C. M. (2011). Temperature and salinity tolerances of embryos and larvae of the deep-sea mytilid mussel "*Bathymodiolus*" *childressi*. *Marine biology*, *158*, 2481-2493. https://doi.org/10.1007/s00227-011-1749-9

Ayata, S. D., Lazure, P., & Thiébaut, É. (2010). How does the connectivity between populations mediate range limits of marine invertebrates? A case study of larval dispersal between the Bay of Biscay and the English Channel (North-East Atlantic). *Progress in Oceanography*, *87*(1-4), 18-36. https://doi.org/10.1016/j.pocean.2010.09.022

Balbar, A. C., & Metaxas, A. (2019). The current application of ecological connectivity in the design of marine protected areas. *Global Ecology and Conservation*, *17*, e00569. https://doi.org/10.1016/j.gecco.2019.e00569

Bayer, S. R., Mullineaux, L. S., Waller, R. G., & Solow, A. R. (2011). Reproductive traits of pioneer gastropod species colonizing deep-sea hydrothermal vents after an eruption. *Marine biology*, *158*, 181-192. https://doi.org/10.1007/s00227-010-1550-1

Benestan, L., Fietz, K., Loiseau, N., Guerin, P. E., Trofimenko, E., Rühs, S., ... & Manel, S. (2021). Restricted dispersal in a sea of gene flow. *Proceedings of the Royal Society B*, *288*(1951), 20210458. https://doi.org/10.1098/rspb.2021.0458

Biastoch, A., Schwarzkopf, F. U., Getzlaff, K., Rühs, S., Martin, T., Scheinert, M., ... & Böning, C. W. (2021). Regional imprints of changes in the Atlantic Meridional Overturning Circulation in the eddy-rich ocean model VIKING20X. *Ocean Science*, *17*(5), 1177-1211. https://doi.org/10.5194/os-17-1177-2021

Bierne, N., Borsa, P., Daguin, C., Jollivet, D., Viard, F., Bonhomme, F., & David, P. (2003). Introgression patterns in the mosaic hybrid zone between *Mytilus edulis* and *M. galloprovincialis*. *Molecular Ecology*, *12*(2), 447-461. https://doi.org/10.1046/j.1365-294X.2003.01730.x

Bierne, N., Welch, J., Loire, E., Bonhomme, F., & David, P. (2011). The coupling hypothesis: why genome scans may fail to map local adaptation genes. *Molecular ecology*, *20*(10), 2044-2072. https://doi.org/10.1111/j.1365-294X.2011.05080.x

Blazewicz-Paszkowycz, M., Bamber, R., & Anderson, G. (2012). Diversity of Tanaidacea (Crustacea: Peracarida) in the world's oceans–how far have we come? *PLoS One*, *7*(4), e33068. https://doi.org/10.1371/journal.pone.0033068

Boavida, J. R. H., Becheler, R., Choquet, M., Frank, N., Taviani, M., Bourillet, J. F., et al. (2019). Out of the Mediterranean? post-glacial colonization pathways varied among cold-water coral species. *J. Biogeogr.* 46, 915– 931. https://doi.org/10.1111/jbi.13570

Brandt, A., Błażewicz-Paszkowycz, M., Bamber, R. N., Mühlenhardt-Siegel, U., Malyutina, M. V., Kaiser, S., ... & Havermans, C. (2012). Are there widespread peracarid species in the deep sea (Crustacea: Malacostraca)?. *Polish Polar Research*, 139-162. https://doi.org/10.2478/v10183-012-0012-5

Brasier, M. J., Wiklund, H., Neal, L., Jeffreys, R., Linse, K., Ruhl, H., & Glover, A. G. (2016). DNA barcoding uncovers cryptic diversity in 50% of deep-sea Antarctic polychaetes. *Royal Society open science*, *3*(11), 160432. https://doi.org/10.1098/rsos.160432

Breusing, C., Biastoch, A., Drews, A., Metaxas, A., Jollivet, D., Vrijenhoek, R. C., ... & Reusch, T. B. (2016) Biophysical and population genetic models predict presence of "phantom" stepping stones connecting Mid-Atlantic Ridge vent ecosystems. *Current Biology*, 26(17), 2257-2267. http://dx.doi.org/10.1016/j.cub.2016.06.062

Breusing, C., Johnson, S. B., Mitarai, S., Beinart, R. A., & Tunnicliffe, V. (2023). Differential patterns of connectivity in Western Pacific hydrothermal vent metapopulations: A comparison of biophysical and genetic models. *Evolutionary Applications*, *16*(1), 22-35. https://doi.org/10.1111/eva.13326

Breusing, C., Johnson, S. B., Tunnicliffe, V., Clague, D. A., Vrijenhoek, R. C., & Beinart, R. A. (2020). Allopatric and sympatric drivers of speciation in *Alviniconcha* hydrothermal vent snails. *Molecular Biology and Evolution*, *37*(12), 3469-3484. https://doi.org/10.1093/molbev/msaa177

Capel, K.C., Zilberberg, C., Carpes, R.M., Morrison, C.L., Vaga, C.F., Quattrini, A.M., Quek, R.Z., Huang, D., Cairns, S.D. and Kitahara, M.V. (2024). How long have we been mistaken? Multi-tools shedding light into the systematics of the widespread deep-water genus *Madrepora* Linnaeus, 1758 (Scleractinia). *Molecular Phylogenetics and Evolution*, *191*, 107994. https://doi.org/10.1016/j.ympev.2023.107994

Castel J., Hourdez S., Pradillon F., Daguin-Thiébaut C., Ballenghien M., Ruault S., Corre E., Tran Lu Y A., Mary J., Comtet T., Gagnaire P.-A., Bonhomme F., Bierne N., Breusing C., Broquet T., Jollivet D. 2022. Inter-specific genetic exchanges despite strong divergence in deep-sea hydrothermal vent gastropods of the genus *Alviniconcha. Genes, special issue: Feature Papers in Population and Evolutionary Genetics and Genomics*. *13*, 985. https://doi.org/10.3390/genes13060985

Castelin, M., Lorion, J., Brisset, J., Cruaud, C., Maestrati, P., Utge, J., & Samadi, S. (2012). Speciation patterns in gastropods with long-lived larvae from deep-sea seamounts. *Molecular Ecology*, *21*(19), 4828-4853. https://doi.org/10.1111/j.1365-294X.2012.05743.x

Catchen, J., Hohenlohe, P.A., Bassham, S., Amores, A. & Cresko, W.A. (2013). Stacks: an analysis tool set for population genomics. *Molecular Ecology* **22**: 3124–3140. https://doi.org/10.1111/mec.12354

Cayuela, H., Rougemont, Q., Prunier, J. G., Moore, J. S., Clobert, J., Besnard, A., & Bernatchez, L. (2018). Demographic and genetic approaches to study dispersal in wild animal populations: A methodological review. *Molecular ecology*, *27*(20), 3976-4010. https://doi.org/10.1111/mec.14848

Chan, J., Pan, B., Geng, D., Zhang, Q., Zhang, S., Guo, J., & Xu, Q. (2020). Genetic diversity and population structure analysis of three deep-sea amphipod species from geographically isolated hadal trenches in the Pacific Ocean. *Biochemical genetics*, *58*, 157-170. https://doi.org/10.1007/s10528-019-09935-z

Chevaldonné, P., Jollivet, D., Vangriesheim, A. & Desbruyères, D. (1997). Hydrothermal-vent alvinellid polychaete dispersal in the eastern Pacific. I. Influence of vent-site distribution pattern, bottom currents and biological features. *Limnology and Oceanography*, **42**, (1), 67-80. https://doi.org/10.4319/lo.1997.42.1.0067

Daguin-Thiébaut, C., Ruault, S., Roby, C., Broquet, T., Viard, F. & Brelsford, A. (2021). Construction of individual ddRAD libraries. *protocols.io*, https://doi.org/10.17504/protocols.io.bv4tn8wn

Dayton, P. K., & Hessler, R. R. (1972, March). Role of biological disturbance in maintaining diversity in the deep sea. In *Deep Sea Research and Oceanographic Abstracts* (Vol. 19, No. 3, pp. 199-208). Elsevier. https://doi.org/10.1016/0011-7471(72)90031-9

Doebeli, M., & Ruxton, G. D. (1997). Evolution of dispersal rates in metapopulation models: branching and cyclic dynamics in phenotype space. *Evolution*, *51*(6), 1730-1741. https://doi.org/10.1111/j.1558-5646.1997.tb05097.x

Faure B., Jollivet, D., Tanguy, A., Bonhomme, F., & Bierne**,** N. (2009). Speciation in the deep sea: Multi-locus analysis of divergence and gene flow between two hybridizing species of hydrothermal vent mussels*.* PlosOne, 4(8): e6485. https://doi.org/10.1371/journal.pone.0006485

Folmer, O., Hoeh, W. R., Black, M. B., & Vrijenhoek, R.C. (1994). Conserved primers for PCR amplification of mitochondrial DNA from different invertebrate phyla. *Molecular Marine Biology and Biotechnology*, *3*(5), 294-299.

France, S. C., Hessler, R. R., & Vrijenhoek, R. C. (1992). Genetic differentiation between spatially-disjunct populations of the deep-sea, hydrothermal vent-endemic amphipod *Ventiella sulfuris*. *Marine Biology*, *114*(4), 551-559. https://doi.org/10.1007/BF00357252

Gagnaire, P. A. (2020). Comparative genomics approach to evolutionary process connectivity. *Evolutionary Applications*, *13*(6), 1320-1334. https://doi.org/10.1111/eva.12978

Gagnaire, P. A., & Gaggiotti, O. E. (2016). Detecting polygenic selection in marine populations by combining population genomics and quantitative genetics approaches. *Current Zoology*, *62*(6), 603-616. https://doi.org/10.1093/cz/zow088

Gagnaire, P. A., Lamy, J. B., Cornette, F., Heurtebise, S., Dégremont, L., Flahauw, E., ... & Lapegue, S. (2018). Analysis of genome-wide differentiation between native and introduced populations of the cupped oysters *Crassostrea gigas* and *Crassostrea angulata*. *Genome biology and evolution*, *10*(9), 2518-2534. https://doi.org/10.1093/gbe/evy194

Gary, S. F., Fox, A. D., Biastoch, A., Roberts, J. M., and Cunningham, S. A. (2020). Larval behaviour, dispersal and population connectivity in the deep sea. *Scientific Reports,* 10 (1), 1–12. https://doi.org/10.1038/s41598-020-67503-7

Génio et al. (2008) New record of "*Bathymodiolus*" *mauritanicus* Cosel 2002 from the Gulf of Cadiz (NE Atlantic) mud volcanoes. *Journal of Shellfish Research*, 27(1), 53-61. https://doi.org/10.2983/0730-8000(2008)27[53:NROBMC]2.0.CO;2

Gollner, S., Kaiser, S., Menzel, L., Jones, D. O., Brown, A., Mestre, N. C., ... & Arbizu, P. M. (2017). Resilience of benthic deep-sea fauna to mining activities. *Marine Environmental Research*, *129*, 76-101. https://doi.org/10.1016/j.marenvres.2017.04.010

Grassle, J. F. (1989). Species diversity in deep-sea communities. *Trends in Ecology & Evolution*, *4*(1), 12-15.

Gutenkunst, R. N., Hernandez, R. D., Williamson, S. H., & Bustamante, C. D. (2009). Inferring the Joint Demographic History of Multiple Populations from Multidimensional SNP Frequency Data. *PLoS Genetics*, 5(10), e1000695. https://doi.org/10.1371/journal.pgen.1000695

Hilario et al. (2011) New perspectives on the ecology and evolution of siboglinid tubeworms. *PloS One*, 6(2), e16309. https://doi.org/10.1371/journal.pone.0016309

Hamilton, W. D., & May, R. M. (1977). Dispersal in stable habitats. *Nature*, *269*(5629), 578-581. https://doi.org/10.1038/269578a0

Handal, W., Szostek, C., Hold, N., Andrello, M., Thiébaut, E., Harney, E., ... & Charrier, G. (2020). New insights on the population genetic structure of the great scallop (*Pecten maximus*) in the English Channel, coupling microsatellite data and demogenetic simulations. *Aquatic Conservation: Marine and Freshwater Ecosystems*, *30*(10), 1841-1853. https://doi.org/10.1002/aqc.3316

Haug, G.H. & Tiedemann, R. (1998) Effect of the formation of the Isthmus of Panama on Atlantic Ocean thermohaline circulation. Nature, 393, 673-676. https://doi.org/10.1038/31447

Henry, L. A., Frank, N., Hebbeln, D., Wienberg, C., Robinson, L., van de Flierdt, T., ... & Roberts, J. M. (2014). Global ocean conveyor lowers extinction risk in the deep sea. *Deep Sea Research Part I: Oceanographic Research Papers*, 88, 8-16. https://doi.org/10.1016/j.dsr.2014.03.004

Hey, J., Chung, Y., Sethuraman, A., Lachance, J., Tishkoff, S., Sousa, V. C., & Wang, Y. (2018). Phylogeny estimation by integration over isolation with migration models. *Molecular biology and evolution*, *35*(11), 2805-2818. https://doi.org/10.1093/molbev/msy162

Huisman, J. (2017). Pedigree reconstruction from SNP data: parentage assignment, sibship clustering and beyond. *Molecular ecology resources*, *17*(5), 1009-1024. https://doi.org/10.1111/1755-0998.12665

Jennings, R. M., Etter, R. J., & Ficarra, L. (2013). Population differentiation and species formation in the deep sea: the potential role of environmental gradients and depth. *PLoS One*, *8*(10), e77594. https://doi.org/10.1371/journal.pone.0077594

Johnson, S. B., Warén, A., & Vrijenhoek, R. C. (2008). DNA barcoding of *Lepetodrilus limpets* reveals cryptic species. *Journal of Shellfish Research*, *27*(1), 43-51. https://doi.org/10.2983/0730-8000(2008)27[43:DBOLLR]2.0.CO;2

Johnson, S. B., Won, Y. J., Harvey, J. B., & Vrijenhoek, R. C. (2013). A hybrid zone between *Bathymodiolus* mussel lineages from eastern Pacific hydrothermal vents. *BMC evolutionary Biology*, *13*, 1-18. https://doi.org/10.1186/1471-2148-13-21

Jollivet, D. Portanier, E., Tran Lu Y, A., Arnaud-Haond, S. (2023) Genetic connectivity maps for deep sea vent and cold-seep fauna and cold-water corals from the North Atlantic. PANGAEA, https://doi.org/10.1594/PANGAEA.961199

Jollivet, D., Portanier, E., Nicolle, A., Thiébaut, E., Biastoch, A. (2023) Atlantic seep mussels larval dispersal simulations and genetic data. PANGAEA, https://doi.org/10.1594/PANGAEA.955455

Jolly, M., Viard, F., Weinmayr, G., Gentil, F., Thiébaut, E. & Jollivet, D. 2003. Does the genetic structure of *Pectinaria koreni* (Polychaeta: Pectinariidae) conform to a source–sink metapopulation model at the scale of the Baie de Seine? *Helgol Mar Res* 56: 238–246. https://doi.org/10.1007/s10152-002-0123-1

Jouganous, J., Long, W., Ragsdale, A. P., & Gravel, S. (2017). Inferring the joint demographic history of multiple populations: beyond the diffusion approximation. *Genetics*, *206*(3), 1549-1567. https://doi.org/10.1534/genetics.117.200493

LaBella, A. L., Van Dover, C. L., Jollivet, D., & Cunningham, C. W. (2017) Gene flow between Atlantic and Pacific Ocean basins in three lineages of deep-sea clams (Bivalvia: Vesicomyidae: Pliocardiinae) and subsequent limited gene flow within the Atlantic. *Deep Sea Research Part II: Topical Studies in Oceanography*, 137, 307-317. https://doi.org/10.1016/j.dsr2.2016.08.013

Le Goff-Vitry, M. C., Pybus, O. G., & Rogers, A. D. (2004). Genetic structure of the deep-sea coral *Lophelia pertusa* in the northeast Atlantic revealed by microsatellites and internal transcribed spacer sequences. *Molecular Ecology*, 13(3), 537-549. https://doi.org/10.1046/j.1365-294x.2004.2079.x

Leigh, J. W., & Bryant, D. (2015). POPART: full-feature software for haplotype network construction. *Methods in ecology and evolution*, *6*(9), 1110-1116. https://doi.org/10.1111/2041-210X.12410

Levin, S. A., Cohen, D., & Hastings, A. (1984). Dispersal strategies in patchy environments. *Theoretical population biology*, *26*(2), 165-191. https://doi.org/10.1016/0040-5809(84)90028-5

Levin, L. A., Etter, R. J., Rex, M. A., Gooday, A. J., Smith, C. R., Pineda, J., ... & Pawson, D. (2001). Environmental influences on regional deep-sea species diversity. *Annual review of ecology and systematics*, *32*(1), 51-93. https://doi.org/10.1146/annurev.ecolsys.32.081501.114002

Levin, L. A., Mengerink, K., Gjerde, K. M., Rowden, A. A., Van Dover, C. L., Clark, M. R., ... & Brider, J. (2016). Defining "serious harm" to the marine environment in the context of deep-seabed mining. *Marine Policy*, *74*, 245-259. https://doi.org/10.1016/j.marpol.2016.09.032

Lutz, R. A., Bouchet, P., Jablonski, D., Turner, R. D., & Warén, A. (1986). Larval ecology of mollusks at deep-sea hydrothermal vents. *American Malacological Bulletin*, *4*(1), 49-54.

Marticorena, J., Matabos, M., Ramirez-Llodra, E., Cathalot, C., Laes-Huon, A., Leroux, R., ... & Sarrazin, J. (2021). Recovery of hydrothermal vent communities in response to an induced disturbance at the Lucky Strike vent field (Mid-Atlantic Ridge). *Marine Environmental Research*, *168*, 105316. https://doi.org/10.1016/j.marenvres.2021.105316

Matabos, M. & Jollivet, D. 2019. Revisiting the species' complex of *Lepetodrilus elevatus* (Vetigastropod, Lepetodrilidae) using gastropod samples from the Galápagos and Guaymas hydrothermal vent systems. *J. Molluscan studies*, 85 (1), 154-165. https://doi.org/10.1093/mollus/eyy061

Matabos, M., & Thiebaut, E. (2010). Reproductive biology of three hydrothermal vent peltospirid gastropods (*Nodopelta heminoda*, *N. subnoda* and *Peltospira operculata*) associated with Pompeii worms on the East Pacific Rise. *Journal of Molluscan Studies*, *76*(3), 257-266. https://doi.org/10.1093/mollus/eyq008

McPeek, M. A., & Holt, R. D. (1992). The evolution of dispersal in spatially and temporally varying environments. *The American Naturalist*, *140*(6), 1010-1027. https://doi.org/10.1086/285453

Methou, P., Guéganton, M., Copley, J. T., Watanabe, H. K., Pradillon, F., Cambon-Bonavita, M. A., & Chen, C. (2023). Juvenile niches select between two distinct development trajectories and symbiosis modes in vent shrimps. *bioRxiv*, 2023-07. https://doi.org/10.1101/2023.07.02.547428

Methou, P., Michel, L. N., Segonzac, M., Cambon-Bonavita, M. A., & Pradillon, F. (2020). Integrative taxonomy revisits the ontogeny and trophic niches of *Rimicaris* vent shrimps. *Royal Society Open Science*, *7*(7), 200837. https://doi.org/10.1098/rsos.200837

Mohrbeck, I., Horton, T., Jażdżewska, A. M., & Martinez Arbizu, P. (2021). DNA barcoding and cryptic diversity of deep-sea scavenging amphipods in the Clarion-Clipperton Zone (Eastern Equatorial Pacific). *Marine Biodiversity*, *51*, 1-15. https://doi.org/10.1007/s12526-021-01170-3

Morato, T., González-Irusta, J. M., Dominguez-Carrió, C., Wei, C. L., Davies, A., Sweetman, A. K., ... & Carreiro-Silva, M. (2020). Climate-induced changes in the suitable habitat of cold-water corals and commercially important deep-sea fishes in the North Atlantic. *Global Change Biology*, *26*(4), 2181-2202. https://doi.org/10.1111/gcb.14996

Mouchi V., Pecheyran C., Claverie F., Cathalot C., Matabos M., Rouxel O., Jollivet D., Broquet T., Comtet T. (2024). A step towards measuring connectivity in the deep-sea: elemental fingerprints of mollusk larval shells discriminate hydrothermal sites. Biogeosciences, 21, 145-160. BioRxiv archive. https://doi.org/10.1101/2023.01.03.522618.

Mullineaux, L. S., Adams, D. K., Mills, S. W., & Beaulieu, S. E. (2010). Larvae from afar colonize deep-sea hydrothermal vents after a catastrophic eruption. *Proceedings of the National Academy of Sciences*, *107*(17), 7829-7834. https://doi.org/10.1073/pnas.0913187107

Nicolle, A., Moitié, R., Ogor, J., Dumas, F., Foveau, A., Foucher, E., & Thiébaut, E. (2017). Modelling larval dispersal of *Pecten maximus* in the English Channel: a tool for the spatial management of the stocks. *ICES Journal of Marine Science*, *74*(6), 1812-1825. https://doi.org/10.1093/icesjms/fsw207

Nussberger, B., Greminger, M. P., Grossen, C., Keller, L. F., & Wandeler, P. (2013). Development of SNP markers identifying European wildcats, domestic cats, and their admixed progeny. *Molecular Ecology Resources*, *13*(3), 447-460. https://doi.org/10.1111/1755-0998.12075

Nye, V., Copley, J., & Plouviez, S. (2012). A new species of *Rimicaris* (Crustacea: Decapoda: Caridea: Alvinocarididae) from hydrothermal vent fields on the Mid-Cayman spreading centre, Caribbean. *Journal of the Marine Biological Association of the United Kingdom*, *92*(5), 1057-1072.

O'Dea, A., Lessios, H. A., Coates, A. G., Eytan, R. I., Restrepo-Moreno, S. A., Cione, A. L., ... & Jackson, J. B. (2016). Formation of the Isthmus of Panama. *Science advances*, *2*(8), e1600883. https://doi.org/10.1017/S0025315411002001

Olu–Le Roy K., von Cosel**,** R., Hourdez, S., Carney, S.L., Jollivet, D. 2007. Amphi-Atlantic cold seep *Bathymodiolus* complexes of species across the Equatorial belt. Deep-Sea Research I, 54, 1890-1911. https://doi.org/10.1016/j.dsr.2007.07.004

O'Mullan, G. D., Maas, P. A. Y., Lutz, R. A., & Vrijenhoek, R. C. (2001). A hybrid zone between hydrothermal vent mussels (Bivalvia: Mytilidae) from the Mid-Atlantic Ridge. *Molecular Ecology*, *10*(12), 2819-2831. https://doi.org/10.1046/j.0962-1083.2001.01401.x

Pante, E., France, S. C., Couloux, A., Cruaud, C., McFadden, C. S., Samadi, S., & Watling, L. (2012). Deep-sea origin and *in situ* diversification of chrysogorgiid octocorals. *PLoS One*, *7*(6), e38357. https://doi.org/10.1371/journal.pone.0038357

Pante, E., Puillandre, N., Viricel, A., Arnaud-Haond, S., Aurelle, D., Castelin, M., ... & Samadi, S. (2015). Species are hypotheses: avoid connectivity assessments based on pillars of sand. *Molecular Ecology*, *24*(3), 525-544. https://doi.org/10.1111/mec.13048

Paulus, E., Brix, S., Siebert, A., Martinez Arbizu, P., Rossel, S., Peters, J., ... & Schwentner, M. (2022). Recent speciation and hybridization in Icelandic deep-sea isopods: An integrative approach using genomics and proteomics. *Molecular Ecology*, *31*(1), 313-330. https://doi.org/10.1111/mec.16234

Pickrell, J. K., & Pritchard, J. K. (2012). User Manual for TreeMix v1.

Pineda, J., Hare, J. A., & Sponaugle, S. U. (2007). Larval transport and dispersal in the coastal ocean and consequences for population connectivity. *Oceanography*, *20*(3), 22-39.

Plouviez, S., Faure, B., Le Guen, D., Lallier, F.H., Bierne, N., Jollivet, D. (2013) A new barrier to dispersal trapped old genetic clines that escaped the Easter Microplate tension zone of the Pacific vent mussels. *PloS One*, 8(12), e81555.

Plouviez S., Le Guen D., Lecompte, O., Lallier F.H. and Jollivet D. (2010) Determining gene flow and the influence of selection across the equatorial barrier of the East Pacific Rise in the tube-dwelling polychaete *Alvinella pompejana*. *BMC Evolutionary Biology*, 10: 220.

Plouviez, S., Shank, T.M., Faure, B., Daguin-Thiébaut, C., Viard, F., Lallier, F.H., Jollivet, D**.** 2009. Comparative phylogeography among hydrothermal vent species along the East Pacific Rise reveals vicariant processes and population expansion in the south. Mol. Ecol. 18 (18), 3903-3917. https://www.jstor.org/stable/24860094

Poitrimol, C., Thiébaut, É., Daguin-Thiébaut, C., Le Port, A. S., Ballenghien, M., Tran Lu Y, A., ... & Matabos, M. (2022). Contrasted phylogeographic patterns of hydrothermal vent gastropods along South West Pacific: Woodlark Basin, a possible contact zone and/or stepping-stone. *Plos one*, *17*(10), e0275638. https://doi.org/10.1371/journal.pone.0275638

Portanier, E., Nicolle A., Rath, W., Kirch, F., Monnet L., Le Goff G., Le Port A.-S., Daguin-Thiébaut, C., Morrison C., Cunha, M., Betters, M., Young C.M., Van Dover C.L., Biastoch, A., Thiébaut E., Jollivet D. 2022. Coupling large-spatial scale larval dispersal modelling with barcoding to refine the amphi-Atlantic connectivity hypothesis in deep-sea seep mussels. Frontiers in Marine Science, in 'Managing deep-sea and open ocean ecosystems at ocean basin scale – volume 2', 10, 1122124. https://doi.org/10.3389/fmars.2023.1122124

Portanier E., Tran-Lu A., Pradillon F., Daguin-Thiébaut C., Ruault, S., Omnes, E., Borowski, C., Carlsson, J., Jollivet D., Matabos M. (2024 - submitted) Genetic connectivity and demographic history of iconic hydrothermal vent gastropods along the Mid-Atlantic Ridge: insights using next-generation sequencing and conservation implications (submitted to Conservation Biology)

Puillandre, N., Sysoev, A. V., Olivera, B. M., Couloux, A., & Bouchet, P. (2010). Loss of planktotrophy and speciation: geographical fragmentation in the deep-water gastropod genus *Bathytoma* (Gastropoda, Conoidea) in the western Pacific. *Systematics and Biodiversity*, *8*(3), 371-394. https://doi.org/10.1080/14772001003748709

Ramirez-Llodra, E., Tyler, P. A., Baker, M. C., Bergstad, O. A., Clark, M. R., Escobar, E., ... & Van Dover, C. L. (2011). Man and the last great wilderness: human impact on the deep sea. *PLoS one*, *6*(8), e22588.Raupach, M. J., Malyutina, M., Brandt, A., & Wägele, J. W. (2007). Molecular data reveal a highly diverse species flock within the munnopsoid deep-sea isopod *Betamorpha fusiformis* (Barnard, 1920) (Crustacea: Isopoda: Asellota) in the Southern Ocean. *Deep Sea Research Part II: Topical Studies in Oceanography*, *54*(16-17), 1820-1830. https://doi.org/10.1371/journal.pone.0022588

Rex, M. A., Stuart, C. T., Hessler, R. R., Allen, J. A., Sanders, H. L., & Wilson, G. D. (1993). Global-scale latitudinal patterns of species diversity in the deep-sea benthos. *Nature*, *365*(6447), 636-639. https://doi.org/10.1038/365636a0

Ritchie, H., Jamieson, A. J., & Piertney, S. B. (2017). Population genetic structure of two congeneric deep-sea amphipod species from geographically isolated hadal trenches in the Pacific Ocean. *Deep Sea Research Part I: Oceanographic Research Papers*, *119*, 50-57. https://doi.org/10.1016/j.dsr.2016.11.006

Rogacheva, A. V., Mironov, A. N., Minin, K. V., & Gebruk, A. V. (2013). Morphological evidence of depth-related speciation in deep-sea Arctic echinoderms. *Invertebrate Zoology*, *10*(1), 143-166.

Rougeux, C., Gagnaire, P. A., & Bernatchez, L. (2019). Model-based demographic inference of introgression history in European whitefish species pairs'. *Journal of evolutionary biology*, *32*(8), 806-817. https://doi.org/10.1111/jeb.13482

Roux, C., Fraisse, C., Romiguier, J., Anciaux, Y., Galtier, N., & Bierne, N. (2016). Shedding light on the grey zone of speciation along a continuum of genomic divergence. *PLoS biology*, *14*(12), e2000234. https://doi.org/10.1371/journal.pbio.2000234

Rozas, J., Ferrer-Mata, A., Sánchez-DelBarrio, J. C., Guirao-Rico, S., Librado, P., Ramos-Onsins, S. E., & Sánchez-Gracia, A. (2017). DnaSP 6: DNA sequence polymorphism analysis of large data sets. *Molecular biology and evolution*, *34*(12), 3299-3302. https://doi.org/10.1093/molbev/msx248

Sarrazin, J., Cathalot, C., Laes, A., Marticorena, J., Michel, L. N., & Matabos, M. (2022). Integrated Study of New Faunal Assemblages Dominated by Gastropods at Three Vent Fields Along the Mid-Atlantic Ridge: Diversity, Structure, Composition and Trophic Interactions. *Frontiers In Marine Science*, *9*, 1192. https://doi.org/10.3389/fmars.2022.925419

Stoeckel, S., Arnaud-Haond, S., & Krueger-Hadfield, S. A. (2021). The combined effect of haplodiplonty and partial clonality on genotypic and genetic diversity in a finite mutating population. *Journal of Heredity*, *112*(1), 78-91. https://doi.org/10.1093/jhered/esaa062

Sundqvist, L., Keenan, K., Zackrisson, M., Prodöhl, P., & Kleinhans, D. (2016). Directional genetic differentiation and relative migration. *Ecology and evolution*, *6*(11), 3461-3475. https://doi.org/10.1002/ece3.2096

Taboada, S., Ríos, P., Mitchell, A., Cranston, A., Busch, K., Tonzo, V., ... & Riesgo, A. (2022). Genetic diversity, gene flow and hybridization in fan-shaped sponges (*Phakellia* spp.) in the North-East Atlantic deep sea. *Deep Sea Research Part I: Oceanographic Research Papers*, *181*, 103685. https://doi.org/10.1016/j.dsr.2021.103685

Teixeira, S., Olu, K., Decker, C., Cunha, R. L., Fuchs, S., Hourdez, S., ... & Arnaud-Haond, S. (2013) High connectivity across the fragmented chemosynthetic ecosystems of the deep Atlantic Equatorial Belt: efficient dispersal mechanisms or questionable endemism? *Molecular Ecology*, 22(18), 4663-4680. https://doi.org/10.1111/mec.12419

Teixeira, S., Serrao, E. A., & Arnaud-Haond, S. (2012). Panmixia in a fragmented and unstable environment: the hydrothermal shrimp *Rimicaris exoculata* disperses extensively along the Mid-Atlantic Ridge. *PLoS One*, *7*(6), e38521. https://doi.org/10.1371/journal.pone.0038521

Thomas, E. A., Molloy, A., Hanson, N. B., Böhm, M., Seddon, M., & Sigwart, J. D. (2021). A global red list for hydrothermal vent Molluscs. *Frontiers in Marine Science*, *8*, Article 713022. https://doi.org/10.3389/fmars.2021.713022

Tran Lu Y A., Ruault, S., Daguin-Thiébaut, C., Castel, J., Bierne, N., Broquet, T., Winkler, P., Perdereau, A., Arnaud-Haond, S., Gagnaire, P.A., Jollivet, D., Hourdez, S., Bonhomme, F. 2022. Subtle limits to connectivity revealed by outlier loci within two divergent metapopulations of the deep-sea hydrothermal gastropod *Ifremeria nautilei*. Mol. Ecol., 31(10): 2793-2813. https://doi.org/10.1111/mec.16430

Tyler, P. A., & Dixon, D. R. (2000). Temperature/pressure tolerance of the first larval stage of *Mirocaris fortunata* from Lucky Strike hydrothermal vent field. *Journal of the Marine Biological Association of the United Kingdom*, *80*(4), 739-740. https://doi.org/10.1017/S0025315400002605

Van der Heijden, K., Petersen, J. M., Dubilier, N., & Borowski, C. (2012). Genetic connectivity between north and south Mid-Atlantic Ridge chemosynthetic bivalves and their symbionts. *PLoS One*, *7*(7), e39994. https://doi.org/10.1371/journal.pone.0039994

Van Dover, C. L. (2011). Mining seafloor massive sulphides and biodiversity: what is at risk?. *ICES Journal of Marine Science*, *68*(2), 341-348. https://doi.org/10.1093/icesjms/fsq086

Versteegh, E. A., Van Dover, C. L., Van Audenhaege, L., & Coleman, M. (2023). Multiple nutritional strategies of hydrothermal vent shrimp (*Rimicaris hybisae*) assemblages at the Mid-Cayman Rise. *Deep Sea Research Part I: Oceanographic Research Papers*, *192*, 103915. https://doi.org/10.1016/j.dsr.2022.103915

Vrijenhoek, R. C. (2009). Cryptic species, phenotypic plasticity, and complex life histories: assessing deep-sea faunal diversity with molecular markers. *Deep Sea Research Part II: Topical Studies in Oceanography*, *56*(19-20), 1713-1723. https://doi.org/10.1016/j.dsr2.2009.05.016

Wilson, G. D., & Hessler, R. R. (1987). Speciation in the deep sea. *Annual Review of Ecology and Systematics*, *18*(1), 185-207.

White, B. N. (1988). Oceanic anoxic events and allopatric speciation in the deep sea. *Biological Oceanography*, *5*(4), 243-259. https://doi.org/10.1080/01965581.1987.10749516

Wilson, G. A., & Rannala, B. (2003). Bayesian inference of recent migration rates using multilocus genotypes. *Genetics*, *163*(3), 1177-1191. https://doi.org/10.1093/genetics/163.3.1177

Yahagi, T., Fukumori, H., Warén, A., & Kano, Y. (2019). Population connectivity of hydrothermal-vent limpets along the northern Mid-Atlantic Ridge (Gastropoda: Neritimorpha: Phenacolepadidae). *Journal of the Marine Biological Association of the United Kingdom*, *99*(1), 179-185. https://doi.org/10.1017/S0025315417001898

Yearsley, J. M., Salmanidou, D. M., Carlsson, J., Burns, D., & Van Dover, C. L. (2020). Biophysical models of persistent connectivity and barriers on the northern Mid-Atlantic Ridge. *Deep Sea Research Part II: Topical Studies in Oceanography*, *180*, 104819. https://doi.org/10.1016/j.dsr2.2020.104819

Young, C. M., He, R., Emlet, R. B., Li, Y., Qian, H., Arellano, S. M., ... & Rice, M. E. (2012). Dispersal of deep-sea larvae from the intra-American seas: simulations of trajectories using ocean models. *Integr. Comp. Biol.* 52, 483–496. https://doi.org/10.1093/icb/ics090

Zheng, X., Levine, D., Shen, J., Gogarten, S. M., Laurie, C., & Weir, B. S. (2012). A high-performance computing toolset for relatedness and principal component analysis of SNP data. *Bioinformatics*, *28*, 3326-3328. https://doi.org/10.1093/bioinformatics/bts606

Zhou, H., Alexander, D., & Lange, K. (2011). A quasi-Newton acceleration for high-dimensional optimization algorithms. *Statistics and computing*, *21*, 261-273. https://doi.org/10.1007/s11222-009-9166-3

6. Document Information

EU Project N°	818123	**Acronym**	iAtlantic
Full Title	Integrated Assessment of Atlantic Marine Ecosystems in Space and Time		
Project website	www.iatlantic.eu		

Deliverable	**N° 1.5**	**Title**	Preferential pathways of dispersal and role of the AMOC in connectivity
Work Package	**N°1**	**Title**	Atlantic Oceanography and Ecosystem Connectivity

Date of delivery	**Contractual**	December 2023	**Actual**	March 2024
Dissemination level	X	PU Public, fully open, e.g. web		
		CO Confidential restricted under conditions set out in Model Grant Agreement		

Authors (Partner)	Sorbonne University	
Responsible Author(s)	**Name(s)** Didier Jollivet	**Email(s)** jollivet@sb-roscoff.fr